SANDIA REPORT

SAND97–2592 • UC–602
Unlimited Release
Printed January 1998

Electrokinetic Demonstration at the Unlined Chromic Acid Pit

Dr. Eric R. Lindgren, Matthew G. Hankins, Earl D. Mattson, Patricia M. Duda

Prepared by
Sandia National Laboratories
Albuquerque, New Mexico 87185 and Livermore, California 94550

Sandia is a multiprogram laboratory operated by Sandia Corporation, a Lockheed Martin Company, for the United States Department of Energy under Contract DE-AC04-94AL85000.

Sandia National Laboratories

Issued by Sandia National Laboratories, operated for the United States Department of Energy by Sandia Corporation.

Available to DOE and DOE contractors from
Office of Scientific and Technical Information
P.O. Box 62
Oak Ridge, TN 37831

Prices available from (615) 576-8401, FTS 626-8401

Available to the public from
National Technical Information Service
U.S. Department of Commerce
5285 Port Royal Rd
Springfield, VA 22161

NTIS price codes
Printed copy: A08
Microfiche copy: A01

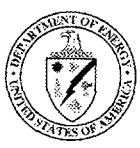

SAND97-2592
Unlimited Release
Printed January 1998

Distribution
Category UC-602

ELECTROKINETIC DEMONSTRATION AT THE UNLINED CHROMIC ACID PIT

Dr. Eric R. Lindgren and Matthew G. Hankins
Sandia National Laboratories
P.O. Box 5800
Albuquerque, NM 87185-0719

Earl D. Mattson
Sat-Unsat, Inc.
Albuquerque, NM 87112

Patricia M. Duda
Ktech Corp.
Albuquerque, NM 87110

Abstract

Heavy-metal contaminated soils are a common problem at Department of Energy (DOE)-operated sites and privately owned facilities throughout the nation. One emerging technology which can remove heavy metals from soil *in situ* is electrokinetics. To conduct electrokinetic (EK) remediation, electrodes are implanted into the ground, and a direct current is imposed between the electrodes. Metal ions dissolved in the soil pore water migrate towards an electrode where they can be removed.

The electrokinetic program at Sandia National Laboratories (SNL) has been focusing on electrokinetic remediation for unsaturated soils. A patent was awarded for an electrokinetic electrode system designed at SNL for applications to unsaturated soils. Current research described in this report details an electrokinetic remediation field demonstration of a chromium plume that resides in unsaturated soil beneath the SNL Chemical Waste Landfill (CWL). This report describes the processes, site investigation, operation and monitoring equipment, testing procedures, and extraction results of the electrokinetic demonstration.

This demonstration successfully removed chromium contamination in the form of chromium(VI) from unsaturated soil at the field scale. After 2700 hours of operation, 600 grams of Cr(VI) was extracted from the soil beneath the SNL CWL in a series of thirteen tests. The contaminant was removed from soil which has moisture contents ranging from 2 to 12 weight percent. This demonstration was the first EK field trial to successfully remove contaminant ions from arid soil at the field scale.

Although the new patented electrode system was successful in removing an anionic contaminant (i.e., chromate) from unsaturated sandy soil, the electrode system was a prototype and has not been specifically engineered for commercialization. A redesign of the electrode system as indicated by the results of this research is suggested for future EK field trials.

Acknowledgments

This work was performed at Sandia National Laboratories, which is operated for the U.S. Department of Energy under Contract No. DE-AC04-94AL85000 and funded by the Department of Energy's Office of Science and Technology through the Subsurface Contaminant Focus Area.

The authors wish to express their appreciation to the following individuals for their invaluable support of this project: Robert Helgesen and Bruce Reavis (both SNL) for drilling, soil sampling, and equipment installation; James Swanson (SNL) for electrical expertise; Christopher Sears (SNL) for electrical design and construction and for system monitoring; and Judy Campbell (GRAM, Inc.) for technical editing and formatting of this report. Without the assistance of these people the project would not have been successfully completed.

Contents

Figures

Tables

EXECUTIVE SUMMARY

Heavy-metal contaminated soils are a common problem at Department of Energy-operated sites and privately-owned facilities throughout the nation. The most common method for remediating heavy-metal contaminated soils is by excavation and subsequent disposal in a hazardous waste landfill. One emerging technology which can remove heavy metals from soil in-situ is electrokinetics. To conduct electrokinetic (EK) remediation, electrodes are implanted into the ground, and a direct current is imposed between the electrodes. Metal ions dissolved in the soil pore water migrate toward either an anode or cathode where they can be removed.

The EK program at Sandia National Laboratories (SNL) has been focusing on EK remediation for unsaturated soils. A major problem to overcome in the application of electrokinetics to unsaturated soils was the lack of an effective way to remove the contamination from the soil once it reached an electrode. A method to remove the contamination was developed by designing an electrode installed within a vacuum lysimeter. Contaminant ions could pass through the porous ceramic casing of the lysimeter to the electrolyte fluid and then subsequently be removed for treatment or disposal. A patent was awarded for this EK electrode that was specifically designed for application in unsaturated soils. Current research described in this report details a field demonstration of the EK remediation of a chromium plume that resides in unsaturated soil beneath the SNL Chemical Waste Landfill (CWL). This report describes the processes, site investigation, operation and monitoring equipment, testing procedures, and extraction results of the EK demonstration.

The SNL EK demonstration successfully removed chromium contamination (in the form of Cr(VI), chromate) from unsaturated soil at the field scale. After 2700 hours of operation, 600 grams of Cr in the form of chromium(VI) was extracted from the soil beneath the SNL CWL in a series of thirteen tests. The contaminant was removed from soil which had moisture contents ranging from 4 to 12 weight percent. This demonstration was the first EK field trial to successfully remove contaminant ions from arid soil at the field scale.

The EK demonstration was terminated prior to complete cleanup of the soil beneath the Unlined Chromic Acid Pit (UCAP) site. During the demonstration, chromium removal efficiencies (grams Cr removed per amp-hr) did not deteriorate, indicating the EK process is stable over long periods of time. The EK demonstration was stopped due to budget and time constraints (the SNL Environmental Restoration Program had scheduled a Voluntary Corrective Action at the site).

Comparison of pretest and post-test soil sample chemical results indicates a cleaning of the soil near the cathodes and an accumulation of chromate in the area near the anodes. No significant changes in chromium concentrations were noted outside of the remediation zone. Soil samples adjacent to the cathodes would pass the toxicity

characteristic leaching procedure (TCLP) criteria, indicating that soil in this area would not be considered hazardous waste if excavated and removed to the surface. Pretest soil samples taken in the area of the cathodes had TCLP extract chromium concentrations as high as 28 ppm prior to conducting the EK demonstration. It is expected that all of the soil between the cathodes and the anodes would have passed the TCLP criteria if the EK demonstration had run to completion.

Electrokinetic remediation can transport only contaminants that are dissolved in the soil water. Contaminants that are in a precipitated solid phase or sorbed onto the soil particles will not be transported until they are brought into the liquid phase. At the EK demonstration site, some of the chromium(VI) has likely co-precipitated with gypsum or has precipitated as anhydrous chromatite ($CaCrO_4$). Both of these solid forms of chromate have slow dissolution rates. In soil zones where the chromate ions have been removed by electromigration, these slowly dissolving solid forms of chromate may recontaminate the water contained in the soil pores after some period of time. This dissolution of chromate will extend the time to complete a remediation effort.

Calculating the contaminant transference numbers from soil samples collected prior to conducting EK remediation prove to be a viable technique to predict the EK extraction performance. Transference numbers calculated from pretest soil samples closely correlated with EK extraction efficiencies. Transference numbers describe the fraction of the current carried by the contaminant ions to the total amount of current applied. Using these numbers, an estimate of the amount of chromium removed per applied charge can be made for individual electrodes. If the total mass of contaminant is known in the remediation zone, the amount of electricity needed to remediate the site can also be estimated.

Although the newly patented electrode system was successful in removing an anionic contaminant (i.e., chromate) from unsaturated sandy soil, the electrode system was a prototype and has not been sufficiently engineered for commercialization. A redesign of the electrode system is suggested for future EK field trials.

This demonstration has also led to the next generation of an innovative electrode system to remove chromium from unsaturated soils. The new electrode system is expected to substantially reduce the cost of EK remediation. A solid matrix chromate capture system eliminates the need for a liquid-control system and a vacuum system. In addition, the new electrodes will be planar in design to better transfer the electrical power to the soil. Electrical costs will be reduced to ½ the present values by operating the system at a lower power, thereby avoiding the expense of actively cooling the EK electrode system. SNL and Sat-Unsat, Inc. have successfully tested a laboratory-scale prototype of this electrode for removing chromate from unsaturated soil.

Acronyms

A"x"	anode "x"
BLS	below land surface
C"x"	cathode "x"
CVOC	chlorinated volatile organic compound
CWL	Chemical Waste Landfill
DOE	Department of Energy
EK	electrokinetic
EPA	Environmental Protection Agency
HDTMA	hexadecyltrimethylammonium
HDTMA-OH	hexadecyltrimethylammonium hydroxide
IC	ion chromatography
ID	inside diameter
KAFB	Kirtland Air Force Base
PCBs	poly-chlorinated biphenyls
PE	polyethylene
PVC	polyvinylchloride
RIM	radio imaging method
SITE	Superfund Innovative Technology Evaluation
SNL	Sandia National Laboratories
SVOC	semi-volatile organic compound
TA III	Technical Area III
TCLP	toxicity characteristic leaching procedure
UCAP	unlined chromic acid pit
VOA	volatile organic analysis
VOC	volatile organic compound
XRF	x-ray fluorescence

Equation Symbols (in order of appearance)

v_{em}	electromigration velocity (m s^{-1})
μ	electric ionic mobility ($m^2V^{-1}s^{-1}$)
τ	tortuosity (unitless)
dV/dx	voltage gradient (V m^{-1})
v_{eo}	electroosmosis velocity (m s^{-1})
ε	fluid permittivity (C $V^{-1}m^{-1}$ = N V^{-2})
ζ	zeta potential (V)
ν	fluid viscosity (Pa * s = (N m^{-2}) * s)
J_i	flux of ion *i* across a plane (mol s^{-1} m^{-2})
C_i	concentration of ion *i* (mol m^{-3})
A	area (m^2)
I	current (Amps = C s^{-1})
z_i	charge on the ion (unitless)
F	Faraday's constant (96500 C mol^{-1})
Q	quantity of charge (C)
t	time (s)
T_{Cr}	chromate transference number (unitless)
$X_{Cr(t)}$	moles of chromate (or chromium) removed over time interval (mol Cr)
z_{Cr}	charge of CrO_4^{2-} = -2
Λ_{Cr}	molar conductivity of chromate (S m^2 mol^{-1})
C_{Cr}	concentration of chromate (mol m^{-3})
σ_w	solution conductivity (S m^{-1})
IS	ionic strength
ϕ	activity coefficient
p	temperature dependent constant (~0.51 at 25 °C)
EC	solution electrical conductivity (mS cm^{-1})
E_{Cr}	extraction efficiency for chromate (g amp^{-1} hr^{-1})
m_{Cr}	mass of chromate expressed as total grams of chromium (g)
$I * t$	charge, Q (amp-hrs)
MW_{Cr}	molecular weight of chromium (52 g mol^{-1})
P	electrical power (W)
V	volts (V)
E_e	energy efficiency of chromium removal (g Cr $kW^{-1}hr^{-1}$)
σ_e	effective soil electrical conductivity (S cm^{-1})
a, m, & n	constants of Archie's formula
φ	porosity (cm^3 cm^{-3})
S	saturation (cm^3 cm^{-3})
σ_{sw}	soil water electrical conductivity (S cm^{-1})
θ	moisture content (wt %)
M	moles
R_{H_2}	rate of hydrogen gas generation (L min^{-1})
R_{air}	rate of air purge (L min^{-1})

1. INTRODUCTION

Heavy-metal contamination of soils and groundwater is a widespread problem at the Environmental Protection Agency (EPA) Superfund sites, Department of Energy (DOE)-operated sites, and privately-owned facilities throughout the nation. Currently, the only viable method for remediating heavy-metal contaminated soil is by excavation followed by soil washing or relocation. One possible technique for *in-situ* removal of such contaminants is EK remediation, in which electrodes are implanted into the ground and a direct current is imposed between the electrodes. Metal ions migrate in pore water toward either an anode or cathode where they can be removed. Contaminants arriving at the electrodes may be removed from the soil in several ways including electroplating or adsorption onto the electrode, precipitation or co-precipitation at the electrode, pumping water near the electrode, or complexing with ion-exchange resins.

The EK program at Sandia National Laboratories (SNL) has been focusing on EK applications to unsaturated soils. One problem in applying EK technology with currently available electrodes to unsaturated soils is the potential for washing the contaminants out of the remediation area. The SNL research has led to a patented (Lindgren & Mattson, 1995) electrode design to remove the contaminants from the soil without the addition of significant amounts of water which could spread the contamination. This electrode design extracts contaminants by moving them into water held under tension (i.e., under partial vacuum) inside a ceramic casing that surrounds the electrode. Previous research at the laboratory scale had proven the concept of transporting and extracting chromium from unsaturated soils (Mattson and Lindgren, 1994). Current research described in this report demonstrates the EK remediation of a chromium plume that resides in the vadose (unsaturated) zone beneath the Unlined Chromic Acid Pit (UCAP) in the Chemical Waste Landfill (CWL) at SNL. Knowledge gained from this field trial can be transferred to any site that has heavy-metal contamination in the unsaturated zone.

This report first will describe the theory of EK remediation and explain the two important transport mechanisms, electromigration and electroosmosis, and then examine ways to evaluate the effectiveness of the EK process. Secondly, it will recount the investigation of the site including the preexisting conditions of the chromium distribution to determine the feasibility of EK treatment. The unique design of the EK electrodes and the instrumentation that controls and monitors the EK remediation process will be described in detail. The report then will describe a series of tests conducted to evaluate the effectiveness of the EK remediation effort. Finally, the report will discuss the extraction results, the final site investigation, the goals met, and the conclusions for this project.

2. THEORY

The application of a direct current imposed between electrodes implanted in soil leads to a number of effects: ionic species and charged particles in the soil water will migrate to the oppositely-charged electrode (electromigration and electrophoresis), and, along with this migration, a bulk flow of water is induced, usually toward the cathode (electroosmosis) (Hunter,

1981). The combination of these phenomena leads to a movement of contaminants toward the electrodes (Figure 2-1).

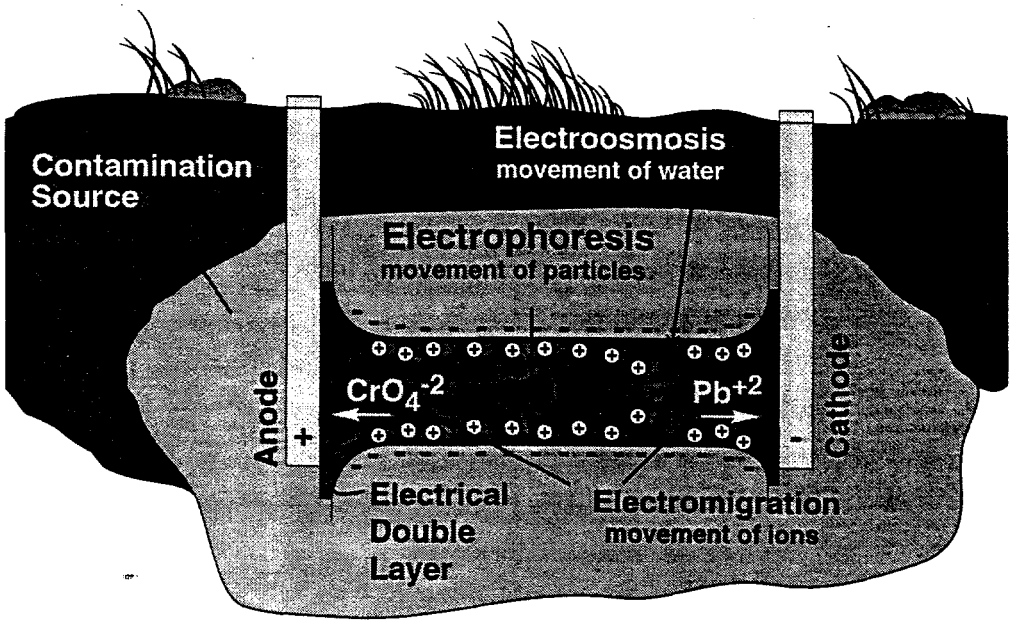

Figure 2-1. Movement of charged particles.

This section will discuss the transport phenomena, several ways to evaluate the effectiveness of contaminant removal, and the effect of soil heating.

2.1 Transport Phenomena

To understand EK remediation, it is necessary to understand the governing equations of the transport phenomena. The two most important transport mechanisms for electrokinetics are electromigration and electroosmosis.

The electromigration velocity of an ion in a dilute solution is a function of the electric ionic mobility and the voltage gradient. Shapiro (1990) incorporated a tortuosity term in the general ionic transport equation to account for the non-linear path an ion must travel in a soil. Equation 2.1 is a general equation for electromigration velocity which includes tortuosity:

$$v_{em} = \frac{\mu}{\tau^2} \frac{dV}{dx} \tag{2.1}$$

where

v_{em} = electromigration velocity (m s^{-1})
μ = electric ionic mobility (m^2 V^{-1} s^{-1})
τ = tortuosity (unitless)
dV/dx = voltage gradient (V m^{-1})

Following a similar argument for electroosmosis to account for the tortuosity of the soil pore, the Helmholtz-Smoluchowski equation (Hunter, 1981) describing the transport of water in an electric field can be extended to a porous media:

$$v_{eo} = \frac{\varepsilon \zeta}{\nu \tau^2} \frac{dV}{dx} \tag{2.2}$$

where

v_{eo} = electroosmosis velocity (m s^{-1})
ε = fluid permittivity (C V^{-1} m^{-1} = N V^{-2})
ζ = zeta potential (V)
ν = fluid viscosity (Pa * s = (N m^{-2}) * s)

The zeta potential is the voltage potential at the surface of shear (Hunter, 1981), an imaginary surface which is considered to lie close to the solid particle surface. Between these two surfaces, the fluid is considered stationary in relation to the particle; therefore, the fluid would migrate with the particle. In an experimental apparatus in which a particle is undergoing electrophoresis, a surface of shear forms around the particle while it is moving. One can calculate the average voltage potential in the surface of shear (zeta potential) by measuring the particle's velocity and the applied voltage gradient using Equation 2.2. In an analogous situation where the particles are stationary but the fluid is moving, the zeta potential determines the fluid flow velocity.

There appears to be confusion in some of the early EK remediation literature which implies that all contaminants were transported by electroosmosis while electromigration had little, if any, effect. This implication may be due to the fact that the early EK remediation research concentrated on cationic contaminants, which move in the same direction as electroosmosis. This emphasis on electroosmosis probably stems from previous civil engineering field studies to dewater clays. In general, electromigration transport is actually the dominant transport mechanism for ions. The charge of the ion determines the electromigration transport direction in an electric field, either towards the cathode if the ion is positively charged or towards the anode if the ion is negatively charged. Due to a negatively-charged zeta potential, the electroosmotic water flow is toward the cathode. Therefore, when the contaminant is anionic, electromigration of the ions is counter to the direction of the electroosmotic flux of water. For a cationic contaminant, electromigration and electroosmotic transport are in the same direction.

2.2 Transference Numbers

One way to evaluate the effectiveness of EK remediation is by normalizing the experimental results in relation to the applied electrical charge. This evaluation method is known as the transference number (Bard and Faulkner, 1980). A transference number is a dimensionless

number which describes the amount of current carried by species *i* compared to the total current. This number can be determined with either currents or conductivities. In terms of the EK experiments described in this report, the current-based transference number relates the amount of contaminant removed (in terms of electrical charge) to the amount of current applied over some period of time (i.e., the total applied charge in coulombs or amp-hours).

A discussion of how current is transported through an electrolyte fluid is necessary before examining the current-based transference number. As mentioned earlier, positive ions migrate in the direction of the negative electrode, and negative ions migrate in the direction of the positive electrode. The flux of an ion can be defined as the moles of that ion per unit time crossing a plane (or per unit area) as follows:

$$J_i = C_i v_{em_i} A \tag{2.3}$$

where

J_i = flux of ion *i* across a plane (mol s^{-1} m^{-2})
C_i = concentration of ion *i* (mol m^{-3})
A = area (m^2)

For current flowing through an ionic fluid, the flux of positive ions across a plane creates a portion of the current. In addition, the flux of the negatively-charged ions, flowing in the opposite direction to the positive ions, also results in a contribution to the current. Since the negatively charged ions have an opposite charge and flow in the opposite direction of the positive ions, the current contribution of the negative ion flux will actually be in the same direction as that resulting from the flux of the positive ions. Therefore, the total current is the sum of the positive ion flux and the negative ion flux. In mathematical terms, the current in an electrolytic solution is defined by the sum of the number of moles of ions crossing an area multiplied by the charge per mole of ions:

$$I = A\sum J_i |z_i| F \tag{2.4}$$

where

I = current (Amps = C s^{-1})
$|z_i|$ = absolute value of the charge on the ion (unitless)
F = Faraday's constant (96500 C mol^{-1})

As discussed in the previous paragraphs and as seen in Equation 2.4, the amount of current applied has a direct effect on the magnitude of the ion flux. In this work, the plane which the ions pass through is the surface of a ceramic electrode casing. Greater applied currents result in large fluxes of ions (including the contaminant ion of interest) through this ceramic casing and into the fluid to be extracted to the soil surface. Multiplying Equation 2.4 by some time interval gives the quantity of electrical charge needed to move a certain number of moles of ions as follows:

$$Q = It \tag{2.5}$$

where

Q = quantity of charge (C)
t = time (s)

The current-based transference number for chromate can be expressed as an equivalent charge of chromate removed per the total amount of applied charge as follows:

$$T_{Cr} = \frac{X_{Cr(t)}|z_{Cr}|F}{Q} \tag{2.6}$$

where

T_{Cr} = chromate transference number (unitless)
$X_{Cr(t)}$ = moles of chromate (or chromium) removed over some time interval (mol Cr)
z_{Cr} = charge of CrO_4^{2-} = -2

The denominator of Equation 2.6 represents the possible equivalent charge of chromate that could be moved across a plane by the application of "Q" coulombs of electricity. The current-based transference number will never approach 1.0 since in reality both cations and anions are migrating in solution. However, the current-based transference number is useful when examining what fraction of the applied current is transporting chromate.

A prediction of the current-based transference number can be made by looking at conductivity-based transference numbers of pretest soil water-extraction samples. Conductivity-based transference numbers are calculated by multiplying the molar conductivity of chromate in the soil water by the concentration of chromate and dividing this product by the measured electrical conductivity of the solution, as shown in Equation 2.7.

$$T_{Cr} = \frac{\Lambda_{Cr} C_{Cr}}{\sigma_w} \tag{2.7}$$

where

Λ_{Cr} = molar conductivity of chromate (S m^2 mol^{-1})
C_{Cr} = concentration of chromate (mol m^{-3})
σ_w = solution conductivity (S m^{-1})

Reference books list the molar conductivity of chromate (as well as many other contaminants) at infinite dilution, which will tend to overestimate the chromate transference number. Molar conductivity, like many other chemical properties, is dependent on the ionic strength of the fluid. The interaction between ions tends to decrease the molar conductivity as the concentration of ions increases. For solutions with ionic strengths of 0.1M or higher, decreases of 20 to 50% can be expected.

To overcome the problem of overestimating the transference number with the infinite dilution molar conductivity, a method to correct the molar conductivity for ionic strength effects

has been developed. The term ionic strength describes the number of electrical charges in solution and was introduced to express the non-ideal dissociation of electrolytes in solutions. Ionic strength can be expressed as:

$$IS = \tfrac{1}{2} \Sigma C_i z_i^2 \tag{2.8}$$

where IS = ionic strength (moles L^{-1}).

The activity coefficient of an ion, which describes the reduced reactivity as the solution concentration increases, can correct for the effects of electrostatic shielding of an ion in an electrolyte solution. Although the activity coefficient was developed to describe the interaction of ions between one another, it likely can also describe the reduced molar conductivity of an ion due to an increase in solution concentration. The Davies Equation, which relates the activity coefficient to the solution ionic strength for solutions with ionic strengths of less than 0.5, is recommended for the expected ionic strengths of soil pore water extracts.

$$\text{Log } \phi = -p\, z\, (IS^{1/2} / (1 + IS^{1/2}) - 0.3\ IS) \tag{2.9}$$

where

ϕ = activity coefficient
p = temperature dependent constant (~0.51 at 25 °C)

In soil pore water extracts, it is unlikely that the concentrations of all the ions are known, thus making it impossible to calculate of the ionic strength of the solution. To overcome this problem, the empirical relationships between ionic strength and the solution electrical conductivity are used. Both of these terms are proportional to the concentration of electrolytes in a solution and exhibit a strong linear relationship to one another. Griffin and Jurinak (1978) developed an empirical relationship between electrical conductivities of saturated paste extracts of 27 alkaline soils and 124 river waters and their ionic strengths. For solutions with an electrical conductivity between 0.64 to 32.4 (milliSeimens per centimeter), their linearly regressed fit is:

$$IS = 0.0127EC - 0.002 \tag{2.10}$$

where EC = solution electrical conductivity (mS cm^{-1}).

Therefore, by measuring the electrical conductivity of the soil water extract and applying Equation 2.10, an estimate of the extract's ionic strength can be made. This ionic strength value then can be substituted into Equation 2.9 to calculate the contaminant's activity coefficient. The activity coefficient can be multiplied by the contaminant's molar conductivity at infinite dilution to find the molar conductivity. This accounts for the contaminant's concentration dependence and provides a better estimate of the transference number as determined in Equation 2.7. If the composition of the pore-water solution does not change throughout the remediation process, the conductivity-based transference number should approximate, relatively due to the infinite dilution error, the current-based transference number values.

2.3 Extraction Efficiency

Closely related to the current-based transference number is the extraction efficiency. The extraction efficiency describes how many grams of contaminant are removed per amount of current applied over some period of time. Both the extraction efficiency and the transference number describe the removal efficiency as a function of applied charge. While the transference number is dimensionless, the extraction efficiency is sometimes preferred because it has more meaningful units. Numerically it is expressed as:

$$E_{Cr} = \frac{m_{Cr} 3600}{It} \tag{2.11}$$

where

E_{Cr} = extraction efficiency for chromate (g amp^{-1} hr^{-1})
m_{Cr} = mass of chromate expressed as total grams of chromium (g)
$I\,t$ = charge, Q (amp-sec)

The chemical analysis results are given in parts per million (ppm) of chromium; therefore, although all chromium removed is assumed to be chromate, data reduction and calculations are given in terms of chromium (in grams) rather than chromate.

The transference number for chromate calculated in Equation 2.6 can be expressed in terms of the extraction efficiency defined in Equation 2.11 by combining Equations 2.5, 2.6, 2.11, and the molecular weight of chromium.

$$T_{Cr} = \frac{E_{Cr} z_{Cr} F}{MW_{Cr} 3600} \tag{2.12}$$

where MW_{Cr} = molecular weight of chromium (52 g mol^{-1}).

The transference number is easily calculated from the extraction efficiency. Substituting the appropriate values for the molecular weight of chromium, ionic charge of chromate, and Faraday's number yields:

$$T_{Cr} = (1.03 \text{amp hr/g}) E_{Cr} \tag{2.13}$$

2.4 Energy Efficiency

A second way to evaluate the EK process is by determining the electrical work required to extract a certain amount of chromium over some time interval. Since electricity is sold by kilowatt-hours, this method of evaluation is desired by some when estimating the monetary cost of removing X grams of contaminant; however, it does not take into consideration many other cost factors. Electrical power is defined as the current multiplied by the voltage as follows:

$$P = I\,V \tag{2.14}$$

where

P = electrical power (W)
V = volts (V)

Therefore, over some period of time, energy efficiency can be calculated as:

$$E_e = \frac{m_{Cr}}{P\,t} \tag{2.15}$$

where E_e = energy efficiency of chromium removal (g Cr $kW^{-1}hr^{-1}$).

Although the evaluation of EK remediation in terms of kilowatt-hours can be useful for determining the amount of chromium removed per dollar of energy expenditure, it has a serious drawback. It is the total number of coulombs that determines the amount of contaminant removed; however, the same number of coulombs can be applied over different time spans resulting in vastly different energy expenditures.

Consider two cases, outlined in Table 2-1, where 10 coulombs of charge are necessary to remove a contaminant ion. In the first case, 1 amp is applied for 10 seconds, whereas 10 amps are applied for 1 second in the second case. Assume that the resistance in both cases is the same, constant over time, and arbitrarily set to 1. Using Ohm's law and the definitions of power and energy, the calculated watts per second is 10 for Case 1 and 100 for Case 2. Therefore, the energy cost would be ten times greater in Case 2 than in Case 1 to transmit the same amount of charge.

Table 2-1. Hypothetical Example Illustrating the Effect of the Relationship Between Number of Coulombs Applied over Two Different Time Periods on the Amount of Energy Used

	Case 1	Case 2
Number of Coulombs C (= A t)	10	10
Current I (A)	1	10
Time t (s)	10	1
Resistance R (ohms)	1	1
Calculated Volts V (= I R)	1	10
Calculated Power P (= I V)	1	100
Calculated Energy W (= P t)	10	100

Therefore, care must be taken when evaluating EK remediation in terms of energy efficiency only. The cost of electricity is only part of the total remediation expenditures. Although it would cost ten times the energy expenditure in Case 2 (as illustrated in the above example), the project would be complete in $1/10^{th}$ the time.

2.5 Soil Heating

The transport of ions due to the application of current will cause an increase in the soil temperature. The greater the rate of current application (i.e., the faster the transport of ions), the greater the rate of heat generation. Generated heat can be expressed as kilowatt-hours per cubic meter. In an adiabatic system, the amount of energy input into the system via electrical power for some period of time will be proportional to the amount of heat generated in the soil. The proportionality constant for soil is given as volumetric heat capacity.

However, soil generally is not considered to be adiabatic, and heat is dissipated from the soil by conduction. In this case, comparison of the rate of energy input (i.e., power) to the rate of heat dissipation will determine the rate of soil temperature change. Heat conduction generally takes place in the soil particles and pore water phase with little heat transfer through the air phase. Heat transport by radiation, convection, and distillation are of secondary importance (Hillel, 1980).

In soils, much of the heat transport takes place through the soil particles; however, soil pore water also plays an important role in the transport phenomena. Although the thermal conductivity of quartz is approximately twenty times higher than that of water, the overall thermal conductivity of a soil is a function of the ratio of the two phases as well as the internal geometry of the soil particles. Soil particles, as thermally conductive as they are, are not well connected to one another physically. For heat to be transferred from one soil particle to the next, it will be transferred mainly from the first particle through the soil water and then to the next particle. As a saturated sandy soil dries, the thermal conductivity basically decreases proportionally to the decrease in volumetric water content. In this case, heat is being transferred through both the solid and liquid phases, and the decrease in thermal conductivity is due chiefly to less water in the soil pores available to transmit the heat. However, as the soil dries further, the amount of water diminishes to the point where the water between the soil grains is affected, and the soil particles are not completely connected thermally. Soil thermal conductivity per volumetric water reduction will decrease as the water connecting the individual soil particles dries up.

The application of current to soil during EK remediation increases the temperature of the soil in the remediation zone. Heat generated by the application of electrical energy is dissipated by thermal conduction out of the zone of remediation. The increase in soil temperature is a function of the rate of energy applied per unit volume of soil (i.e., kilowatts per cubic meter); the volumetric heat capacity; the thermal conductivity of the soil; and the location, geometry, and type of heat sinks. Needless to say, calculating the actual soil temperature increase is not a trivial matter. However, applying more power to the soil generally results in a corresponding increase in soil temperature.

During EK remediation, the electrical currents tend to focus in more conductive areas of the remediation zone. Electrical current pathways tend to be concentrated in soil horizons that exhibit the greater electrical conductivity. These soil horizons likely have the greatest power density in the remediation zone and therefore, the greatest heat generation. As the temperature of

this soil horizon increases above that of the surrounding soil, the soil water viscosity decreases and, hence, the electrical conductivity of this soil horizon increases. As the EK process continues, this cascading effect due to the interrelationship between power density, temperature, and electrical conductivity results in certain soil horizons transmitting a disproportionately high amount of the current. The increasing soil temperature induces movement of the soil water out of the soil zone (i.e., by thermally induced flow or evaporation and vapor transport). At some point, the soil moisture content then decreases, which significantly decreases its electrical conductivity, and the current pathways are affected again.

The process of bioremediation is also affected by soil heating. Bioremediation, either actively managed or by natural attenuation, therefore could be either enhanced or inhibited by EK remediation. Most bacteria are sensitive to temperature fluctuation. Bioremediation appears most promising in soil temperatures from 0 to 25 °C. In cold climates, EK remediation could be beneficial in keeping the soil temperature in ranges that would support many of the organisms effective for bioremediation. However, soil temperatures exceeding 40 °C can severely limit many bacteria's metabolic rates (Stanier et al., 1986). In addition, soil drying due to EK heating effects would also limit bacteria activity.

Enhanced vaporization of VOCs through soil heating could be accomplished in conjunction with EK remediation. Vapor pressures of VOCs increase with increasing temperature. If an EK remediation zone contains VOCs, the increase in soil temperature results in higher VOC concentrations in the soil pores. This enhanced phase could be extracted from the EK remediation zone with soil-venting techniques, making EK and soil venting complimentary technologies. However, bacteria present in the soil would probably be killed with large temperature increases.

Limited research has been performed on the secondary effects of soil heating in conjunction with EK remediation. Some soil heating can be beneficial from the standpoint of reduced soil electrical conductivity and enhanced bioremediation. However, too much soil heating would be detrimental by focusing electrical current pathways, killing indigenous bacteria, and transporting VOC contamination out of the EK remediation zone.

3. SITE INVESTIGATION & PREPARATION

3.1 Background

The CWL was the chemical disposal site for SNL from 1962 to 1985. During this time, chemicals were separated by type and disposed of in unlined trenches. It is estimated that over 4290 gallons of chromic sulfuric acid solution were disposed of in the chromic acid pits (SNL, 1991). The chromium was disposed of in the form of hexavalent chromium, and the very low organic fraction present in the native soil suggests the chromium should stay in the hexavalent form. Such anionic hexavalent chromium adsorbs weakly to soil beneath the CWL (Persaud and Wierenga, 1982). Thus, in its present form, the chromium is mobile in the environment and has apparently migrated to a depth of at least 75 feet below the ground surface.

3.1.1 Facility Description

SNL is located southeast of Albuquerque, New Mexico, in Bernalillo County. SNL facilities are located within the boundaries of Kirtland Air Force Base (KAFB). Within SNL there are five designated technical areas. The area which contains the CWL is called Technical Area III (TA III). Figure 3-1 is a general map of the area which shows the KAFB and TA III boundaries. The CWL is approximately four miles south of the nearest drinking water supply well and at least three miles from any natural groundwater discharge point. Figure 3-2 shows the location of the UCAP at the EK site and the local CWL coordinate system (the southwest fence post is 0,0).

The climate of the region is semi-arid. Average annual precipitation is approximately 8 inches (20 centimeters). Most of the precipitation occurs as thunderstorms during late summer to early fall; there is also a limited amount of snow. Average daytime summer temperatures are around 90°F (32°C), while average daily winter temperatures are about 50°F (10°C). At the CWL, the water table is located approximately 485 feet below the land surface and does not play a role in this EK remediation demonstration.

The near surface geology at the CWL consists of alluvial fan deposits with some eolian deposits. The individual beds are not extensively laterally continuous and consist of coarse-grained material to caliche-cemented sediments. Little organic matter (0 to 0.2%) was measured in samples taken in TA III from the top 9 meters of the soil profile (Persaud and Wierenga, 1982).

Three boreholes were geologically logged during an investigation at the UCAP (IT, 1992). Samples were collected at five-foot intervals using a 2-foot, split-spoon sampler. The visual description of these logs beneath the UCAP indicates that the sediments consist of intercalated fine-to-coarse grained, well-sorted to poorly-sorted sands, gravels, and cobbles. Sediments are typically tan to brown in color and are composed of subrounded to subangular fragments of granite, limestone, and quartzite. Unsurprisingly, the clast composition is similar to outcrops found in the Sandia and Manzano Mountains. This section is generally uncemented to poorly cemented. Caliche cement and grain coatings act as the primary means of formation induration when present. Individual two-foot samples displayed homogeneous lithologic samples indicating thick-bedded stratigraphic layers.

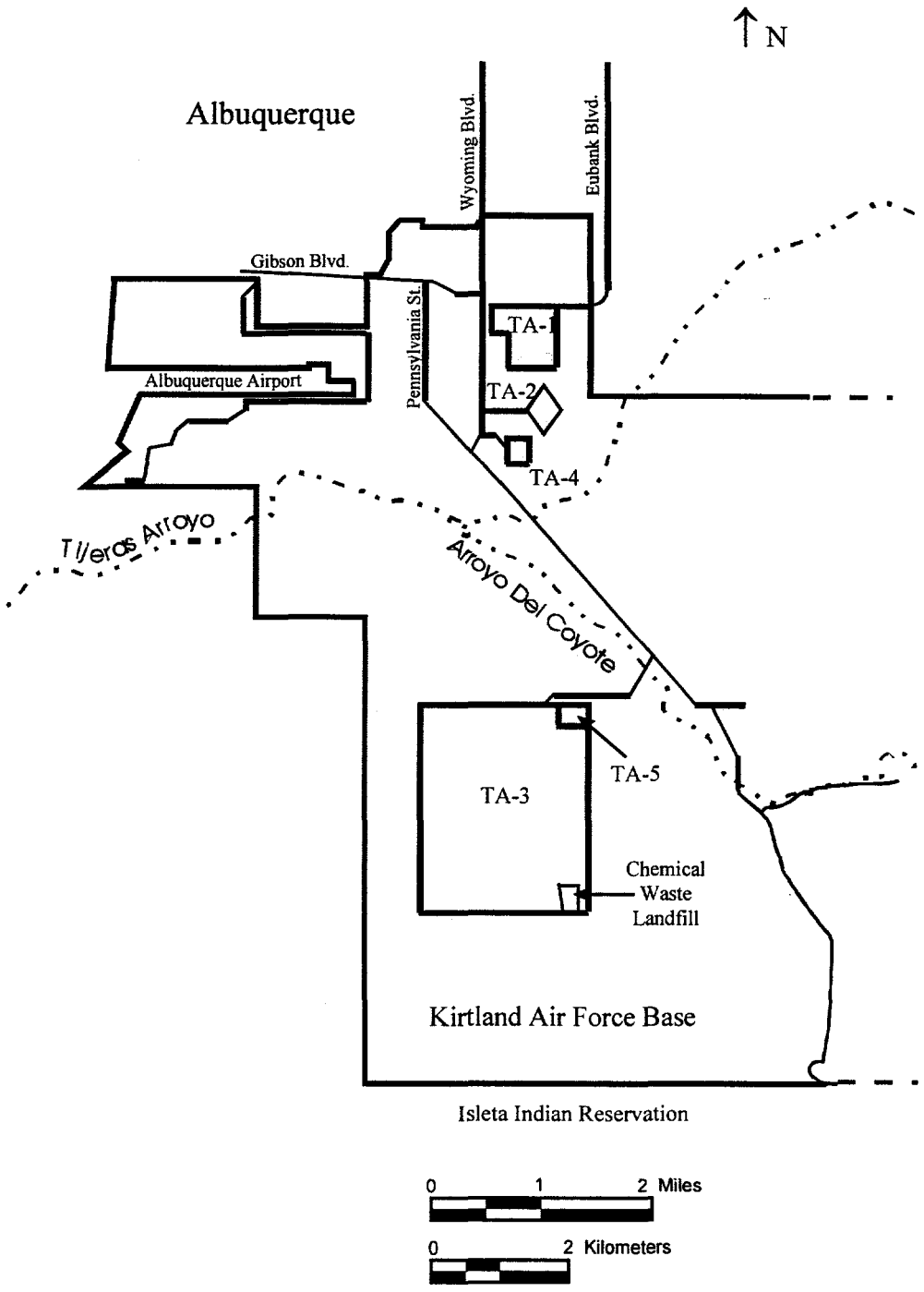

Figure 3-1. Map of Kirtland Air Force Base and the Chemical Waste Landfill.

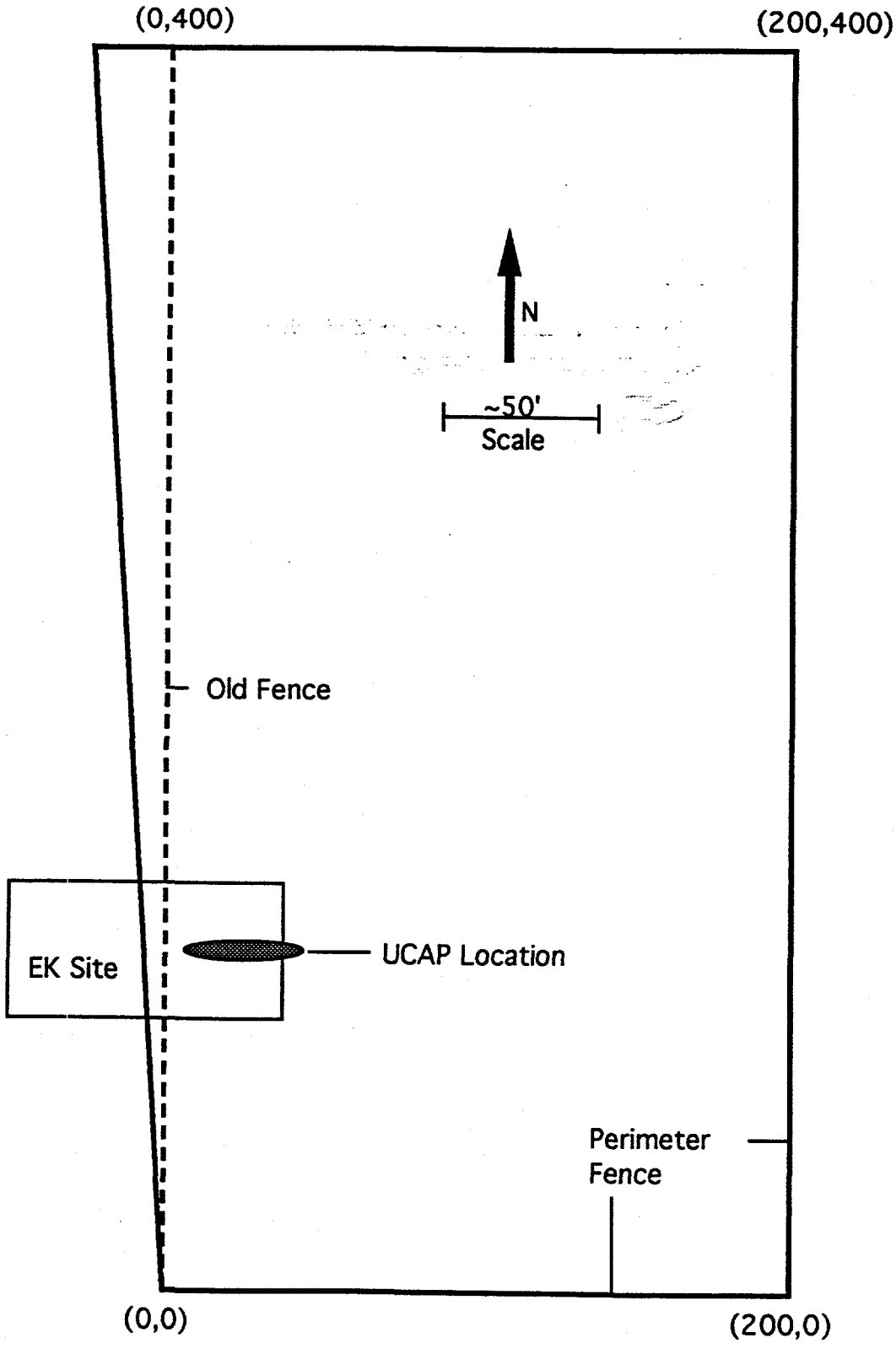

Figure 3-2. Location of the UCAP, the EK site, and the coordinate system of the CWL.

3.1.2 Waste Characterization

The chromium disposed of in the UCAP was in the form of chromic sulfuric acids. Within the pH and Eh range of soils, chromium can exist as two oxidation states: (1) Cr(III) either as a cation or as CrO_2^-, an anion, or (2) as Cr(VI) either as CrO_4^{2-} or $Cr_2O_7^{2-}$, both anions. Cr^{3+} will sorb readily to most soils. The anionic form of chromium, on the other hand, exhibits little to no adsorption to soils (Persaud and Wierenga, 1982). It is to be expected that in and immediately below the UCAP, some of the chromium was reduced to its trivalent form and sorbed to the soil. However, due to the alkaline nature of the soil and the little organic matter at depth (i.e., a few feet from the bottom of the pit), much of the chromium in the soil will be in its hexavalent form in the soil water.

Stein (1994) reported that analytical results from soil samples taken from the UCAP site indicate that Cr(VI) co-precitates primarily in a gypsum form. It was concluded that significant amounts of CrO_4^{2-} can be substituted for the SO_4^{2-} in the gypsum. Cr(VI) can also precipitate as anhydrous $CaCrO_4$, although this form was not seen in the sediments beneath the UCAP. The dissolution of this species is slow, requiring weeks to reach an equilibrium between the solid phase and the dissolved species; however, the solubility is relatively high (0.01 to 0.02 moles/L).

3.2 Further Investigations of the Site

In 1987, a series of boreholes were drilled to investigate the extent of chromium contamination from the UCAP in the southwest corner of the CWL (SNL, 1991). These holes were spatially located in a east-west orientation (Figure 3-3). Results of the chemical analyses for water-soluble chromium concentrations are shown in Figure 3-4. The chromium concentrations are highest immediately beneath the disposal pit with soil concentrations greater than 200 ppm. This zone of high contamination looked promising for the EK demonstration, but additional investigations were required to ensure the adequacy of the site.

Further investigations were conducted during the fall of 1995 and early winter of 1996 to decide the X-Y location and depth of the EK treatment zone. These investigations were designed to gain insight into the subsurface spatial distribution and form of the chromium, and the subsurface electrical conductivity of the proposed EK treatment zone. The most desirable placement for the EK treatment zone was in the area of the highest concentration of water-soluble chromium where there were no metallic objects. A geoprobe survey was conducted to collect data on the vertical profile of the soil conductivity and to collect soil samples at depth for physical and chemical analysis. A surface geophysical survey was also conducted to determine if any metallic debris was located within the proposed EK treatment zone. After a treatment zone was decided upon, EK treatment remediation and monitoring equipment was installed at the appropriate locations and depths. Additional soil samples were collected during equipment installation to further define the spatial distribution of the chromium. Finally, a radio-imaging survey was conducted through some of the neutron access tubes as another means of examining the soil conductivity throughout the EK treatment zone. All EK equipment positions and soil borings were surveyed to the local CWL X-Y coordinate system. These further investigations are described below.

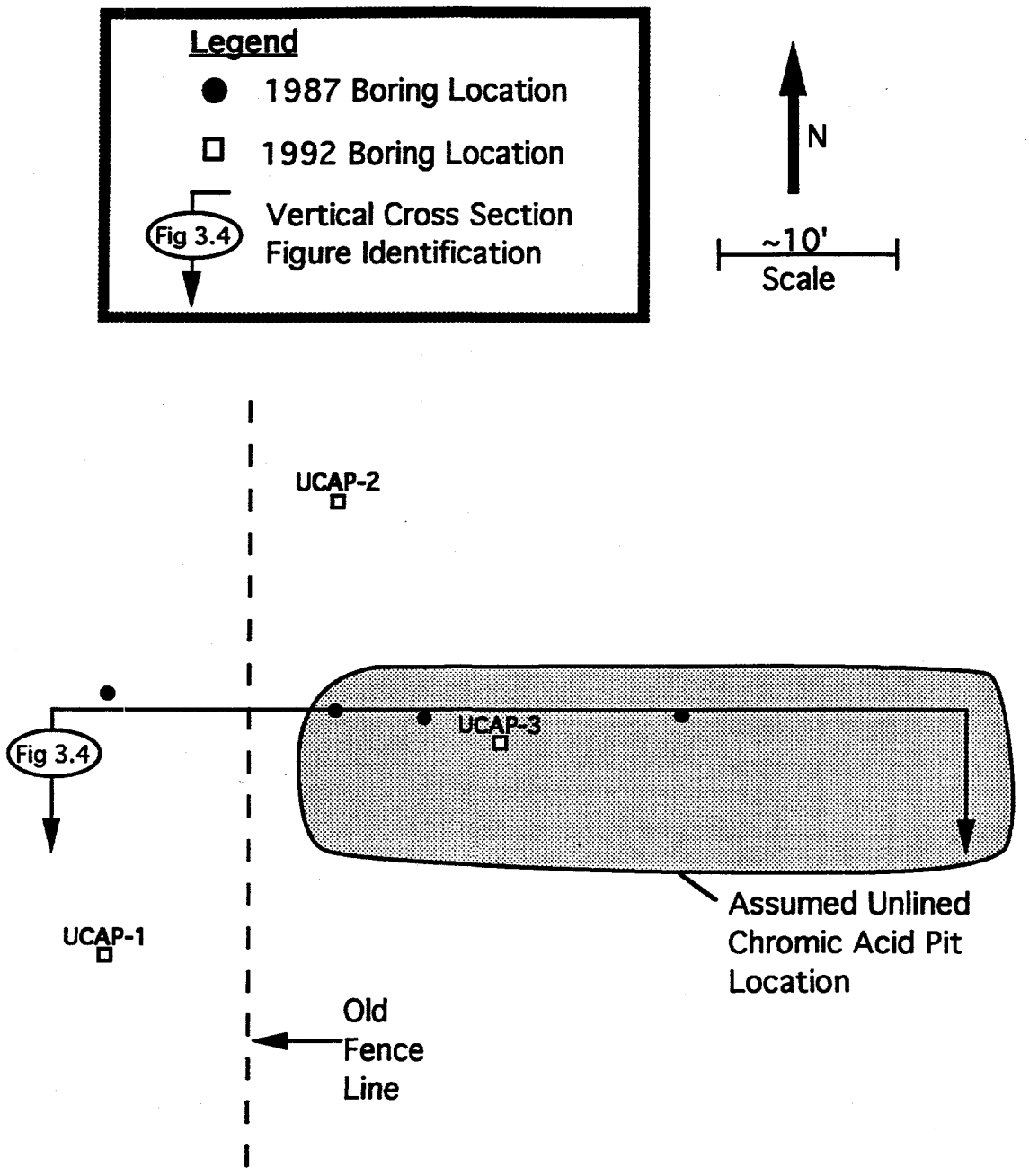

Figure 3-3. Location of 1987 and 1992 soil boreholes and approximate location of UCAP.

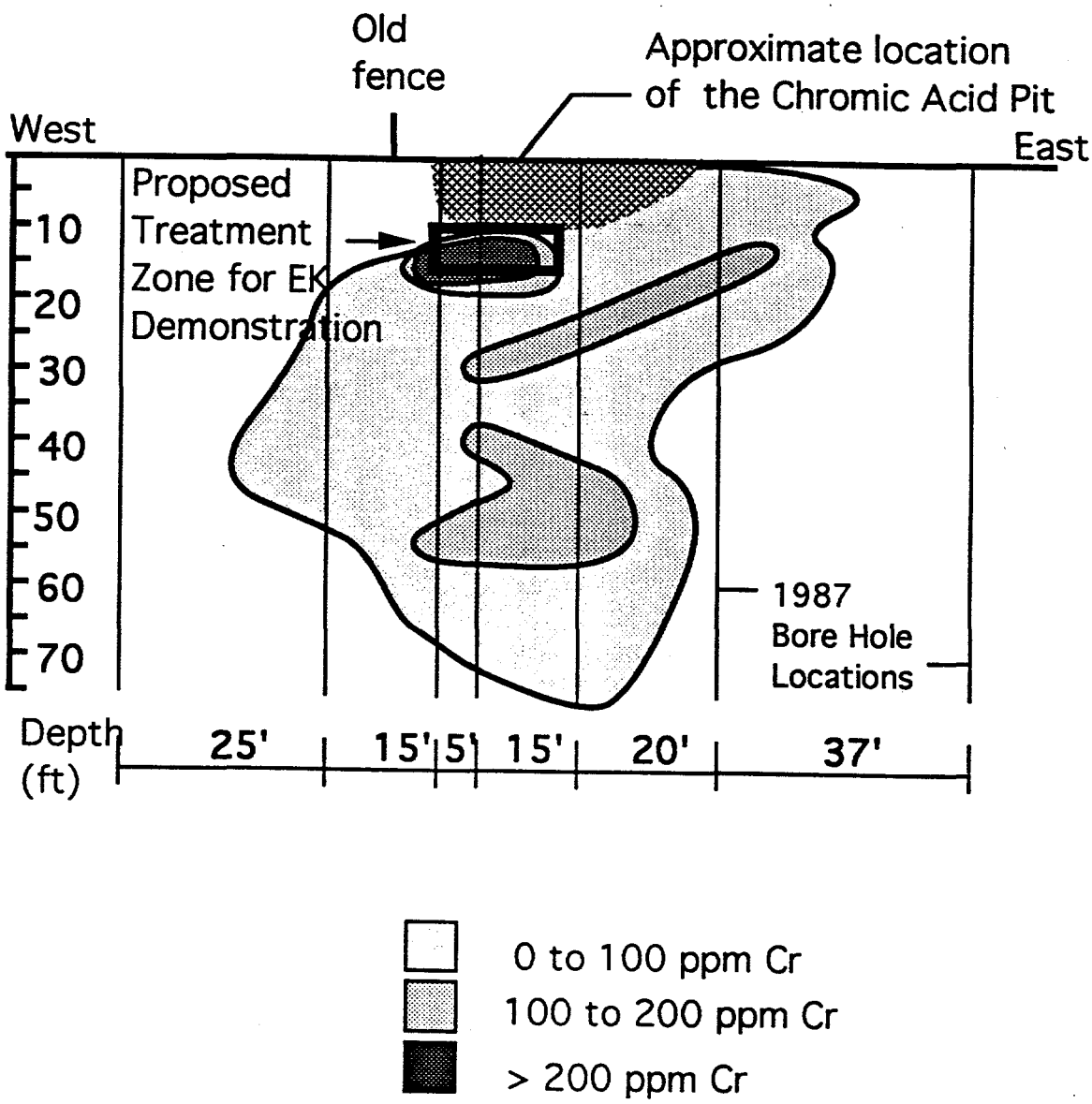

Figure 3-4. East-west cross section of water-soluble chromium concentrations from the 1987 chromic acid pit investigation.

3.2.1 Geoprobe Survey

Twenty-one pneumatically-pounded "Geoprobe®"[1] holes were made either to collect soil samples for physical and chemical analysis or to conduct soil conductivity measurements. Figure 3-5 shows the location of the 21 geoprobed holes and Table 3-1 gives the coordinates and types of geoprobe holes. Figure 3-5 also shows the subsequent electrode casing boreholes, which are given on all the maps for spatial comparisons.

3.2.1.1 Soil Conductivity Measurements

Geoprobe® soil-conductivity measurements were collected at one-foot intervals using the Geoprobe® electrical-conductivity probe pneumatically pounded into the soil by a Hurricane Sampling System™[2]. The electrical-conductivity probe consists of a slightly tapered, approximately one-foot long, one-inch diameter Geoprobe® rod tip which contains four electrically isolated stainless steel rings. Each ring is connected to a wire conductor that leads to the surface. A 150 Hz AC sine wave was applied to the two outer electrodes via a Tektronix®[3] FG 502 Function Generator. The voltage and current was measured on dual Fluke®[4] 45 meters. The ratio of the applied current at the two outer rings to the resulting voltage at the two inner rings is proportional to the electrical conductivity of the medium surrounding the stainless steel rings. The electrical conductivity probes were calibrated in a plastic, 30-gallon water bath with water of a known conductivity.

Figures 3-6 and 3-7 are the east-west and north-south electrical conductivity cross-sections. In general, the soil near the surface and at depths over 15 feet have soil conductivities of less than 10 mS/m. However, soil conductivities within the UCAP itself range to over 100 mS/m in localized areas. These zones of higher soil conductivity values are likely due to increased concentrations of mobile ions resulting from the disposal of wastes and/or from higher moisture contents.

It is generally assumed that the rocks and the soil matrix by themselves are poor conductors of electricity. Water which fills the pores is the main contributor to the conduction of current. Therefore, the amount of water, the interconnectiveness of the water, and the electrical conductivity of the water are all important contributors to the soil electrical conductivity. Archie (1942) developed an empirical formula to describe the functionality of the above parameters to that of the effective soil resistivity. Archie's formula is shown below for the effective soil conductivity (i.e., the inverse of soil resistivity):

---

[1] Geoprobe® is a registered trademark of Geoprobe Systems

[2] Hurricane Sampling System™is a trademark of Universal Environmental Engineering, Inc.

[3] Tektronix® is a registered trademark of Tektronix, Inc.

[4] Fluke® is a registered trademark of John Fluke Manufacturing Company

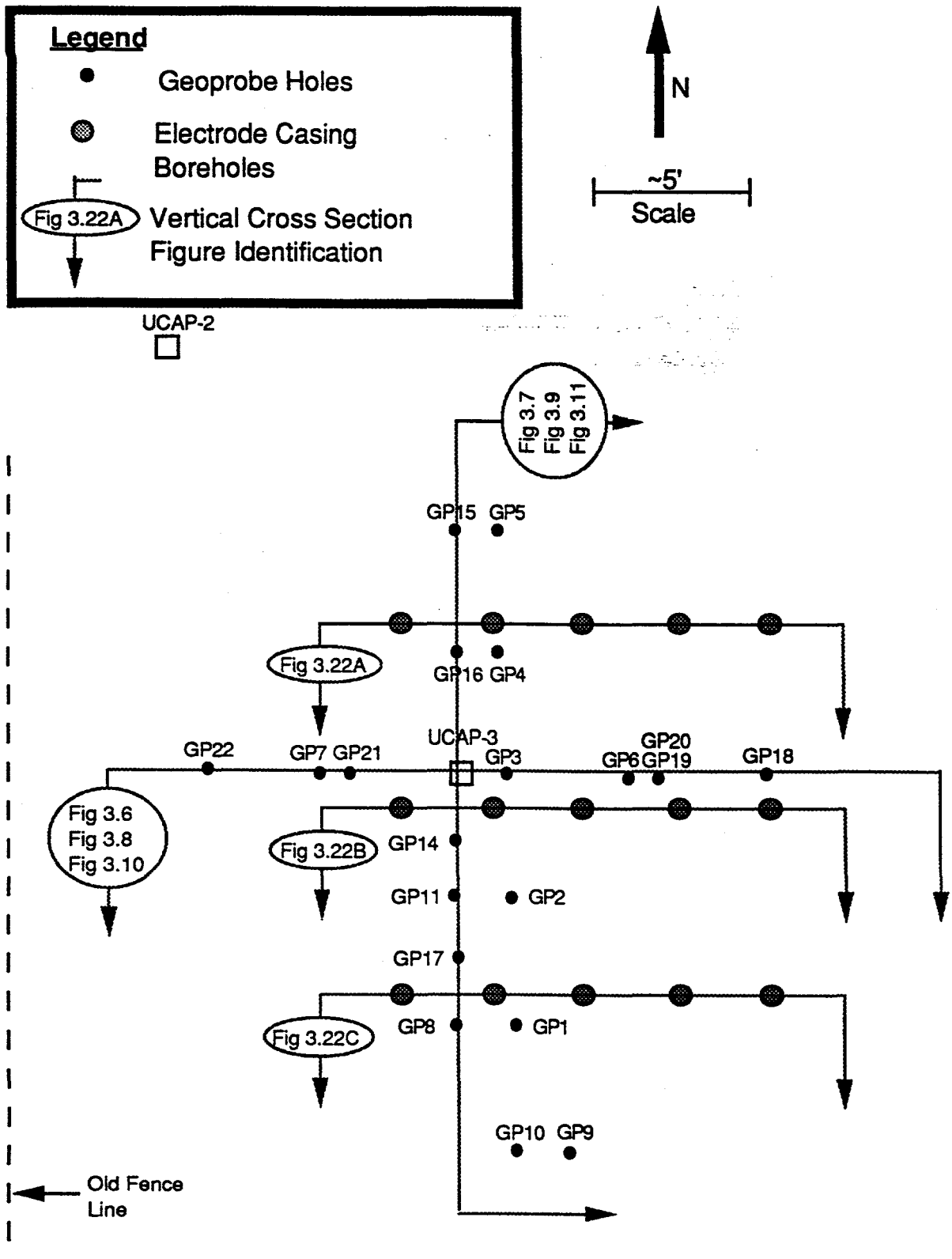

Figure 3-5. Location map of pre-EK geoprobe holes and subsequent EK electrode casings.

Table 3-1. Location and Type of Geoprobe Holes

Hole Number	X Coordinate	Y Coordinate	Max. Depth (ft BLS)	Comments
GP-01	16.5	104.0	16	Resistivity Measurements
GP-02	16.5	108.0	31	Resistivity Measurements
GP-03	16.5	112.0	12.6	Resistivity Measurements
GP-04	16.5	116.0	13.3	Resistivity Measurements
GP-05	16.5	116.0	18	Resistivity Measurements
GP-06	20.5	112.0	11	Probe Testing
GP-07	11.0	112.0	15.5	Resistivity Measurements
GP-08	15.0	104.0	22	Resistivity Measurements
GP-09	18.5	100.0	3	Resistivity Measurements
GP-10	16.5	100.0	10	Resistivity Measurements
GP-11	15.0	108.0	15	6' to 15' Soil Sampling
GP-12	45.0	112.0	19	Resistivity Measurements
GP-13	45.0	112.0	20	2' to 20' Soil Sampling
GP-14	15.0	110.0	22	16.5' to 22' Soil Sampling
GP-15	15.0	120.0	22	8' to 22' Soil Sampling
GP-16	15.0	116.0	22	8' to 22' Soil Sampling
GP-17	15.0	106.0	22	16' to 22' Soil Sampling
GP-18	25.0	112.0	14	Resistivity Measurements
GP-19	21.0	112.0	14	Resistivity Measurements
GP-20	21.0	112.5	15	6' to 14' Soil Sampling
GP-21	10.5	112.0	15	6' to 14' Soil Sampling
GP-22	7.0	112.0	13.5	Resistivity Measurements

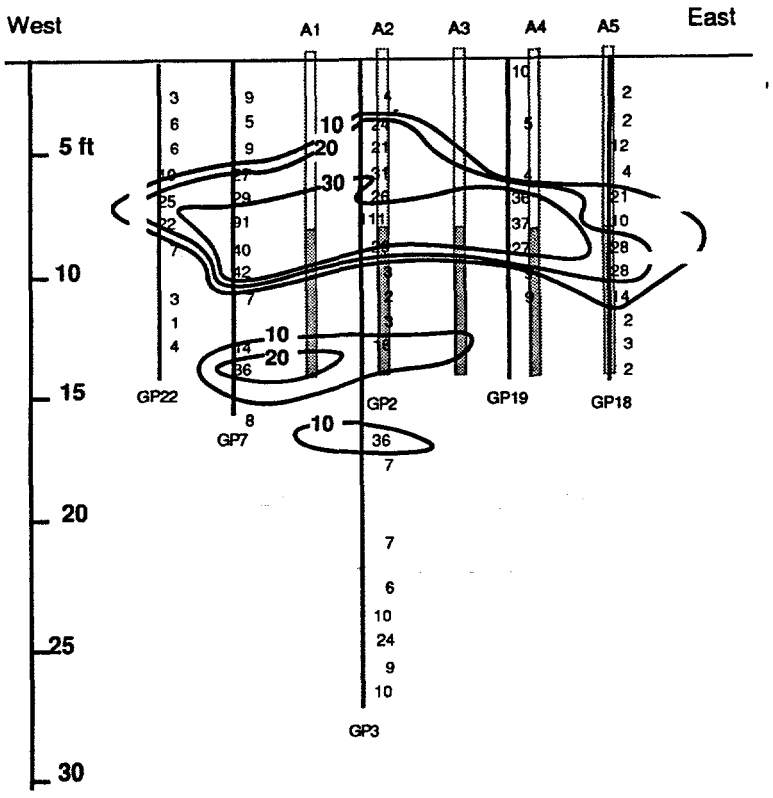

Figure 3-6. East-west cross section of soil electrical conductivity (mS/m) by the geoprobe method.

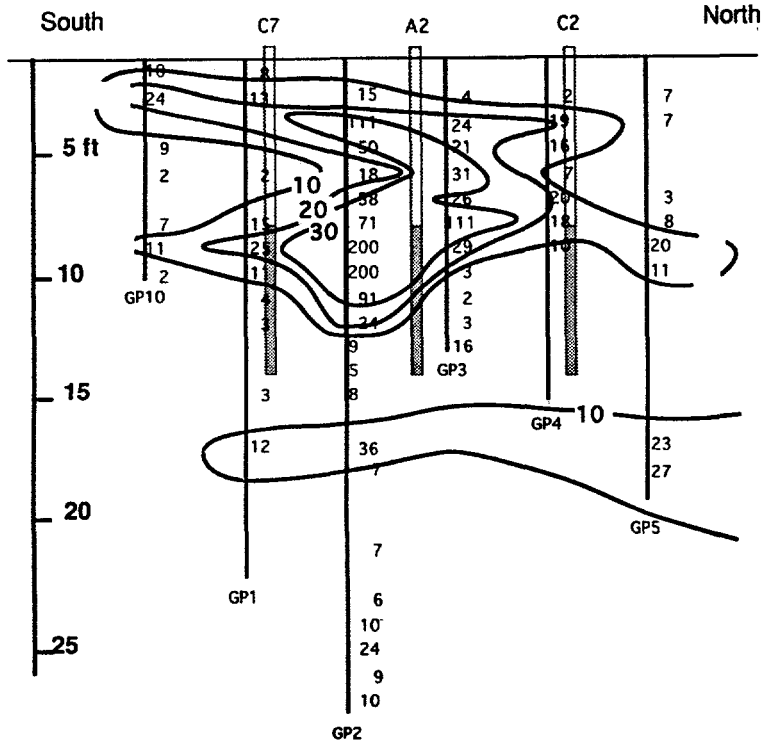

Figure 3-7. North-south cross section of soil electrical conductivity (mS/m) by the geoprobe method.

$$\sigma_e = \frac{1}{a}\phi^m S^n \sigma_{sw} \quad (3.1)$$

where

σ_e= effective soil electrical conductivity (S cm^{-1})
a, m & n = constants
φ = porosity (cm^3 cm^{-3})
S = saturation (cm^3 cm^{-3})
σ_{sw}= soil water electrical conductivity (S cm^{-1})

For rocks, values of the constants of Archie's formula are $0.5 < a < 2.5$; $1.3 < m < 2.5$; and $n \sim 2$.

Equation 3.1 illustrates the direct relationship between effective electrical conductivity of the soil and that of the water contained in the soil pores. The chromic sulfuric acid solutions disposed of in the UCAP likely exhibit solution electrical conductivities much higher than natural water in chemical equilibrium with the soil. In soils where the chromate solutions have displaced the native water, the soil should exhibit much higher electrical conductivities than those in non-perturbed areas. This would allow the electrical conductivity profiles shown in Figures 3-6 and 3-7 to be used as a tool to estimate the zone of chromic acid infiltration.

In addition to the dependence of soil electrical conductivity on porewater conductivity, Equation 3.1 also shows a strong dependence of the effective electrical conductivity on the moisture content. For example, if constants m and n are both equal to 2, Equation 3.1 can be reduced to

$$\sigma_e = \frac{1}{a}\theta^2 \sigma_w \quad (3.2)$$

where

θ =volumetric moisture content (cm^3 cm^{-3})

In this case, the soil electrical conductivity is proportional to the square of the volumetric moisture content. A doubling of the moisture content quadruples the soil electrical conductivity. This doubling is due not only to supplying twice the number of ions but also to providing better connectivity between the water contained in the soil pores. In the scenario described above where the chromic acid solution displaces native soil water, it is likely that the moisture content will also be higher, resulting in higher electrical conductivity. Both of these factors, higher solution conductivity and higher moisture contents, would support the use of electrical conductivity to define zones of contamination.

3.2.1.2 Soil Samples for Physical and Chemical Analysis

Soil samples were collected via the Hurricane Sampling System® using the Geoprobe® large-bore samplers. The large-bore sampler is approximately 24 inches long and has an inside diameter (ID) of 1 inch. Each sample was contained in a plastic sleeve housed in the sampler. The sampler has a front point which is stationary while driving the sampler to the sampling depth

and then is allowed to slide up a plastic sleeve while the soil sample is being taken. This retractable point system allows no borehole sluff into the sampler. A number of samples were taken consecutively in the geoprobed holes using this method. The large-bore sampler was decontaminated between samples by a scrub wash with Alconox™[5] solution followed by a clean-water rinse and then allowed to air dry prior to reassembly. A new plastic liner was used for each soil sample.

Soil samples were stirred to achieve some homogeneity, then split into two fractions. The first fraction of soil was oven dried for gravimetric soil moisture content as per ASTM standard 2216. An approximately one-hundred-gram sample was then placed in a pre-weighed aluminum drying pan, weighed with the soil, and placed in an oven at 100 °C for a 24-hour period. The dry soil and drying pan were weighed again, and the percent moisture by weight was calculated. Figures 3-8 and 3-9 show the north-south and east-west moisture content cross sections. These figures illustrate that the background soil moistures are in the 2 to 4 wt% range. There is a zone of higher moisture content within the assumed disposal pit between 7 and 12 feet below land surface (BLS). The 25% moisture content by weight at approximately 9 feet BLS is anomalously high and is likely due to breaking a solution bottle in the disposal pit during geoprobe sampling.

As discussed in Section 3.2.1.1, there should be a correlation between higher moisture contents and higher electrical conductivity. Figures 3-8 and 3-9 also illustrate the electrical conductivity contours shown in Figures 3-6 and 3-7 in light gray shading. Moistures greater than 5% appear to correspond well with electrical conductivities greater than 10 mS/m.

An x-ray fluorescence (XRF) determination for total chromium was run on a portion of the oven-dried soil. The XRF procedure can be used as a quick field-screening method for determining total chromium concentrations. Although much of the total chromium will be irreversibly bound to the soil and cannot be removed from the soil without significantly reducing the soil pH, the method can locate quickly the areas of highest concentrations within the site. Appendix A.1 gives the XRF results.

The second portion of the geoprobe soil sample was used for an in-house, water-extraction (Method A, Appendix A.1) to determine the amount of water-soluble chromium in the soil. The procedure used a 2-to-1 ratio by weight of deionized water to soil to make a liquid slurry. The slurry was shaken for approximately 5 minutes; then the eluent was filtered through a 0.45 micron filter for analysis by ion chromatography for chromate concentrations. Conductivity and pH of the extracts were also measured (Table A-1, Appendix A.1).

Figures 3-10 and 3-11 illustrate the water-soluble chromium contour-profile concentrations in east-west and north-south orientations. These figures also show the electrical conductivity profiles of Figures 3-6 and 3-7 as light gray shaded contours. There is a general positive correlation between the chromium concentrations and the electrical conductivity measurements. Chromium concentrations over 1000 are suspected to be the byproduct of bottle breakage in the disposal pit during sampling.

[5] Alconox™ is a trademark of Alconox, Inc.

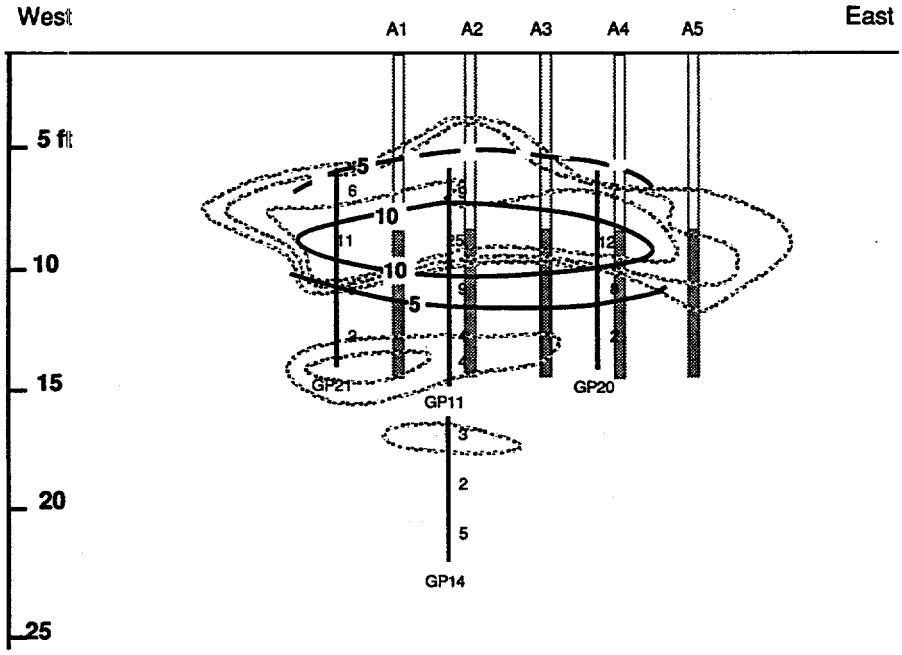

Figure 3-8. East-west cross section of moisture content (W%).
(Electrical conductivity contours are shown in gray.)

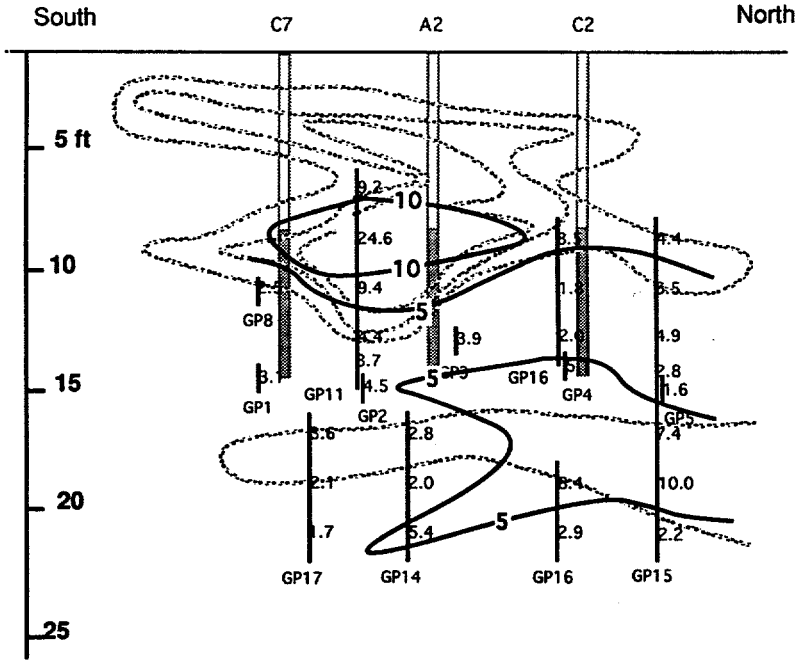

Figure 3-9. North-south cross section of moisture content (W%).
(Electrical conductivity contours are shown in gray.)

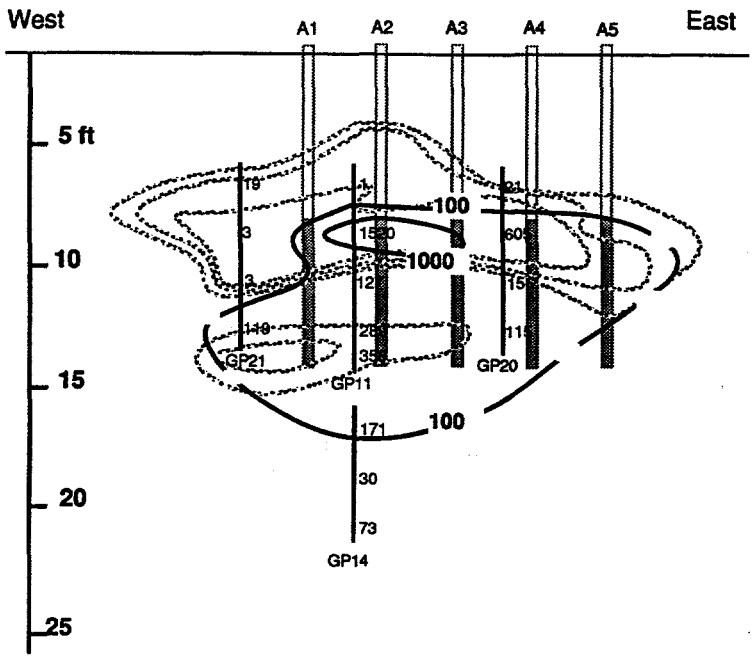

Figure 3-10. East-west cross section of water soluble Cr (ppm by weight). (Electrical conductivity contours are shown in gray.)

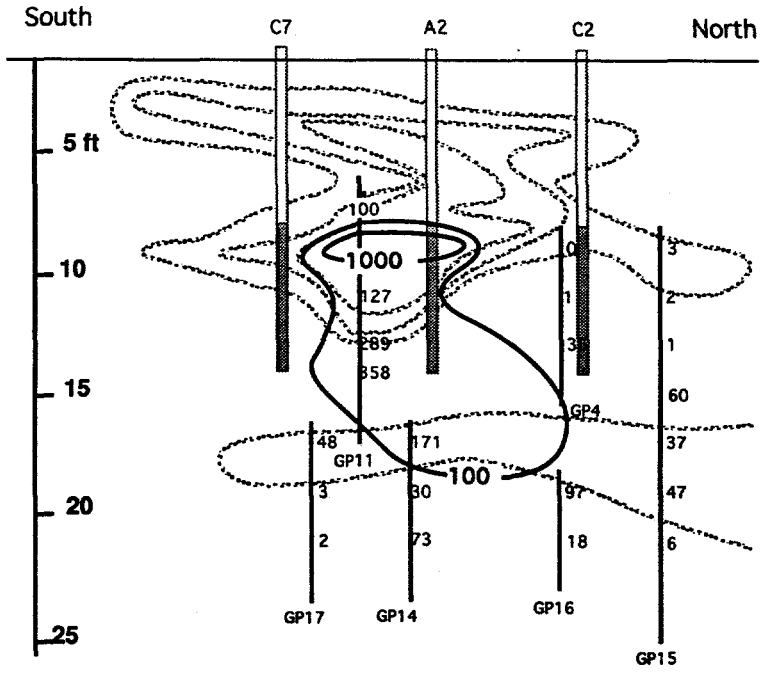

Figure 3-11. North-south cross section of water soluble Cr (ppm by weight). (Electrical conductivity contours are shown in gray along with electrode locations.)

3.2.2 Surface Geophysics Survey

A high density, surface geophysical survey was conducted over the UCAP site by Sunbelt Geophysics (Hyndman, 1995) to determine if any significant buried metal was located within the UCAP pit. The survey consisted of a magnetometer survey, an electromagnetic metal detection survey, and an electromagnetic ground conductivity survey.

The survey grid was established over a 66 ft (E-W) by 54 ft (N-S) area (the southwest corner had coordinates of -16, 95) which included the UCAP pit (Figure 3-12). The grid consisted of parallel north-south traverses separated by 1.5 ft spacing.

The magnetic survey was conducted with a GeoMetric®[6] G-858 cesium vapor magnetometer. Data was collected every 1.25 ft along the north-south traverses. Magnetic surveys are designed to measure anomalies in the earth's magnetic field generated by ferromagnetic objects. Large and shallow ferrous objects generate large anomalies. Smaller and deeper ferrous objects generate smaller anomalies. No metallic objects were detected in the area of interest; however, there were indications of buried metallic objects in the pit to the north of the EK demonstration area.

The electromagnetic metal detection survey was conducted with a Geonics®[7] EM-61 high-precision, metal locator. Data was collected on the transect every 0.67 ft. The EM-61 is a time-domain electromagnetic instrument specifically designed for mapping buried conductive (does not have to be magnetic) metal to an approximate depth of 10 ft. A transmitter coil generates a magnetic field that penetrates the soil, inducing eddy currents in the subsurface. These eddy currents dissipate rapidly in soil but persist in buried metal objects. The long-lived eddy currents induce a signal in the receiver coils, which integrate over the late portion of the time gate between transmissions.

The electromagnetic survey indicated metallic debris immediately to the north and northeast of the proposed EK demonstration. A response was also noted to the east of the EK demonstration, indicating a vertical rod may be present, but it is well outside the influence of the EK demonstration. The magnetic survey results mirror the results of the electromagnetic survey, indicating that the buried metallic objects in the pit to the north of the EK demonstration are iron or steel.

For the last survey, a Geonics® EM-31 meter acquired data every two feet along the north-south transects of the electromagnetic ground conductivity. The EM-31 provides average ground conductivity measurements in mS/m to a depth of approximately 18 ft. The EM-31 also provides an in-phase response that is very sensitive to metal objects and provides a useful quality-control indicator for determining where the borehole/geoprobe conductivity measurements are valid. A well-tuned instrument will have an in-phase response of +/- 1 parts per thousand. When metal is near by, whether at the surface or buried in the ground, the in-phase response will be several parts per thousand.

---

[6] GeoMetric® is a registered trademark of GeoMetrics, Inc.

[7] Geonics® is a registered trademark of Geonics Ltd.

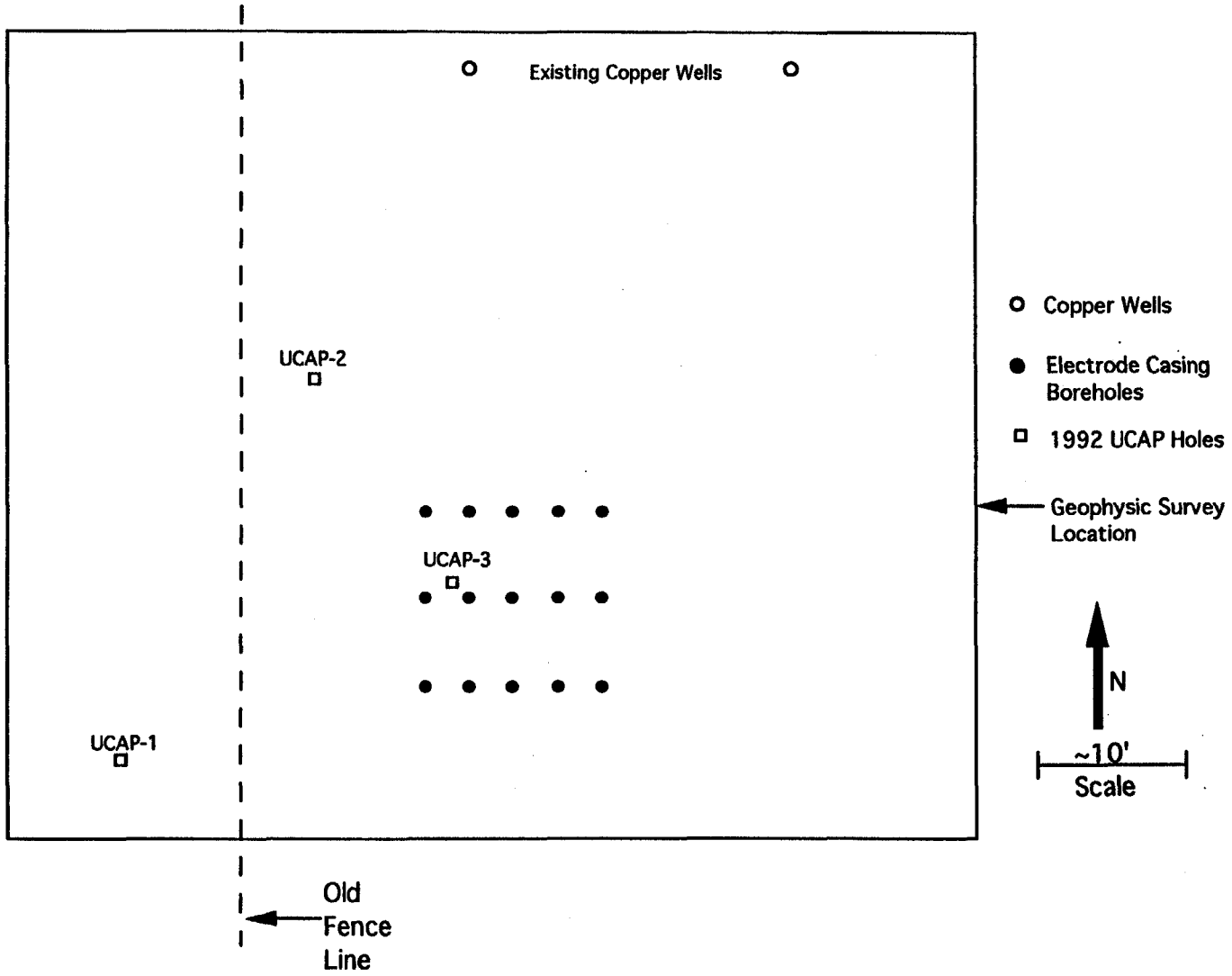

Figure 3-12. Geophysical survey location map.
(Shaded area was surveyed.)

The electromagnetic ground conductivity survey results indicate that much of the survey area was out of phase due to the buried metallic debris and other surface metallic objects. The EM-31 phase contours illustrate that most of the region was greater than 1 unit. Fortunately, a small area located over the proposed EK demonstration area exhibited an in-phase response within 1 unit and showed a ground conductivity in the range of 23 to 30 mS/m.

3.2.3 EK Demonstration Site Selection

Drilling and sampling activities associated with the EK demonstration indicated that there are basically four major geologic profiles within the upper 40 feet beneath the disposal pit. The first 15 feet consist of fine- to medium-grained sands with a few pebbles in the 0.125- to 0.25-inch range. A caliche layer approximately 1 ft thick was noted at 5 ft BLS outside the UCAP area. At 15 ft an approximately 1-ft thick cobble layer was encountered, causing problems with drilling and sampling. Beneath this cobble layer to a depth of 22 ft, the soil is fairly homogenous and consists of medium- to fine-grained sands with many 0.125- to 0.25-inch pebbles. Below 22 ft, the lithology is fine- to medium-grained sand with a few 0.25- to 0.375-inch pebbles.

In general, the surface geophysical survey and the depth-profiling soil-conductivity survey did not reveal any large buried metallic debris within the proposed EK demonstration site. However, small individual metallic items could be present and not be detected by either survey method.

The soil conductivities determined by the surface geophysics and those measured by the Geoprobe® depth profile survey generally agree. The EM-31 measured a weighted average conductivity in which 80% of the response was derived from the upper 18 ft. The greatest response was located at approximately 12 to 15 ft BLS. The geoprobe depth profile survey (Figures 3-6 and 3-7) show that values in this location are in the range of those measured by the EM-31.

In addition to water-soluble chromium concentration profiles and soil conductivity contour intervals shown in Figures 3-10 and 3-11, the chosen locations for placement of the EK anode and cathode casings are shown in light gray shading. The EK electrodes were placed in locations of highest water-soluble chromium concentrations. The zone between the southern row of cathodes and the anode row exhibited higher water-soluble chromium concentrations than the zone between the northern cathodes and the anodes (see Figure 3-10). The active portion of these casings (i.e., where electricity can be transmitted) were in the 8- to 14-ft interval. This treatment zone was bisected by a zone of soil exhibiting electrical conductivities greater than 10 mS/cm above approximately 11 ft BLS, underlain by soil exhibiting electrical conductivities less than 10 mS/cm. This configuration would imply that most of the applied current for the EK remediation would flow through the soil of high conductivity zones (e.g., at the upper portion of the electrodes). (Section 3.2.4.3 describes measures taken to even out the moisture content by injecting water into the soil.) Therefore, the EK site as described was chosen and given an EK coordinate system where the center electrode corresponds to (19,111) on the local CWL coordinates given in Section 3.1.1 where the southwest fence post was (0,0).

Figure 3-13 shows the locations of the fifteen electrodes that are pictured on subsequent maps for spatial comparisons. The electrodes were placed in three rows of five electrodes each. The electrodes were spaced at approximately 3 foot increments within a row, and the rows were spaced approximately 6 feet apart. The five anodes (A1 to A5) were placed in the center row, allowing for a variety of possible electrode configurations.

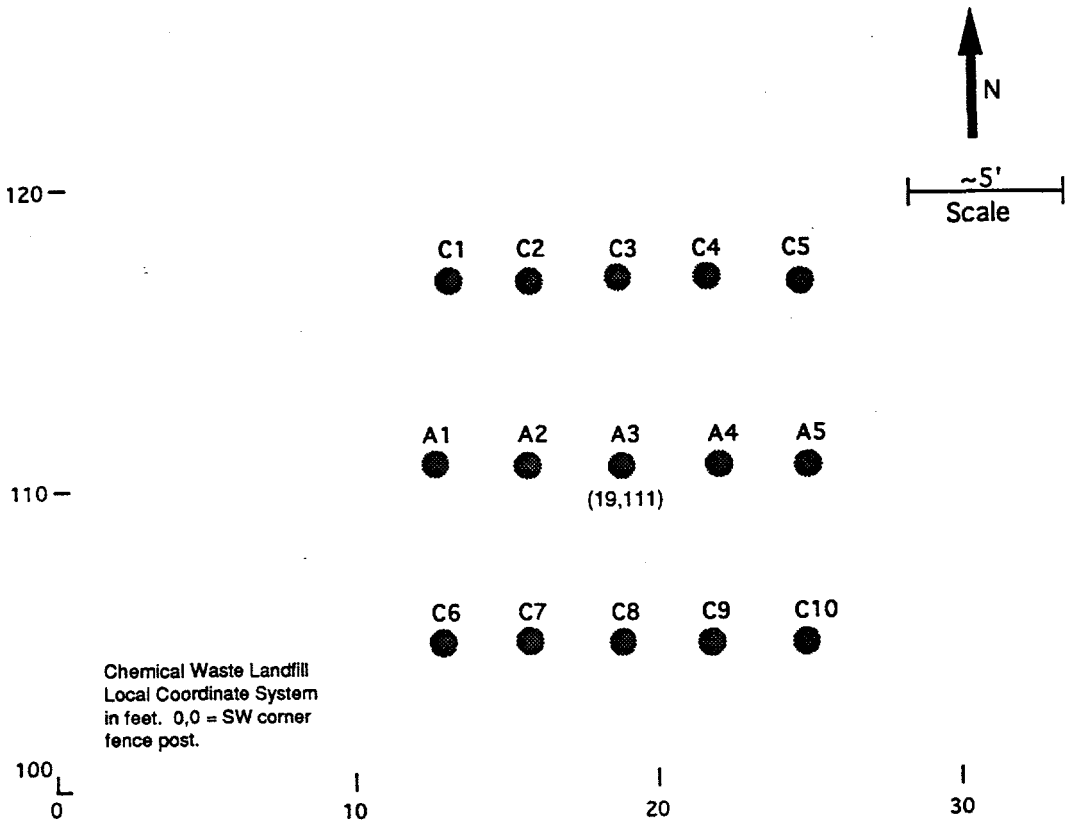

Figure 3-13. Electrode positions.

3.2.4 EK Equipment Installation

Once the site was selected, a number of holes had to be drilled and punched in and around the UCAP to install the EK remediation and monitoring equipment. This equipment placement with the collection of additional soil samples to further assess the initial site conditions is described below. Further descriptions of the equipment, the electrodes in particular, can be found in Section 4.

3.2.4.1 Electrodes

Based on the results of the geoprobe and geophysics surveys, fifteen EK casings were installed at the EK demonstration site as shown on the various previous figures. Each casing was installed in a 6-inch borehole made with the Hurricane Sampling System® rig using hollow-stem augers. For further site characterization, boreholes were initially drilled to 5 ft, and then 2-ft consecutive samples were taken in the same manner as the geoprobed holes described in Section 3.2.1.2. Results of analyses of these pretest soil samples are discussed in Section 6.2 and Appendix A. All boreholes then were drilled to 20 ft except electrode C3, which was drilled to only 16 feet due to auger refusal. Table 3-2 lists the location and type of EK electrode casings (Coors®[8]) installed. Normally the boreholes stayed open to approximately 16 to 17 ft BLS after auger removal. A dry bentonite plug approximately 3 inches in height was installed on top of the borehole sluff, and borehole cuttings were added to bring the borehole depths up to 15 ft BLS (Figure 3-14 [C]). Another layer of dry bentonite powder was added to seal the bottom of the boreholes. The electrode casings were lowered into the borehole so that the ceramic portion of the casing was between 8 and 14 ft BLS and suspended at the surface. Next a slurry of clean surface soil, with the greater than #10 mesh soil fraction removed, was made with drinking water to a consistency of pancake batter. This slurry mix was poured into the boreholes until the top of the slurry was at least 6 inches above the top of the electrode ceramic. The function of the soil slurry was to ensure good hydraulic and electrical contact between the electrode ceramic and the subsurface soil similar to the function of a slurry when installing a tensiometer cup. The remainder of the holes were filled with native soil cuttings to 1 ft of the surface. Final bentonite caps were placed and covered with approximately 2 inches of native soil. A vacuum was applied to each electrode for approximately a week to remove excess water from the soil slurry mixture.

Table 3-2. Location and Type of Electrode Casings

Electrode	X Coordinate	Y Coordinate	Max. Depth (ft BLS)	Comments ("C" indicates cathode; "A", anode)
C1	13.3	117.1	15	Coors type PC-6 ceramic
C2	16.0	117.1	15	Coors type PC-6 ceramic
C3	19.0	117.3	15	Coors type PC-6 ceramic
C4	22.0	117.3	15	Coors type PC-6 ceramic
C5	25.1	117.1	15	Coors type PC-6 ceramic
A1	12.8	111.0	15	Coors type PC-3 ceramic, treated
A2	15.8	111.0	15	Coors type PC-3 ceramic, treated
A3	19.0	111.0	15	Coors type PC-3 ceramic, treated
A4	22.4	111.0	15	Coors type PC-3 ceramic, treated
A5	25.3	111.0	15	Coors type PC-3 ceramic, treated
C6	13.0	105.0	15	Coors type PC-3 ceramic
C7	15.9	105.0	15	Coors type PC-3 ceramic
C8	19.0	105.0	15	Coors type PC-3 ceramic
C9	22.0	105.0	15	Coors type PC-3 ceramic
C10	25.8	105.0	15	Coors type PC-3 ceramic

[8] Coors® is a registered trademark of Coors Ceramic

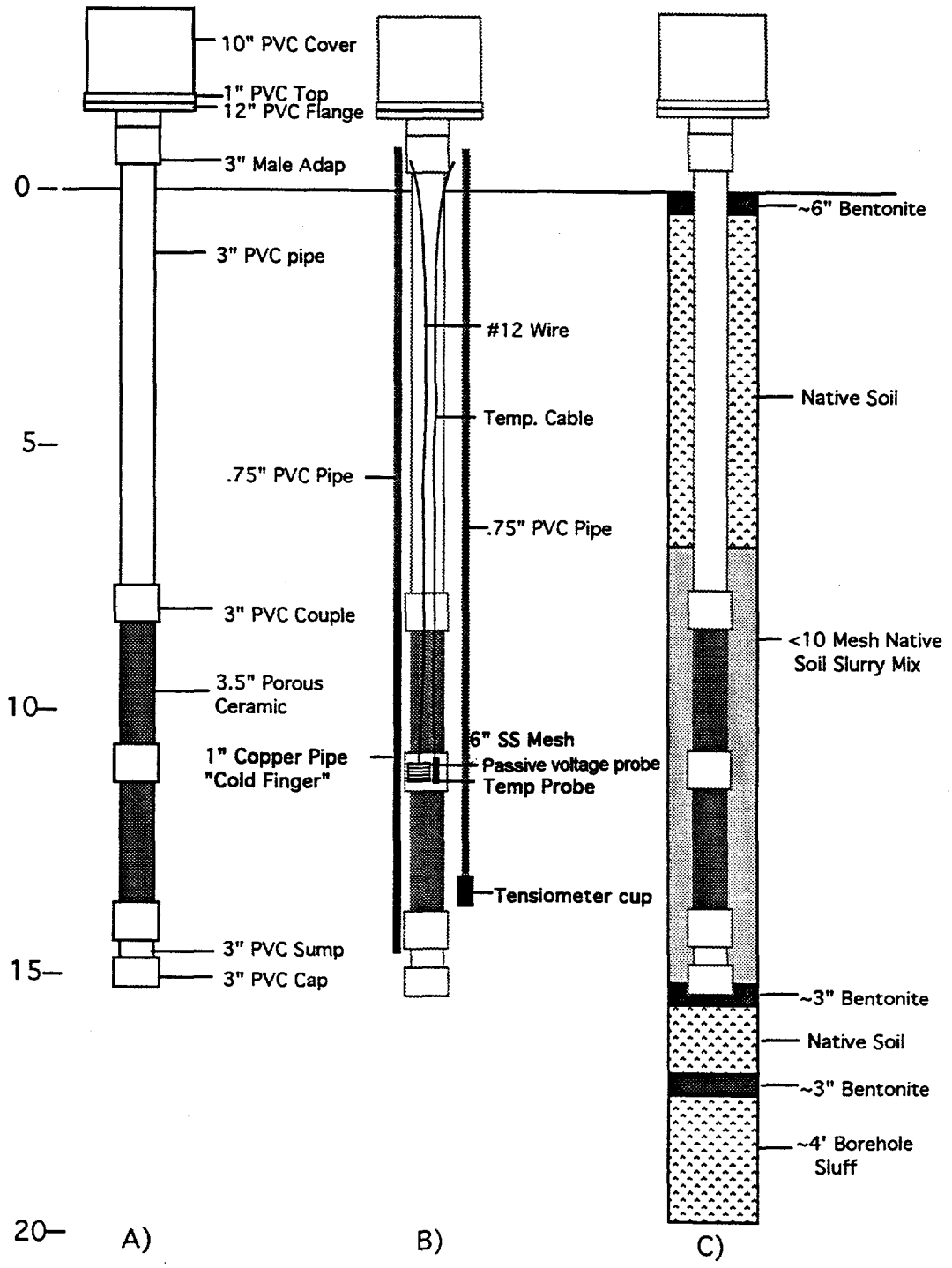

Figure 3-14. Electrokinetic electrode construction cross section: (A) casing, (B) associated monitoring equipment, and (C) borehole backfill.

3.2.4.2 Neutron Access Tubes

Neutron access tubes were installed in ten locations to allow for moisture measurements with the CPN® 503 DR Neutron HYDROPROBE®[9] (Figure 3-15). For further site characterization, boreholes were sampled every two feet with a two-inch ID split spoon as they were drilled (see Appendix A for sample analyses results). The neutron access tubes were installed in boreholes drilled using 7-inch, hollow-stem augers. The access tubes were lowered through the hollow-stem auger, and then the auger flights were removed leaving the access tube in place. The remainder of the holes were filled with drill cuttings, and dry bentonite caps were placed at the surface. The access tubes were made of 2.5-inch, threaded, schedule 40 polyvinlychloride (PVC) pipes. The PVC has the advantage of being an electrically nonconducting material; however, PVC is a hydrogen-based compound which reduces the sensitivity of the neutron probe. The 2.5-inch diameter is slightly larger than that normally used for neutron access tubes and was chosen to accommodate the use of radio imaging probes from New Mexico State University (see Section 3.2.5). Table 3-3 lists the location and depths of the 10 neutron access tubes.

3.2.4.3 Vadose Zone Infiltration Wells

To increase the moisture content (and electrical conductivity) in the lower portion of the remediation area so that it would be similar to that in the upper area , a series of 40 infiltration wells were installed between the electrode casings as shown in Figure 3-16. These wells were installed in geoprobed holes using the 1.5-inch pre-probe. The geoprobed boreholes were pushed to a depth of approximately 11 to 13 feet. After the pre-probe was extracted, 0.5-inch, schedule 40 PVC pipes with about 20 approximately 1/8-inch wide slots in the lower 1-ft section of the pipes were lowered into the borehole. Enough 10/20 silica sand was added as a gravel pack to cover the slotted intervals. The remainder of the holes were filled with dry granular bentonite. Table 3-3 lists the location and completion depths of the vadose zone wells.

Each well was capped with a slip elbow that contained two, 0.25-inch polyethylene (PE) tubes sealed in a slip PVC plug. The first PE tube was used to inject water into the well and extended from an infiltration well board, located approximately 20 feet from the electrode casings, to near the bottom of the PVC infiltration well. The second PE tube was used to determine if an infiltration well was full. This tube started approximately 6 inches below the top of the infiltration well and ended at the infiltration well board. All of the wells and associated tubing were underground, except at the infiltration well board, to facilitate uninhibited movement about the demonstration site.

[9] CPN® 503 DR Neutron HYDROPROBE® is a registered trademark of CPN Corporation

Table 3-3. Location and Depth of Installed Equipment

Equipment Number	X Coordinate	Y Coordinate	Max. Depth (ft BLS)	Equipment Number	X Coordinate	Y Coordinate	Max. Depth (ft BLS)
Neutron Tube				**Tensiometer Holes**			
NT1	14.7	118.8	41	TS1	18.8	119.8	13
NT2	24.0	119.2	41	TS2	19.0	115.7	13
NT3	20.0	114.8	41	TS3	14.6	114.3	13
NT4[1]	15.0	112.0	39	TS4	23.6	114.0	13
NT5	7.0	111.7	41	TS5	19.0	112.7	12
NT6	28.5	111.6	41	TS6	19.0	109.5	13
NT7	23.0	110.3	41	TS7	14.6	107.6	13
NT8	18.0	107.8	31	TS8	23.5	108.2	10.3
NT9	13.9	103.1	41	TS9	19.3	106.3	13
NT10	24.0	104.1	40	TS10	19.0	102.6	12
Vadose Zone Wells				**Temperature Probe**			
I1	14.5	117.0	11.4	T1	18.8	119.8	11
I2	17.5	117.0	10.5	T2	19.0	115.7	11
I3	20.5	117.0	11.0	T3	14.6	114.3	11
I4	23.5	117.0	10.0	T4	20.0	114.6	6
I5	13.0	115.0	12.0	T5	19.3	114.3	11
I6	15.0	115.0	10.8	T6	20.0	114.6	16
I7	17.0	115.0	11.4	T7	23.6	114.0	11
I8	19.0	115.0	11.1	T8	19.0	112.7	10
I9	21.0	115.0	10.4	T9	19.0	109.5	11
I10	23.0	115.0	10.0	T10	14.6	107.6	11
I11	25.0	115.0	11.5	T11	18.0	107.8	6
I12	13.0	113.0	12.5	T12	20.0	108.0	11
I13	15.0	113.0	12.8	T13	18.0	107.8	16
I14	17.0	113.0	12.8	T14	23.5	108.2	8.3
I15	19.0	113.0	12.3	T15	19.3	106.3	11
I16	21.0	113.0	12.3	T16	19.0	102.6	10
I17	23.0	113.0	11.3	**Passive Voltage Probes**			
I18	25.0	113.0	11.4	P1	18.8	119.8	10.5
I19	14.5	111.0	11.0	P2	19.0	115.7	10.5
I20	17.5	111.0	12.0	P3	14.6	114.3	10.5
I21	20.8	111.0	12.0	P4	20.3	114.3	10.5
I22	23.5	111.0	12.0	P5	23.6	114.0	10.5
I23	13.0	109.0	12.8	P6	19.0	112.7	9.5
I24	15.0	109.0	11.8	P7	19.0	109.5	10.5
I25	17.0	109.0	12.8	P8	14.6	107.6	10.5
I26	19.0	109.0	12.2	P9	20.0	108.0	10.5
I27	21.0	109.0	12.0	P10	23.5	108.2	7.75
I28[2]	23.0	109.0		P11	19.3	106.3	10.5
I29	25.0	109.0	11.2	P12	19.0	102.6	9.5
I30	13.0	107.0	12.3	**Cold Finger**			
I31	15.0	107.0	12.4	CF1	13.1	114.1	8.58 - 13.58
I32	17.0	107.0	11.6	CF2	16.0	114.0	8.0 - 13.0
I33	19.0	107.0	12.6	CF3	18.8	114.3	9.0 - 14.0
I34	21.0	107.0	12.3	CF4	21.9	114.2	8.5 - 13.5
I35	23.0	107.0	12.0	CF5	25.0	114.0	9.0 - 14.0
I36	25.0	107.0	12.0	CF6	12.8	108.0	9.0 - 14.0
I37	14.5	105.0	11.9	CF7	15.9	108.0	9.0 - 14.0
I38	17.5	105.0	11.9	CF8	19.0	108.1	7.75 - 12.75
I39	20.5	105.0	11.3	CF9	22.3	108.0	7.5 -12.5
I40	23.5	105.0	12.0	CF10	25.2	108.0	8.25 -13.25

[1] Same as UCAP 3 (collapsed at 19 ft BLS)
[2] Not installed

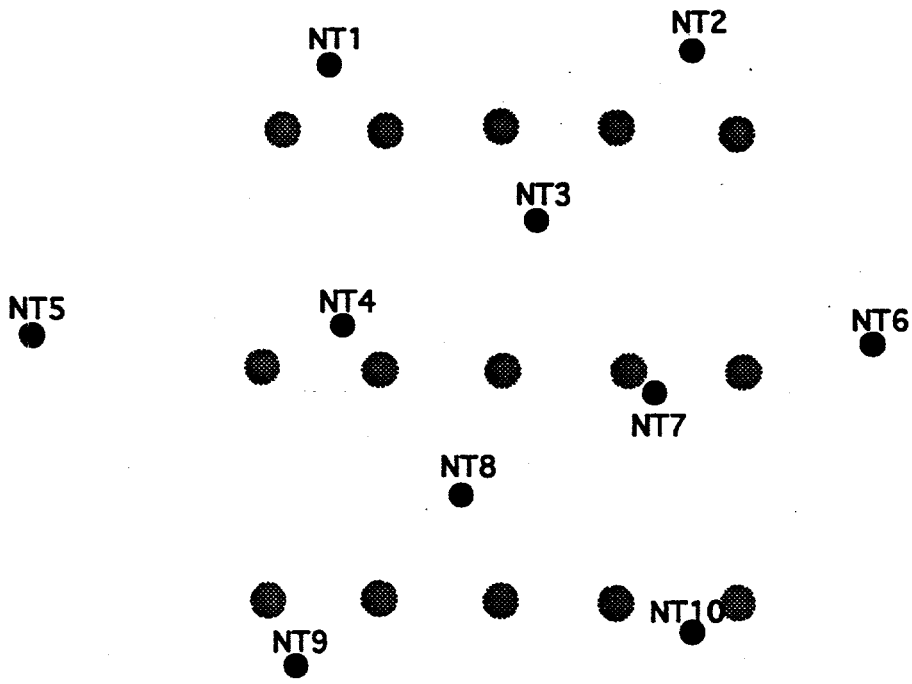

Figure 3-15. Neutron probe moisture logging locations.

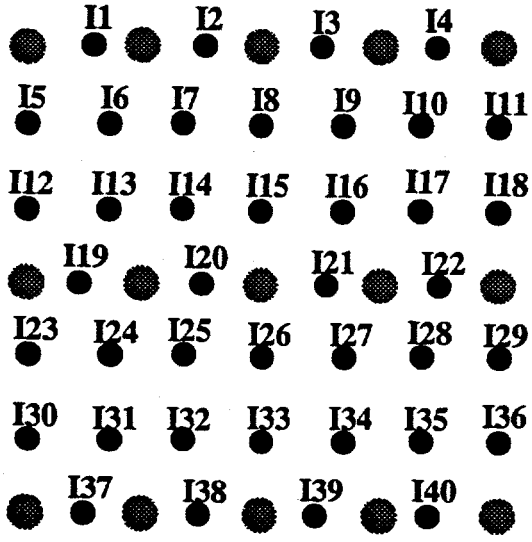

Figure 3-16. Vadose zone infiltration well locations.

3.2.4.4 Tensiometer Cups

Ten tensiometer cups for measuring soil moisture content were placed throughout the remediation area, and an additional 18 tensiometer cups were placed on the electrode casings. Figure 3-17 illustrates the location of the tensiometer cups. The tensiometer cups were a porous ceramic (Soil Moisture Corp.) with a bubbling pressure of 1 bar. These cups were attached to a six-inch section of 0.5-inch schedule 40 PVC pipe using 3M®[10] 2216 epoxy adhesive (Figure 3-18). The upper end of the six-inch PVC pipe was machined to accept a #1 rubber stopper. In order to insert the rubber stopper, a 0.75-inch PVC pipe, to act as a casing, was glued to the top of the tensiometer and extended to the surface.

The 1.5-inch Geoprobe® pre-probe was used to make access holes to install the tensiometers in the ground. A <10-mesh, clean, native-soil slurry was added to the hole to assist in making hydraulic contact between the ceramic cup and the subsurface soil. The remainder of the hole was filled with granular bentonite to the surface. Tensiometers located at the electrode casings were attached to the electrode casings prior to installing the electrodes. Table 3-3 lists the location and depths of the tensiometer cups.

These tensiometers were installed to better measure the soil matrix potential, which is related to the moisture content of the soil, if needed. However, moisture contents never increased to levels where the tensiometers would be needed.

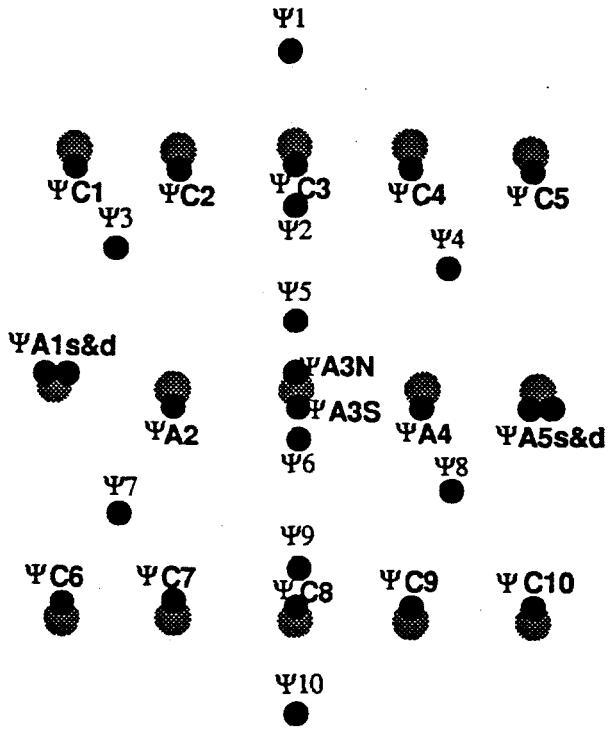

Figure 3-17. Tensiometer cup locations.

[10] 3M® is a registered trademark of 3M

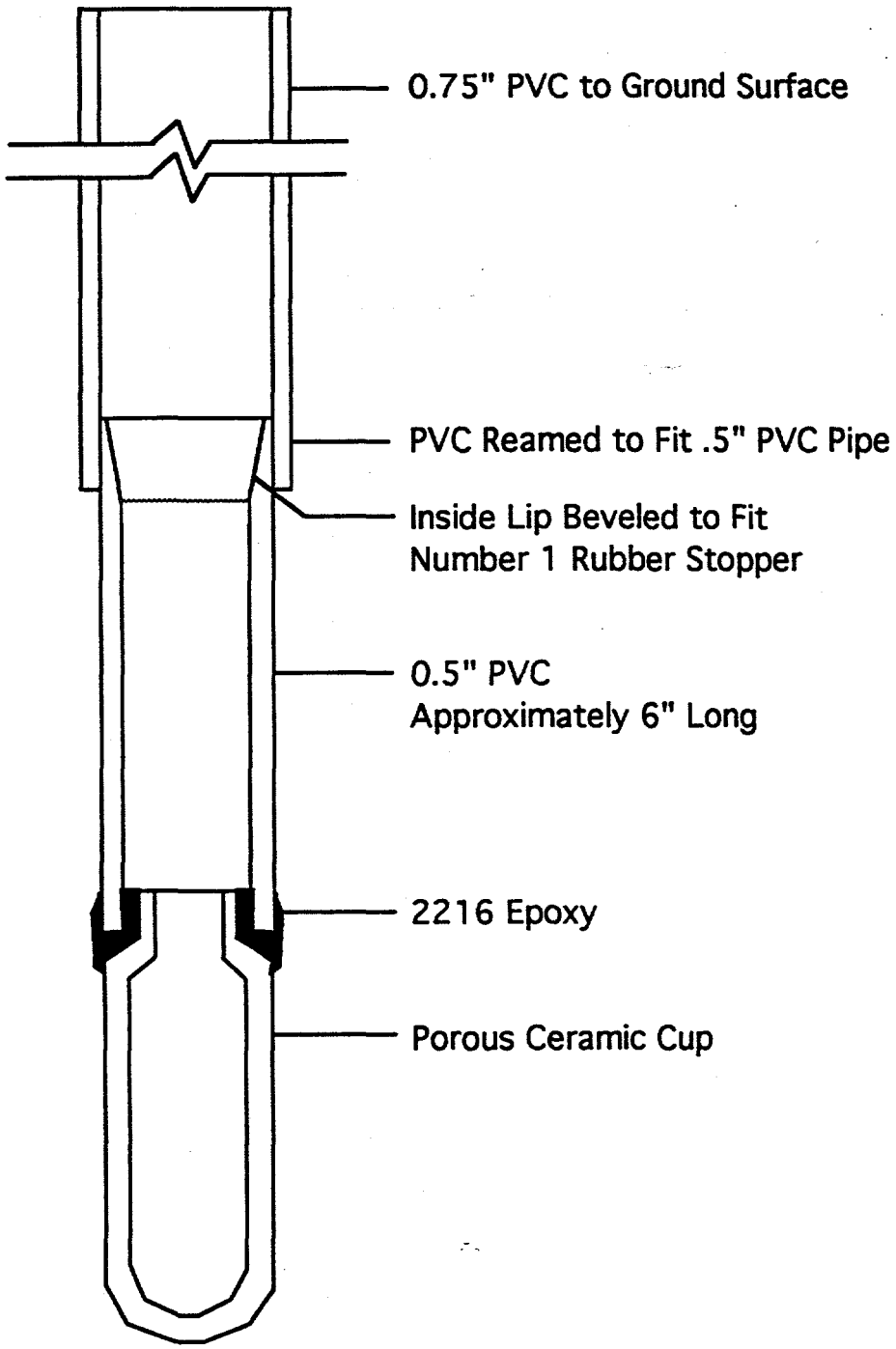

Figure 3-18. Tensiometer design.

3.2.4.5 Temperature Probes

Sixteen temperature probes were placed in the remediation area, and an additional sixteen were placed on the electrode casings. Figure 3-19 illustrates the locations of the Campbell Scientific®[11] 108B thermocouple temperature probes. Temperature probes were attached to the 0.75-inch PVC tensiometer pipes at approximately 11 feet BLS. Temperature probes at the electrode casings were attached to the PVC couple between the two ceramic pieces at 11 feet BLS (see Figure 3-14 [B]). Table 3-3 lists the temperature locations and depths of placement.

3.2.4.6 Passive Voltage Probes

Voltage potential maps can be constructed from a series of passive voltage probes implanted in the subsurface. Twelve passive voltage probes were placed in conjunction with the tensiometers through out the remediation area. An additional twenty passive voltage probes were placed on the electrode casings (Figure 3-20).

The passive voltage probes were made of approximately 2-inch square pieces of 50-mesh stainless steel screen that had insulated wires extending to the surface. The stainless steel screen was attached to the 0.75-inch PVC pipe approximately 10 feet BLS. See Table 3-3 for locations and depths of the passive voltage probes.

3.2.4.7 Cold Fingers

Additional electrodes were deployed across the site to be used either as active "bare" electrodes to increase the voltage gradient or as "cold fingers" if the resistive heating of the soil was excessive. The cold finger gets its name from the ability to circulate chilled water through the interior of the pipe to dissipate heat generated in the vicinity. Ten "field" cold fingers were installed midway between the anode/cathode pairs (Figure 3-21). Twenty additional cold fingers were installed in conjunction with the electrode casings (see Table 3-3 for locations).

The field cold fingers were constructed with 0.75-inch copper pipe 5 feet in length. The bottom portions were stopped with a pipe cap while the top ends were fitted to a 0.75-inch schedule 40 PVC pipe that extended to the surface. Polyethylene tubing ran down the inside of the cold finger to deliver water, and the water flowed back up inside the copper/PVC pipe. Number 10 insulated wires were soldered to the copper pipes and brought to the surface for optional electrical connections. Both copper pipe ends and the copper wire connections were wrapped with electrical tape to protect the solder joint. The cold fingers attached to each of the EK cathode casings were similar in design to the field cold fingers, except these copper tubes were 1 inch in diameter and 6.67 ft in length. Figure 3-14 (B) illustrates the location of the cold fingers in relation to the electrode casing.

[11] Campbell Scientific® is a registered trademark of Campbell Scientific, Inc.

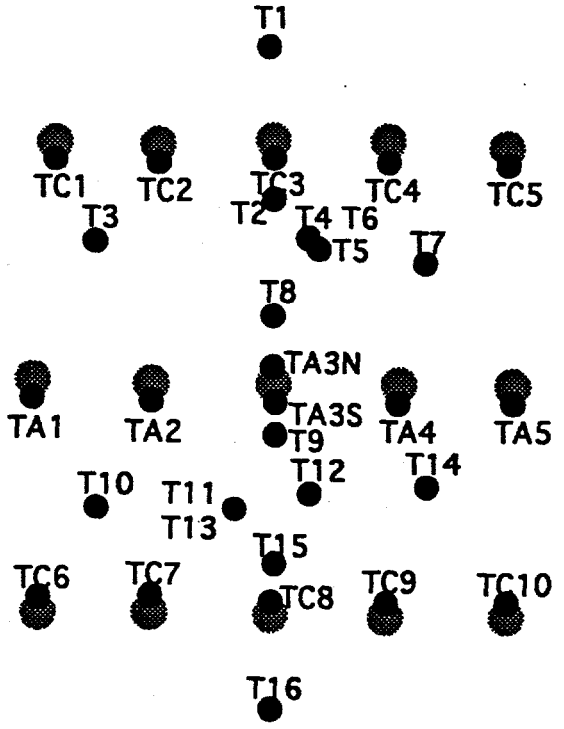

Figure 3-19. Temperature probe location.

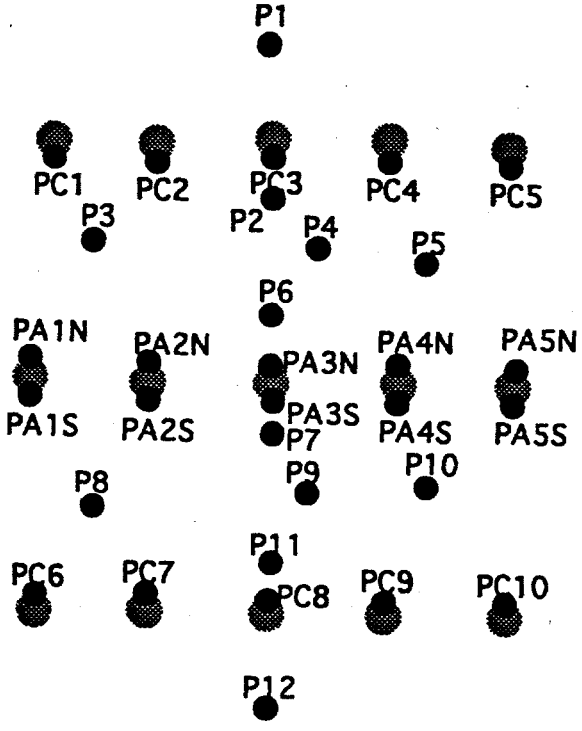

Figure 3-20. Passive voltage probe location.

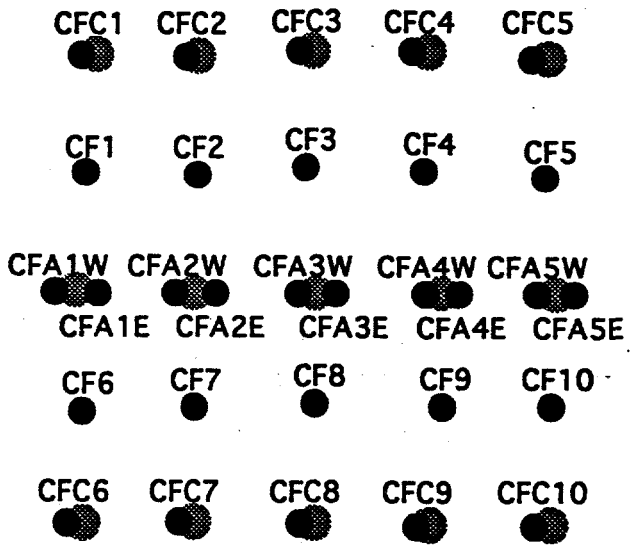

Figure 3-21. Cold finger layout.

The field cold fingers were installed in 1.5-inch diameter pre-punched holes. A soil slurry was poured into the 1.5 inch-diameter hole, and the cold finger immediately installed, submerging the metallic portion of the cold finger in the slurry. The remainder of the hole was backfilled with native soil and capped with a bentonite plug.

Of the twenty cold fingers attached to the EK electrode casings, ten were attached to the five EK anode casings. The anode cold fingers were of the same basic design as those described above but were constructed of a different material. One-inch iridium-coated titanium tubes were used instead of the copper pipes. The bottom ends were plugged with Swagelok®[12] tube plugs, and the top ends with Swagelok male adapters to connect the titanium tubes to the 0.75-inch PVC pipe. The 10-gauge wires were connected to the copper male adapters via ring spade lugs and bolts tapped into the male adapter collars. Both ends were wrapped with self-welding tape and then with standard PVC electrical tape to prevent the brass Swagelok ends from oxidizing if the cold fingers were to be used as bare anodes.

3.2.5 Radio Imaging

The Physical Science Laboratory from New Mexico State University conducted radio imaging method (RIM) surveys for the EK project (McCorkle and King, 1997). These surveys were to examine pretest/post-test changes in the vertical conductivity profile beneath the UCAP site. A transmitter was placed in one of the neutron access tubes, and a receiver in a different neutron access tube measured the strength of the applied signal. Depending on the vertical

[12] Swagelok® is a registered trademark of Swagelok Company

location of the transmitter and receiver, either a direct ray measurement was obtained if the transceiver and receiver were at the same vertical depth, or a tomography image was produced if a suite of data was collected by varying the depth of the transmitter and receiver. Unfortunately, with all of the other equipment described above already installed, the post-test radio imaging was inconclusive.

3.2.6 Initial Chromium Mass Calculations

The initial mass of water-soluble chromium in the EK treatment zone (i.e., 8 to 14 ft BLS between the anodes and the cathodes) was calculated from chemical analysis of pretest soil samples collected while installing the EK electrodes. The EK treatment zone was divided into a series of rectangular blocks that measured 2 ft in height (the soil sampling zone), 3 ft in width (the distance between similar electrodes), and 3 ft in length (one half the distance between the anodes and cathodes). Assuming a soil bulk density of 1.8 g/cc, each of these blocks had a mass of 917 kg of soil. This soil mass was multiplied by the chromium concentrations obtained for the soil samples. Chromium concentrations were obtained by a refined, in-house water-extraction method (Method B) followed by ion chromatography analysis and by an outside laboratory EPA toxicity characteristic leaching procedure (TCLP). A discussion of these methods and analyses results are given in Appendix A. In locations where no samples were collected, estimates of the chromium concentrations were made. Figure 3-22 illustrates the water-soluble chromium concentrations (mg Cr/kg soil) for the northern set of cathodes, the anode electrodes, and the southern set of cathodes.

An estimate of the initial chromium mass within the northern and southern treatment zones was calculated by summing the product of the soil sample chromium concentrations and a representative soil mass within the EK treatment zone. Results of this mass calculation exercise are listed in Table 3-4. In general, the water-soluble chromium estimates were lower than the TCLP chromium estimates (the bulk of the contamination is in the lower portion of the remediation area), and the Southern Zone of the remediation area exhibited higher contamination levels than the Northern Zone. Approximately 1.3 kg of water-soluble chromium were present in the EK treatment zone bounded by Cathodes 1 to 5 and Anodes 1 to 5. Almost twice that amount of chromium, 2.2 kg, was estimated to be in the southern EK treatment area bounded by Anodes 1 to 5 and Cathodes 6 to 10. The north-south water soluble-chromium cross section (see Figure 3-11) also illustrates a higher mass of water soluble-chromium between the southern anode/cathode pair.

Chromium mass in the treatment zone was also estimated using a different type of chemical analysis of soil samples that were collected while drilling boreholes for some neutron access tubes and some EK electrodes. These soil samples were analyzed for chromium using the TCLP. This method uses a weak organic acid in a 20-parts acid to a 1-part soil mixture that is shaken for approximately 18 hours. A similar method of assigning a corresponding mass of soil to each soil sample was used to calculate the total mass of TCLP chromium. Using this method of estimating the chromium mass, the northern portion of the EK treatment zone contains 5.2 kg of chromium while the southern EK treatment zone contains 6.0 kg of chromium.

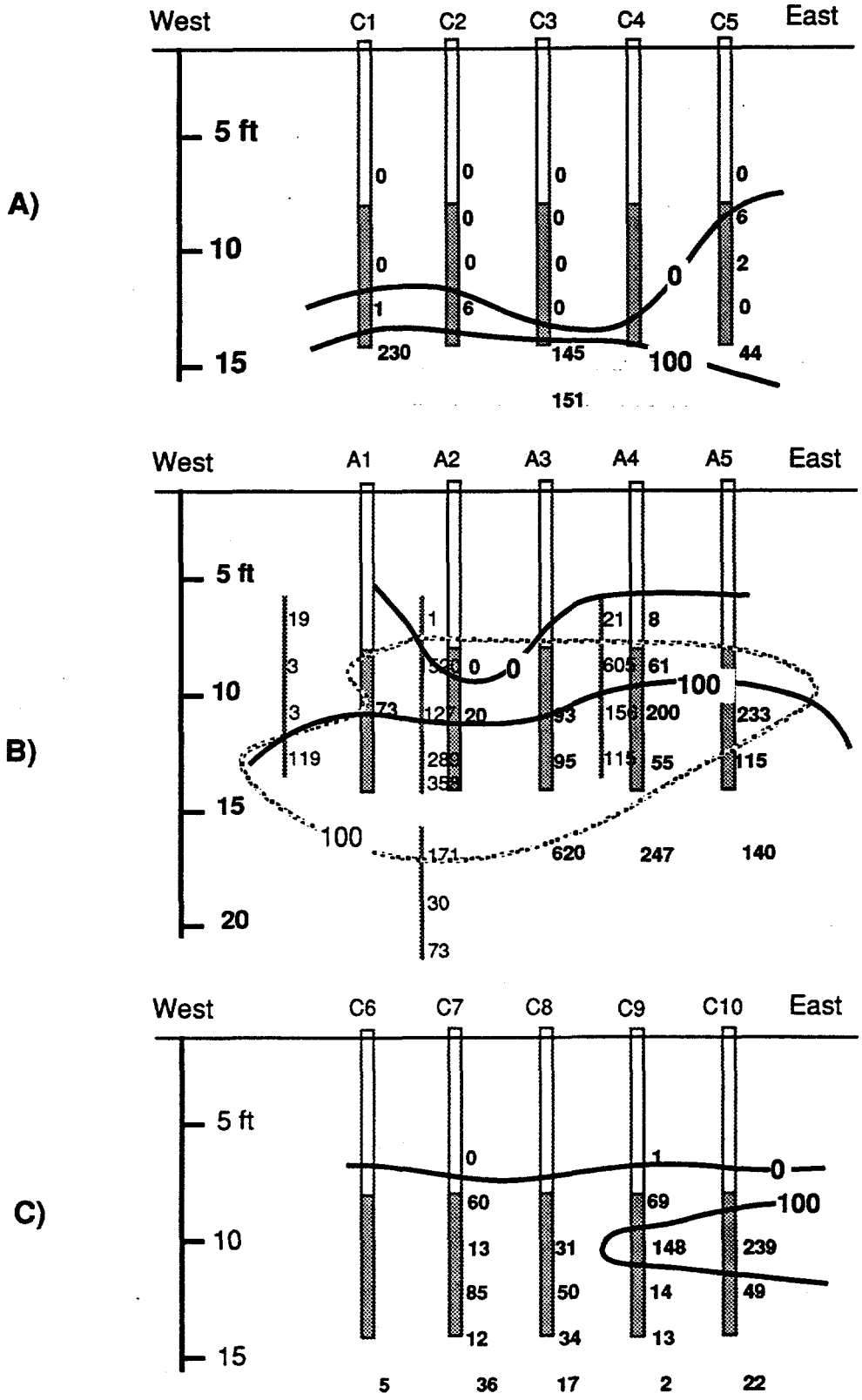

Figure 3-22. East-west cross section of water-soluble Cr through electrodes. (ppm by weight) (A) north row of cathodes, (B) anode row (light contours are from geoprobe cross-section concentrations), and (C) south row of cathodes.

The TCLP-calculated chromium mass is approximately three times greater than the water-soluble chromium mass in the EK treatment zone. This is expected since the TCLP uses a more aggressive extraction procedure and a longer agitation time that will dissolve chromium that is precipitated in the soil matrix. The amount of chromium (as chromate) removed from the EK treatment area was expected to be closer to the water-soluble estimated mass than the TCLP estimated mass since water was the extraction fluid used during the EK demonstration.

Distribution of the chromium in the EK treatment zone was not uniform, as seen in Table 3-4. The upper portion (8 to 10 feet BLS) of the EK treatment zone contained the least amount of chromium, as estimated by both the water-soluble and TCLP chromium extraction methods. The middle portion (10 to 12 feet BLS) of the EK treatment zone contained the bulk of the chromium (44 to 67%), whereas 20 to 40 percent of the calculated chromium mass was located in the lower portion (12 to 14 feet BLS) of the EK treatment zone.

Table 3-4. Chromium Distribution as a Function of Depth
(Water-soluble chromium determined by UV/VIS; chromium in soil by standard TCLP method)

Depth Interval	Water Soluble Chromium				TCLP Chromium			
	Northern Zone		Southern Zone		Northern Zone		Southern Zone	
(ft)	(kg)	%	(kg)	%	(kg)	%	(kg)	%
8 - 10	0.139	10.41	0.386	17.57	0.651	12.46	0.682	11.30
10 - 12	0.577	43.22	0.973	44.29	3.416	65.38	4.04	66.92
12 - 14	0.619	46.37	0.838	38.14	1.158	22.16	1.315	21.78
Total	1.335	100	2.197	100	5.225	100	6.037	100

Unfortunately, the electrical conductivity profiles (see Figures 3-6 and 3-7) indicated that higher conductive soil is located above 10 feet BLS. With no perturbation of the electrical conductivity profile, most of the current would travel in this higher conductive zone between the anodes and cathodes bypassing the zones of highest chromium mass. Efforts were made to redirect the current through zones that are more highly contaminated by installing vadose infiltration wells (Section 3.2.4.3). Results of these efforts are discussed in Section 5.3.3.

4. EXPERIMENTAL CONTROL SYSTEMS

The EK demonstration was housed in two main buildings, the EK Control Trailer and the Greenhouse (Figure 4-1 and Photograph 1 in Appendix B). The Control Trailer was located immediately outside the CWL boundary fence and housed the electrode operation control panels (Figure 4-2 and Photograph 2 in Appendix B), the data logging system, and other data analysis equipment. The Greenhouse was located on the CWL and protected the on-site equipment, electrodes, secondary containment, and personnel from the weather as well as provided an operational exclusion zone while the electrodes were energized (Photograph 3, Appendix B). The two buildings were approximately 75 ft apart and were connected by four, 3-inch electrical conduits that provided protection for the numerous signal and control cables.

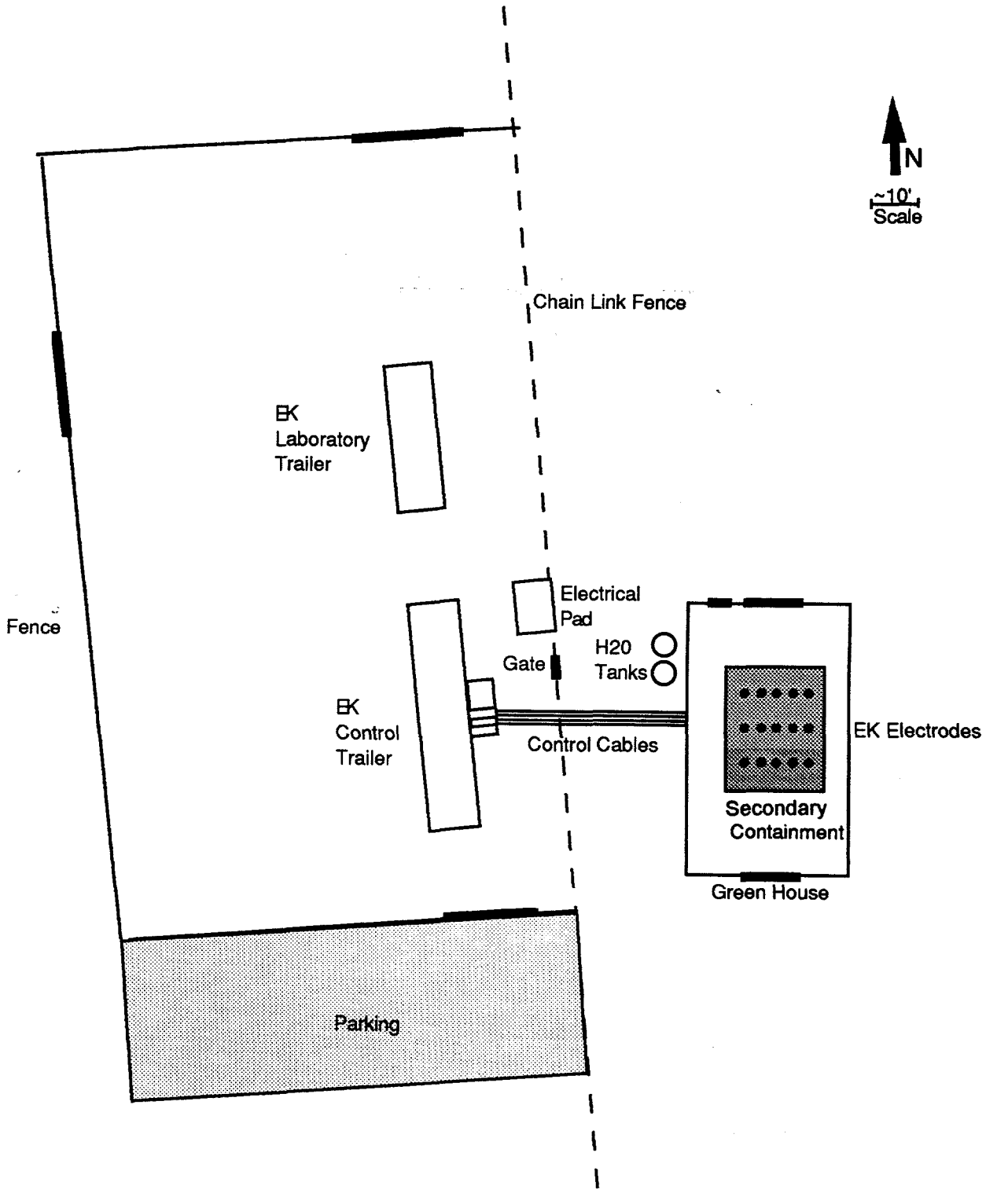

Figure 4-1. Electrokinetic demonstration plan view.

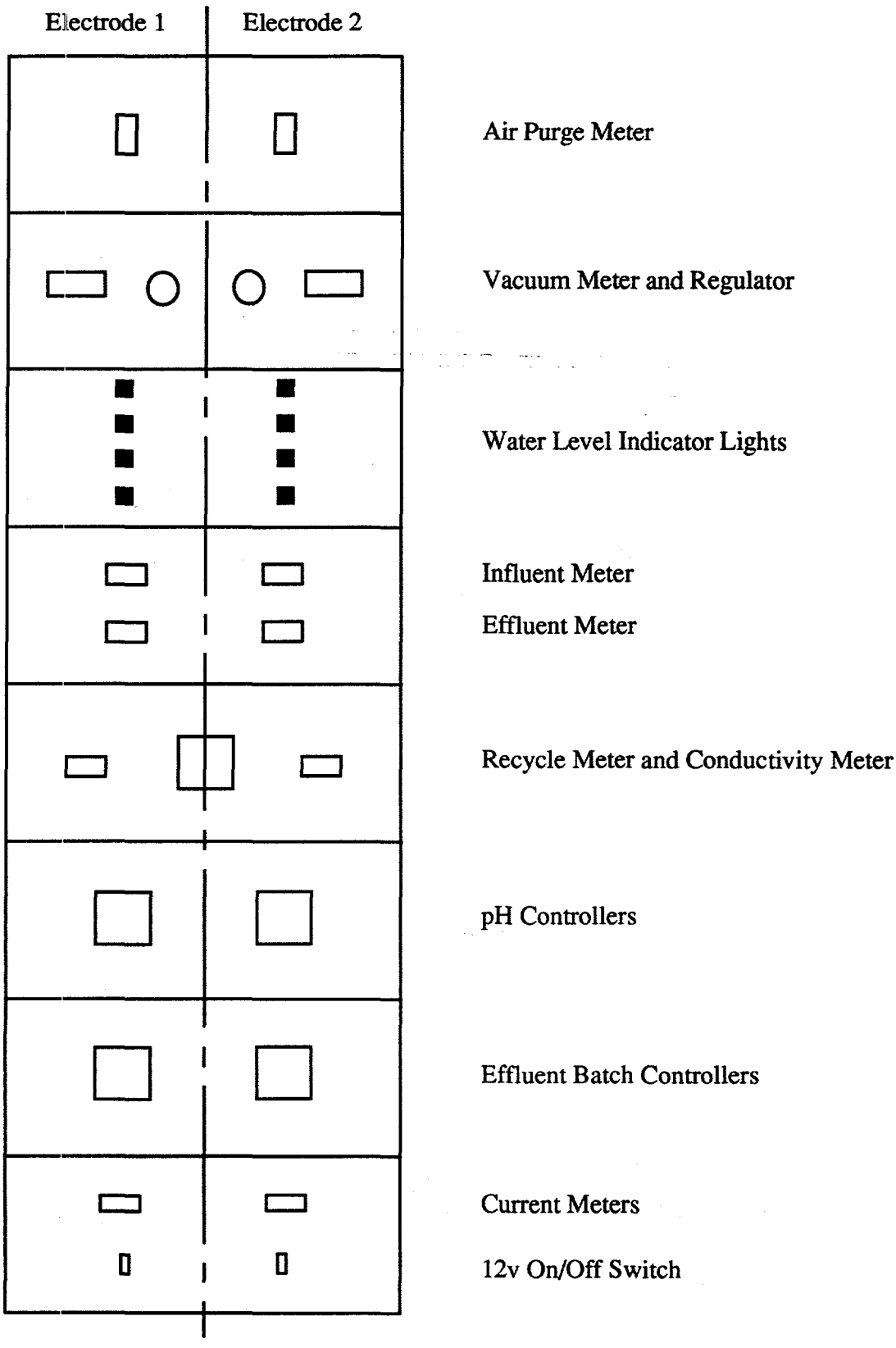

Figure 4-2. Control panel layout.

4.1 Introduction To Electrode System

The electrode system for conducting EK remediation in the unsaturated zone is a unique, patented (Lindgren and Mattson, 1995) design. Unlike groundwater in saturated soil, pore water in the unsaturated zone is held under tension in the soil pores. (Soil tension can describe the moisture content of the soil: the greater the soil tension, the dryer the soil.) This soil tension prevents the pore water in the unsaturated zone from entering simple groundwater extraction wells as it does in the saturated zone. Therefore, an effluent extraction system at an EK electrode must be specifically designed to overcome the soil tension problems for use in unsaturated soils.

In addition, as discussed earlier, when an electric current is applied to soil between electrodes, water will flow by electroosmosis in the soil pores, usually towards the cathode. This process occurs in both saturated and unsaturated soils. The movement of this water causes a depletion of soil moisture adjacent to the anode and a collection of moisture near the cathode. The electrode design overcomes this problem as well.

Electrode systems to meet these needs have been designed for testing in both laboratory and field applications by SNL and Sat-Unsat, Inc. of Albuquerque, New Mexico. These electrode systems overcome the difficulty of the soil tension problems for use in unsaturated soils, thus allowing operation of the EK process in unsaturated soils for much longer periods of time than if simple electrodes were implanted in direct contact with the soil. Also, the effluent extraction system allows water to enter the soil at the anode, thus replenishing the pore water adjacent to the electrode, and permits removal of effluent which contains contaminants from the soil. The EK remediation system designed for this demonstration includes the extraction electrode and four main operational units: a vacuum control system, a liquid control system, a power application system, and a monitoring system. The following section describes the equipment and operation in more detail.

4.2 Electrode System Operation

For the EK remediation system described in this report, a portion of the electrode casing functioned as a suction lysimeter, and an electrode was placed inside the lysimeter. A suction lysimeter is a device which uses a porous material that exhibits a high bubbling pressure (the pressure at which air will pass through a material when submersed in water) to extract pore water samples from the vadose zone. To collect a pore water sample, a vacuum is applied to the inside of the lysimeter. Depending on the magnitude of the applied vacuum and the tension in the vadose zone around the lysimeter, the direction of the pressure gradient across the porous material will either cause water to flow into or out of the lysimeter. Therefore, suction lysimeters offer a technique to control the addition and extraction of water in the vadose zone. By the application of a vacuum to the lysimeter, water can be added to the soil, but saturated conditions can never develop.

A 6-ft portion of the electrode casing was constructed of porous ceramic that acted as the lysimeter. The upper portion of the electrode was constructed of an impermeable, non-conducting PVC material. The fluid between the electrode and the ceramic casing was continuously recirculated to remove contaminants that entered the electrode, to clear the electrode of gas bubbles formed by water electrolysis, and to mitigate hydrolysis reactions. The solution extracted from the electrode lysimeter could be treated at the ground surface.

All electrode casings were constructed in a similar manner. The portion of the casing that allowed the transfer of current and water was constructed of porous ceramic. This porous-ceramic section of the electrode was constructed from two, 3-ft tube sections. The porous ceramic was positioned between 8 and 14 ft BLS. The remainder of the electrode casing was made of 3-inch, schedule 40 PVC pipe and fittings. Figure 3-14 (A) illustrates an electrode casing assembly. The ceramic was connected to the PVC fittings by grinding the interior surface of the PVC fitting with a drum sander and gluing the ceramic to the reamed PVC fitting using 3M® 2216 epoxy adhesive.

The electrode casings were made of two different types of porous ceramic. The northern cathode row, C1 through C5, was constructed of Coors® ceramic PC6 material. The southern row of cathodes, C6 through C10, and the anodes, A1 through A5, were constructed with PC3 material. The main difference between PC3 and PC6 ceramic is the pore-size distribution. PC3 is a tighter material having a smaller pore-size diameter (~3 μm) than the PC6 (~6 μm diameter pores). Bubbling pressure of the PC3 is 19 to 28 psi, while the PC6 bubbling pressure is 7 to 9 psi.

Due to the high negative zeta potential on the ceramic surface and the direction of the voltage gradient, the surfaces of the ceramic in the anodes were treated to prevent movement of water out of the anodes by electroosmosis. By treating the ceramic with a surfactant material to alter the charge on the ceramic surface, electroosmosis can be significantly decreased. The ceramic was first acid washed with a 0.1 molar HCl solution until the pH of the effluent equaled that of the influent. At this time, it was assumed that all of the surface sites were loaded with hydrogen ions. A deionized water rinse was used to remove the excess acid from the ceramic pores. Finally, a 0.01 molar hexadecyltrimethylammonium (HDTMA) hydroxide solution was purged through the ceramic. The reaction of the HDTMA-OH with the hydrogen ions on the ceramic surface replaced the hydrogen ions with HDTMA molecules. The HDTMA likely formed a double layer on the surface of the ceramic reversing the effective charge from negative to positive on the ceramic surface. The ceramic material for the cathode electrode casings was not treated.

4.2.1 Vacuum Control System

To retain water in the porous-ceramic electrode casing, a vacuum was applied to the air head space within the EK electrode (Figure 4-3). This vacuum system also allowed an air-purge system to be incorporated into the electrode design to prevent explosive conditions from developing in the head space. Each electrode type (anode or cathode) had a separate vacuum system to prevent mixing of the hydrogen and oxygen gases.

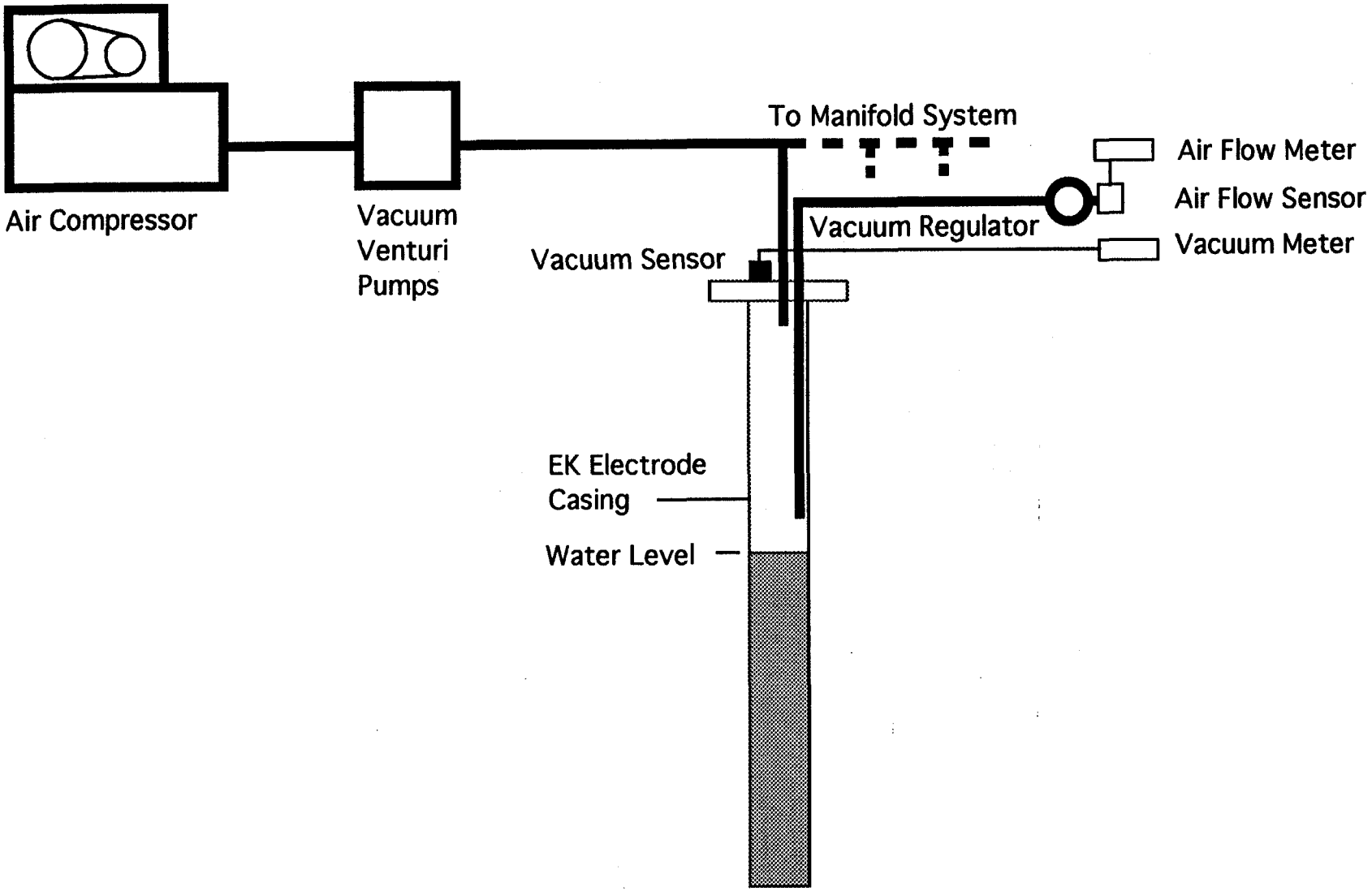

Figure 4-3. Vacuum control system.

The transfer of current from an electrode to an electrolytic fluid involves the oxidation or reduction of the fluid or an ion within the fluid. If water is the oxidized/reduced species, then the reduction reaction at the cathode is:

$$4\,H_2O + 4\,e^- \rightarrow 4\,OH^- + 2\,H_2\uparrow \tag{4.1}$$

Similarly, the oxidation reaction at the anode is:

$$2\,H_2O - 4\,e^- \rightarrow 4\,H^+ + O_2\uparrow \tag{4.2}$$

An air stream was allowed to enter through the cathodes to prevent hydrogen levels from reaching explosive limits. The lower explosive limit of hydrogen gas is 4% (CRC, 1970). Assuming that 15 amps is the maximum current each cathode could transfer (set by the power supplies and the in-line fuse) and that all of the current transferred between the electrode and the electrolytic fluid produced hydrogen via Equation 4.1, the amount of air purge needed to maintain hydrogen levels at the lower explosive limit could be calculated.

Fifteen amps will transfer 9.3 mmol of charge per min as illustrated in Equation 4.3.

$$15A*1\frac{C}{A\cdot s}*\frac{1M_{charge}}{96500C}*\frac{60s}{\min}=9.3\frac{mM_{charge}}{\min} \tag{4.3}$$

Since each mole of charge produces 0.5 moles of hydrogen gas (Equation 4.1), 4.65 mmoles of H_2 will be produced per minute.

The volume rate of hydrogen gas production can be calculated via the Ideal Gas Law. Assuming atmospheric conditions at Albuquerque (0.85 atm), 0.13 liters of hydrogen gas is produced each minute by the application of 15 amps (Equation 4.4).

$$R_{H_2}=4.65\frac{mM_{H_2}}{\min}*\frac{82.06cm^3*atm}{mol*K}*\frac{293K}{0.85atm}=0.13\frac{L}{\min} \tag{4.4}$$

where R_{H_2} = rate of hydrogen gas generation (L/min).

Finally, the rate of air purge need to maintain hydrogen gas at the lower explosive limit is 3.3 L/min as calculated below.

$$R_{air}=0.13\frac{L_{H_2}}{\min}*\frac{1}{0.04}=3.3\frac{L_{air}}{\min} \tag{4.5}$$

where R_{air}= rate of air purge required (L/min).

The purge alarm rates were set at 3.5 L/min, and the actual purge rate was maintained at approximately 8 L/min to ensure the hydrogen gas concentrations were maintained well below

the explosive limit. Air was also purged through each cathode at a rate of 2 L/min to dilute the oxygen gas produced at that electrode.

A 10 HP Quincy®[13] Model 370 air compressor provided compressed air to operate a series of PIAB™[14] vacuum ejector pumps. The compressed air was driven through a series of venturies within the vacuum pump causing additional air to be drawn through the venturi system. This air-driven venturi system has the additional safety feature of being explosion proof.

The vacuum of the cathode system was created with a series of three parallel PIAB® MLD25 pumps which were able to produce 27.5 inches Hg. The anode vacuum system used four parallel PIAB® LX10 vacuum pumps. Each vacuum system was connected to separate manifold systems to evacuate five anodes or five cathodes. The compressed air pressure was set for each vacuum system so that each system operated at its optimal performance.

Rather than directly regulating the vacuum applied to the EK electrode, Moore®[15] Model 44-20 vacuum regulators allowed air to enter the electrode to dilute hydrogen and oxygen gases being generated by the electrode reactions. This air flow was monitored by McMillan®[16] flow sensors (Model 100-8 for the anodes or Model 100-10 for the cathodes) connected to McMillan® bar graph displays. The vacuum regulators were adjusted to provide adequate flow rates through the electrodes, and generally the vacuum was maintained at 14 inches of Hg for both the anodes and the cathodes.

4.2.2 Liquid Control System

The liquid control system can be divided into two separate parts, the water-circulation system (Figure 4-4 and Photograph 4 in Appendix B) and the electrode water-level control (Figure 4-5).

The water-circulation system was powered by a QED®[17] P1101S bladder pump contained in the EK drive electrode with the screen portion of the pump extending into the electrode casing sump. All parts of this pump were plastic to prevent corrosion. The pump housed a dura-flex teflon bladder which, when inflated, filled with liquid. During subsequent deflation of the bladder, the liquid contained in the bladder was driven through the circulation system and returned back to the EK electrode casing just above the drive electrode (Figure 4-4).

---

[13] Quincy® is a registered trademark of Coltec Industries, Quincy Compressor Division

[14] PIAB™ is a trademark of PIAB Vacuum Technique, Sweden

[15] Moore®is a registered trademark of Moore Products Co.

[16] McMillan® is a registered trademark of McMillan Company

[17] QED® is a registered trademark of Q.E.D. Environmental Systems, Inc.

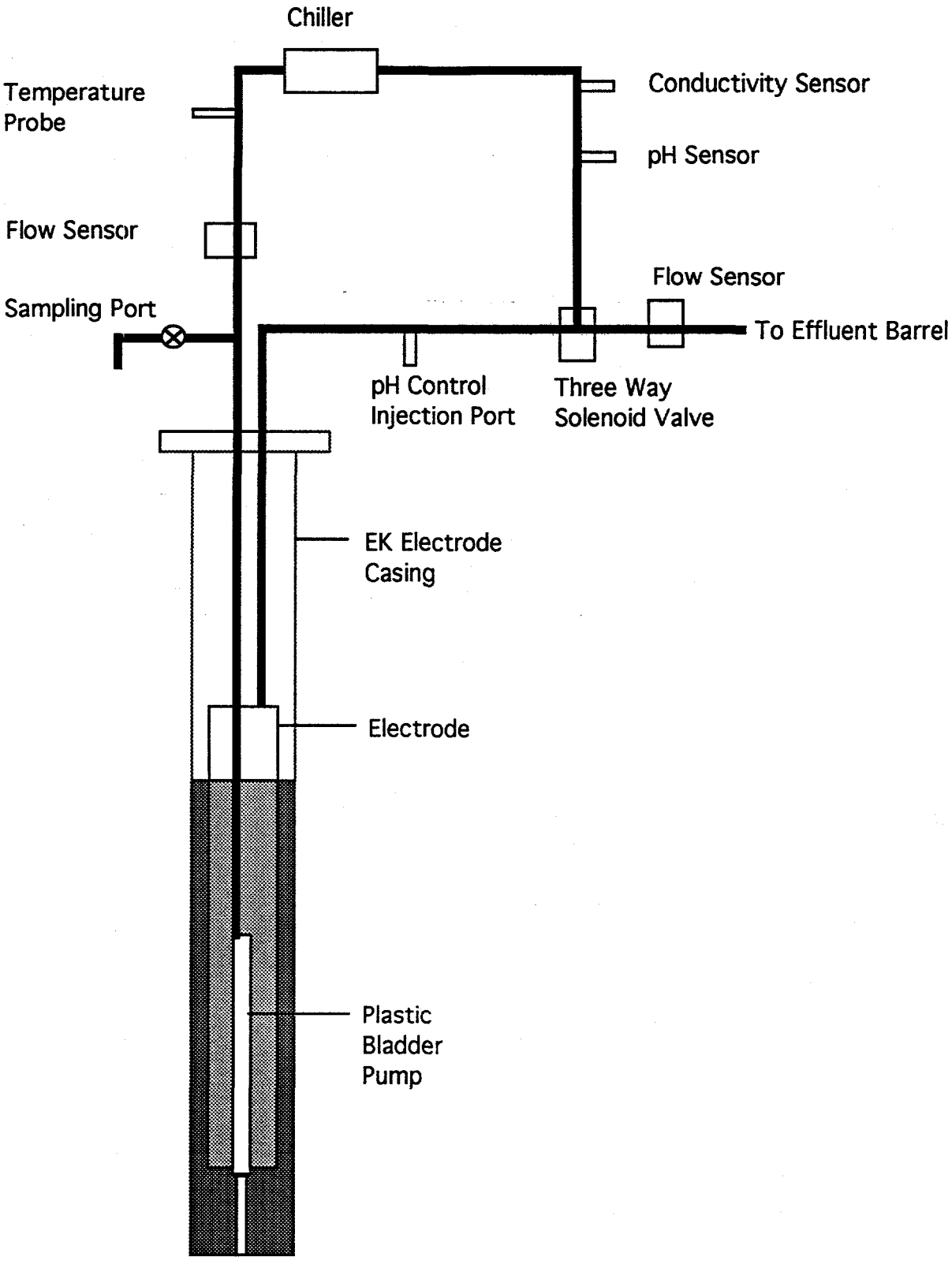

Figure 4-4. Water-circulation system.

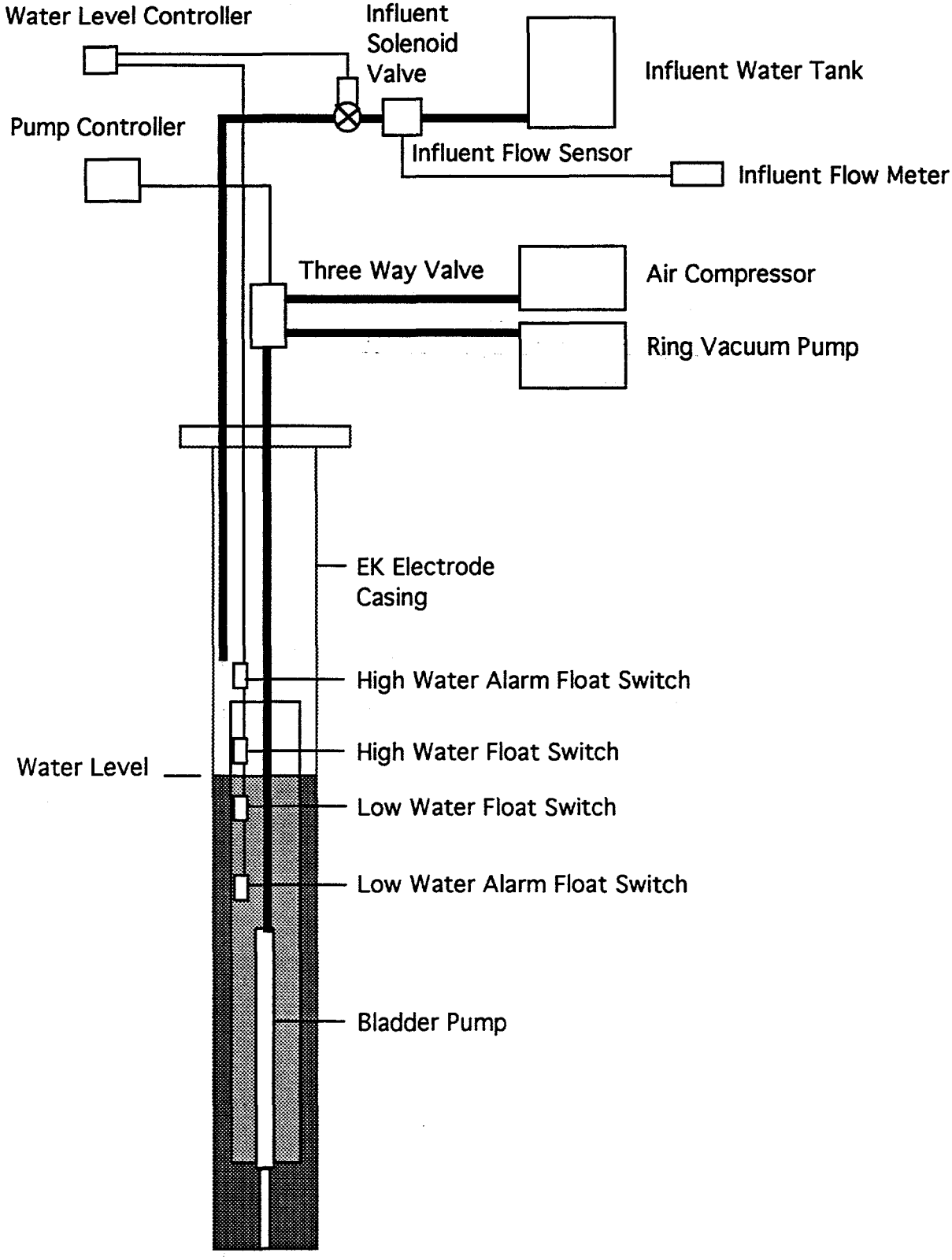

Figure 4-5. Electrode water-level control.

The circulation system was employed to monitor the chemical condition of the liquid in the electrode, to cool the liquid in the electrode, and to sample and remove liquid from the electrode. A manual sampling port was located at the ground surface, just after the liquid left the EK electrode. This sampling port had a PVC ball valve which, when opened, allowed a sample to be collected while the bladder was deflating. With the sampling port in the normally closed position, the liquid then passed through a McMillan® Model 100-8T flow sensor, and the output was displayed on a McMillan® 220 flow rate/total digital display in the control rack (Figure 4-2).

Due to ohmic heating of the water in the electrode and of the surrounding soil, the temperature of the recycle water was monitored by a Campbell Scientific® 108B temperature probe. An ITT Bell & Gossett BP Honeycomb™[18] heat exchanger (Model 410-30 for cathodes and Model 410-40 for anodes) cooled the recycle water. Remcor®[19] (Model CH-3002-A) chillers circulated deionized water at approximately 6 °C at a rate of 1.5 gallons per minute to each heat exchanger to remove the excess heat. This cooling system maintained the water temperature in the electrodes at approximately 8 to 10 °C.

After water passed through the heat exchanger, the recycle water conductivity was measured by an inline Signet®[20] 2820 conductivity sensor. This sensor was connected to a Signet® 9050 Intelek-Pro™[21] conductivity controller in the field trailer. The conductivity controller was used only as a display to observe the electrode fluid conductivity. Each conductivity controller had two separate input channels allowing two electrodes to be monitored by one conductivity meter.

At 30-minute intervals, the effluent batch controllers (Signet® 9020 Intelek-Pro® Batch Controller) in the control trailer sent a signal to a three-way, air-operated, PVC solenoid valve (Figure 4-4) to redirect the recycle water to the effluent barrels. The effluent was collected in 55-gallon, closed-top, polypropylene barrels. The flow of recycle water to the effluent barrels was monitored by a McMillan® (Model 100-5T) flow sensor. After a set amount passed the effluent sensor (user specified at rates of 0.1 to 0.5 liters/30 minutes depending the test), the conductivity controller sent a signal to de-energize the three-way valve to let the recycle water return to the electrode.

A Squire-Cogswell®[22] M30A02 liquid ring vacuum pump was used to re-inflate the bladder in the bladder pump causing water to enter the bladder. Normally, these bladder pumps are used to sample groundwater from monitoring wells. In typical groundwater sampling situations, the static pressure of the water column allows water to fill the bladder. In our system, the water pressure at the pump in the EK electrode is sub-atmospheric due to the vacuum applied to the head space of the electrode, hence the need to re-inflate the bladder. The water was expelled by squeezing the bladder with pressurized air set at approximately 20 psi. A

---

[18] ITT Bell & Gossett Honeycomb™ is a trademark of ITT Bell & Gossett

[19] Remcor® is a registered trademark of Remcor Products Company

[20] Signet® is a registered trademark of George Fischer Signet, Inc.

[21] Intelek-Pro™ is a trademark of George Fischer Signet, Inc.

[22] Squire-Cogswell® is a registered trademark of Squire-Cogswell Company

ChronTrol®[23] (Model XT 4 S) timer module activated a three-way valve at three-second intervals to alternate between air pressure and vacuum to the pump bladder (Figure 4-5). This system resulted in recycle flow rates of approximately 4 L/min.

The water level in the EK electrode was maintained above the ceramic/PVC interface with two sets of reed-type, water-level, float switches (Flowline®[24] Model LV10 series). The two middle switches, spaced approximately 6 inches apart, were connected to a dual-float switch controller (Levelite®[25] Model GLL 100000) which opened and closed an influent solenoid valve (Figure 4-5) to allow water to enter the electrode. The upper and lower floats acted as high and low alarm switches for water-level control failure. The water entering the electrode was monitored by a McMillan® (Model 100-5T) flow sensor connected to a McMillan® digital flow-rate/total-flow meter. Separate 250-gallon PE storage tanks (one for the anodes and one for the cathodes) contained the influent water source; these tanks were monitored visually for water use.

4.2.3 Power Application System

The EK electrodes were energized using a series of four 10-kW power supplies (Sorensen®[26] Model DTR-600-16T). Each power supply was capable of outputting 16 A at 600 V dc. The power supplies could either be operated in parallel mode using a parallel interface controller (PIC) (Sorensen® Model PICTM9A) providing up to 64 amps at 600 volts to the system (Figure 4-6A) or be operated independently so that each power supply energized one set of electrodes (Figure 4-6B).

In either case, the system contained a manual main disconnect to lockout power application while performing maintenance on the EK system. The amount of current to each electrode was limited by 15-amp in-line fuses and monitored by measuring the voltage drop across a 20 amp/100mV shunt with a Newport®[27] Model 504 isolated current transmitter. This current transmitter output a 4 to 20 milliamp signal that was subsequently converted to a 1- to 5-volt signal with a precision 250-ohm resistor. The current was displayed on the control panel through a Simpson®[28] M235 digital display.

Care was taken in choosing and installing monitoring equipment to ensure it was electrically isolated from the DC power supplies and earth ground. Anodes and cathodes can have voltage differentials as high as 600 volts between them as well as hundreds of volts between the electrodes and earth ground. In addition, the liquid contained in the electrodes and recirculation systems can also have sufficient voltage potentials to require monitoring equipment to be electrically isolated. Equipment that is not electrically isolated will allow some of the applied current to short circuit between the electrodes.

---

[23] ChronTrol® is a registered trademark of Linberg Enterprises

[24] Flowline® is a registered trademark of Flowline Inc.

[25] Levelite® is a registered trademark of Levelite/Genelco, Div. Of Bindicator Co.

[26] Sorensen® is a registered trademark of Sorensen Company, A Division of ELGAR Corporation

[27] Newport® is a registered trademark of Newport Electronics, Inc.

[28] Simpson® is a registered trademark of Simpson Electronic Company

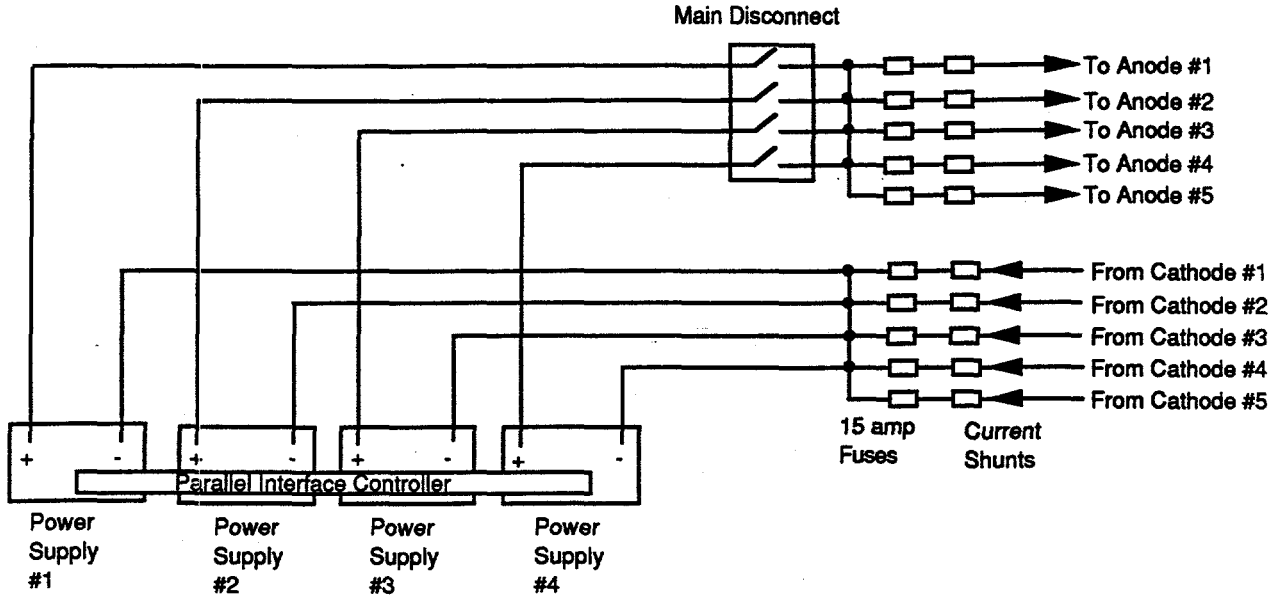

A) Five Anode-Cathode Pairs Operated by the Parallel Interface Controller

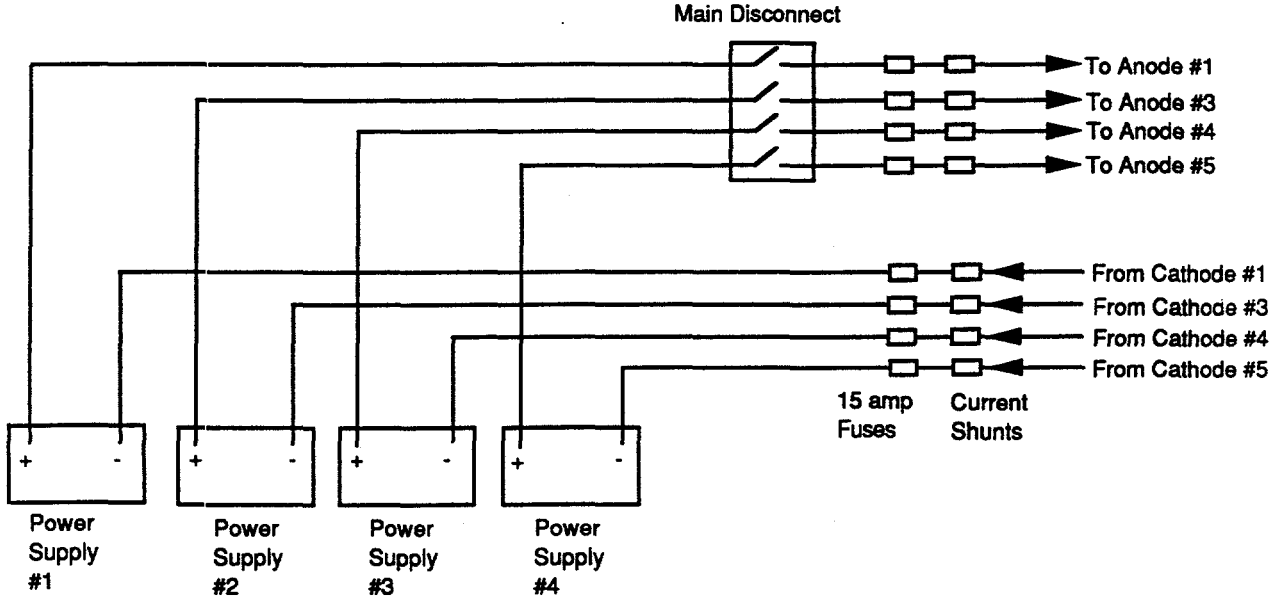

B) Four Anode-Cathode Pairs Controlled by Individual Power Supplies

Figure 4-6. Current distribution schematic.

4.2.4 pH Control System

The pH of the electrode solutions was controlled in the range of 8.8 for the anodes and 5.5 for the cathodes. As illustrated above in Equations 4.1 and 4.2, hydroxyl ions are produced in the cathodes and hydrogen ions are produced in the anodes due to the electrolysis reactions at the electrodes. Researchers (Acar et al., 1989 and 1990) who have not neutralized these electrode reactions have reported pH values adjacent to anodes and cathodes of 2 and 12, respectively. These extreme pH values can have geochemical effects such as precipitation of contaminant ions and dissolution of calcium carbonate in the soil. By neutralizing the electrode reactions, the dissolution of the soil and the build up of precipitates in the pores in the of the soil, which could hinder electromigration, can be minimized.

A series of pH sensors, transmitters, controllers, and chemical feed pumps monitored and controlled the pH of the recycle water (Figure 4-7). A Cole-Parmer®[29] (Model 27001-97) pH electrode emitted a signal which was converted to a milliamp signal by a Jenco®[30] (Model 695PH) current transmitter. A Signet® 9030 pH controller in the control panel subsequently converted this signal to a pH value. The pH controller emitted a pulse signal at a rate proportional to the user specified pH set point, deviation range, and maximum pulse rate. The pulse signal controlled the pumping rate of a ProMinent®[31] (Model G/4a) chemical feed pump located on top of a 55-gallon, polypropylene drum adjacent to the EK demonstration site. This drum contained either 10 wt% NaOH to control the pH in the anodes or 20 wt% acetic acid for cathode pH control. A 30 psi stainless steel pressure relief valve provided adequate back pressure of the neutralization solution to prevent siphoning of the solution into the electrode.

4.2.5 Monitoring System

A CR7 data logger (Campbell Scientific®, Inc.) recorded the operating parameters of the EK demonstration and automatically shut the system down and notified the operators if any parameters were out of tolerance. The data logger monitored operational parameters at one-minute intervals and stored the average of each of these parameters in a storage module each hour. If a measured parameter was out of tolerance during a one-minute reading, the data logger would store that set of parameter readings on the storage module and send a coded message, identifying the type of problem, via a cellular phone to two separate pagers held by two operators.

The data logger monitored the vacuum level and the air purge rate for the vacuum system (Section 4.2.1). The system would shut down if the vacuum level was below 3 inches of Hg (the required vacuum to keep the water column in the EK electrode under tension) or if the air purge rate of the cathodes was below 3.5 liters per minute (the minimum rate necessary to dilute the hydrogen gas to 4%).

---

[29] Cole-Parmer® is a registered trademark of Cole-Parmer Instrument Company

[30] Jenco® is a registered trademark of Jenco Electronics, Ltd.

[31] ProMinent® is a registered trademark of ProMinent Fluid Controls, Inc.

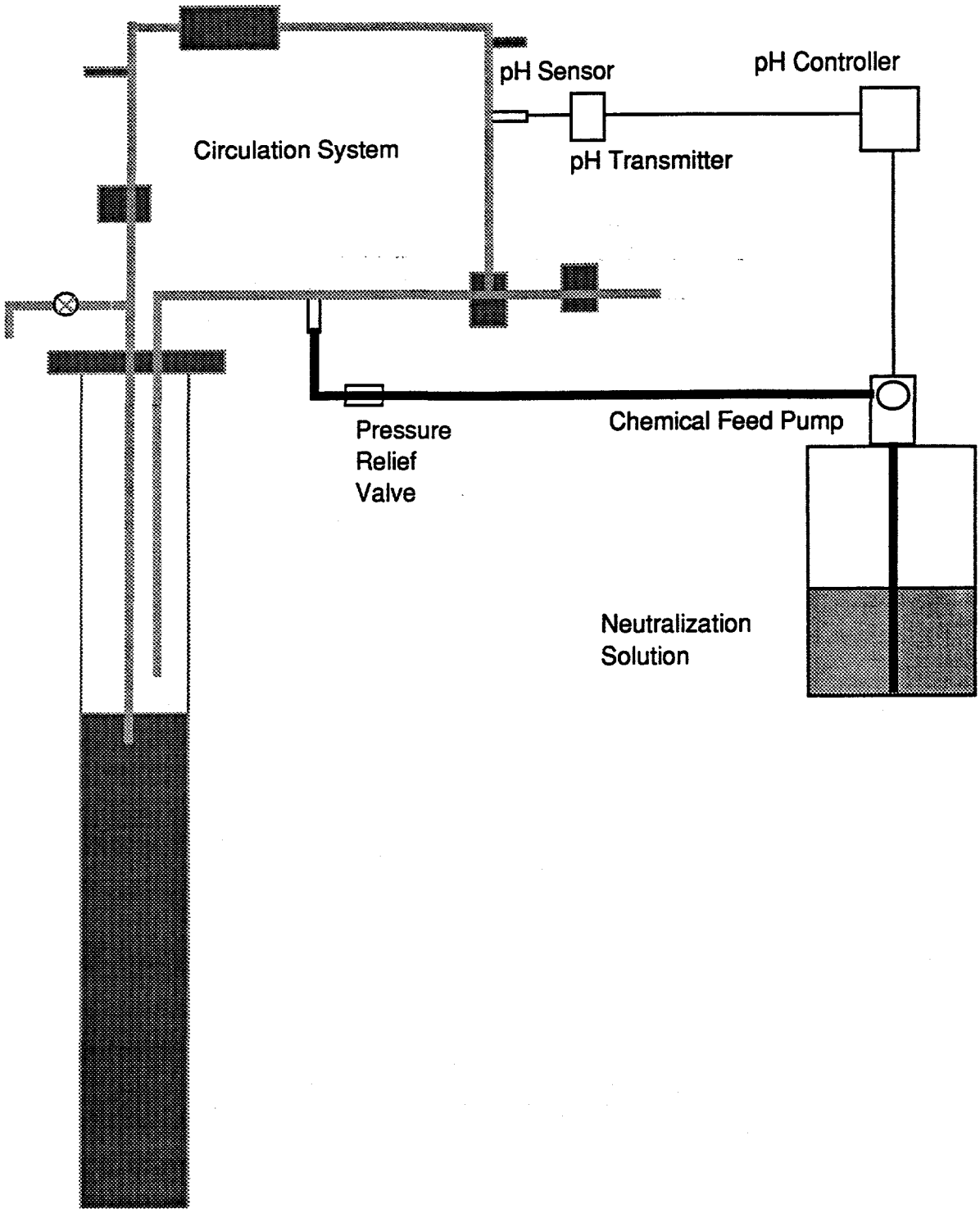

Figure 4-7. pH control system.

The influent, effluent, and recycle rates, water temperature, conductivity, and high-low water level alarms were monitored for the liquid circulation system (Section 4.2.2). The influent, effluent, and recycle rates were qualitatively recorded by the CR7. It was originally thought that quantitative numbers could be obtained, but stray voltages produced some false readings by the CR7. To compensate for the lack of automatic recording of flow data, readings were recorded manually from the control panel meters approximately once per day. Of the three flow sensors, only the recycle rate would activate the CR7 alarm system if no recycling was detected. An electrode water temperature of over 60 °C would trigger an alarm response. The high and low water alarm floats (Figure 4-5) would also activate the CR7 alarm system if either float was switched from its normal position. The current for each electrode also was recorded by the CR7 through the power system (Section 4.2.3), but no alarms were necessary.

The pH of each electrode was also monitored. An alarm was activated if any cathode pH was less than 3 or greater than 11 or any anode pH was less than 5.5 or greater than 11. The lower pH level of the anodes was set higher than the cathode pH level due to the treatment of the ceramic on the anodes (see Section 4.2). At low pH levels the ceramic treatment could have desorbed from the ceramic surface.

In addition to monitoring each individual EK electrode, the CR7 also recorded some field measurements. The soil temperatures immediately outside of the active EK electrodes, as well as an additional fourteen temperature locations in the field (see Figure 3-14 and 3-19 and Table 3-3 for locations) were monitored. Temperatures over 60 °C would shut down the process and notify the operators.

A series of 27 voltage probes also was monitored by the CR7. These voltage probes consisted of stainless steel screens placed in the ground and connected to voltage divider devices so that the voltages could be recorded by the CR7. The only alarm activation would have been a measurement of a step potential over 10 volts at a location approximately 8 feet west of the EK demonstration (see Figure 4-1).

The CR7 data logger also monitored a number of secondary containment float detectors for leaks, full effluent barrel sensors, an alarm which indicated an open gate to the green house exclusion zone, and a "panic" button shut down of the system. If any of the above described sensors were activated, the system would be shut down and the operator notified.

An automatic shutdown controlled by the CR7 consisted of turning off the power to the EK electrodes, closing the water influent valves, de-energizing all influent and effluent solenoids, and discontinuing the pumping of neutralization solutions to the electrodes. In some cases, pumping the electrode water through the recycle board would also be terminated.

5. ELECTROKINETIC OPERATIONS

Thirteen electrokinetic tests were performed during the Sandia electrokinetic field demonstration. Parameters such as anode/cathode geometry, cathode type, applied voltage gradient, anode electrolyte adjustment, and water infiltration to the soil were varied to evaluate chromate removal efficiency.

5.1 Summaries of Test Operating Parameters

The electrokinetic demonstration was operated for 6½ months (from May 15 to November 24, 1996). A counter recorded the cumulative hours that current was applied to the soil. The total run time for the demonstration was 2757 hours (i.e., approximately 60% of the total time). Future tables and graphs show either the counter reading (i.e., at the beginning of a test) or the run time (i.e., the amount of time current was applied to the soil). Down time (i.e., non-operational hours) was due to equipment failure, automatic shutdowns, switching distribution lines between tests, chemical sampling, effluent barrel removal, and weekly monitoring of the soil moisture.

Tests were designed to examine different operating parameters and energized electrode geometries. Table 5-1 lists the thirteen tests, the testing area, an abbreviated description of the operational parameter being changed for that particular test, and the test type category. These tests can be placed into five major testing categories: initial, electrode configuration changes, power application adjustments, electrolyte fluid adjustments, and soil adjustments.

Table 5-1. Description of Test Summary

Test #	Test Area	Remarks	Category				
			Initial	Config.	Power	Electro-lyte	Soil
1-1	Southern Zone	Initial testing of the system	X				
1-2		Removed A2 (inefficient)		X			
1-3		Removed C7 (corresponding to A2)		X			
1-4		Increased current			X		
1-5		Increased effluent flow rate				X	
1-6		Decreased power			X		
2-1	Northern Zone	Started using simpler cathodes (cold fingers)	X				
2-2		Decreased power, reduced effluent rate			X		
2-3		Infiltrated water					X
2-4	S 1/2 of North. Zone	Moved cathodes to northern set of cold fingers		X			
3-1	Southern Zone	Reran Test 1-6 to collect missing soil gas data	X				
3-2	N 1/2 of South. Zone	Moved cathodes to southern set of cold fingers		X			
3-3	Mid Portion	Used cold fingers on both sides of the anodes		X			

As seen in Table 5-1, many of the tests involved changing the energized electrode configuration and/or type of electrode being used. Most of these changes were intentional; however, some of them were due to equipment failure and problems with soil heating. These changes are illustrated in Figure 5-1 and summarized in Table 5-2.

The process information for each test is listed in Table 5-3. This information includes the total time current was applied to the soil for the test, average current applied to the electrodes, average voltage differential between anodes and cathodes, average power applied, and information pertaining to the rate and volume of effluent extracted from the anodes. The process information given is the average value for all of the electrodes for each test.

Although the overall process information listed in Table 5-3 gives the big picture, these numbers may not reflect the major parameter for each electrode if one of the electrodes was not operating properly. Table 5-4 lists the average current, voltage, resulting power, and average extraction rate for each of the operating anodes. The differences between the average parameter values given in Table 5-3 and the specific values for the anodes given in Table 5-4 will be discussed in more detail in the following text.

5.2 Tests Conducted in the Southern Zone

Six tests were initially conducted on the Southern Zone of the demonstration site and are designated as the Phase 1 testing. This early testing had a two-fold purpose. The first purpose was to allow operators to learn the system, its strengths and pitfalls, and how to handle and manage all of the interconnected systems. The second purpose was to determine the optimal operating conditions for a long-term test (Phase 3).

5.2.1 Test 1-1: Initial Operation of the System

The first test of the electrokinetic extraction system commenced on May 15, 1996. The purpose of this test was to provide initial extraction rate data and to ensure that all of the equipment was operating correctly. This test operated with all five ceramic-cased anodes (A1-A5) in conjunction with the five southern ceramic-cased cathodes (C6-C10) (see Figure 5-1).

The anodes and cathodes were operated in a similar manner with the exception that the cathode electrolyte pH levels were conditioned to be more acidic than the anode electrolyte fluid. The pH of the cathode electrolyte fluid was maintained at approximately 6.5 to 7, whereas the anode electrolyte fluid pH was maintained at a higher level of 8.5 to 9. As discussed in Section 4.2.4, the electrolysis reaction at the cathode produces hydroxyl ions. If not conditioned, the cathode's porous ceramic casing was expected to clog due to precipitation reactions. Therefore, the electrolyte fluid in the cathode ceramic casings was maintained at neutral to slightly acidic.

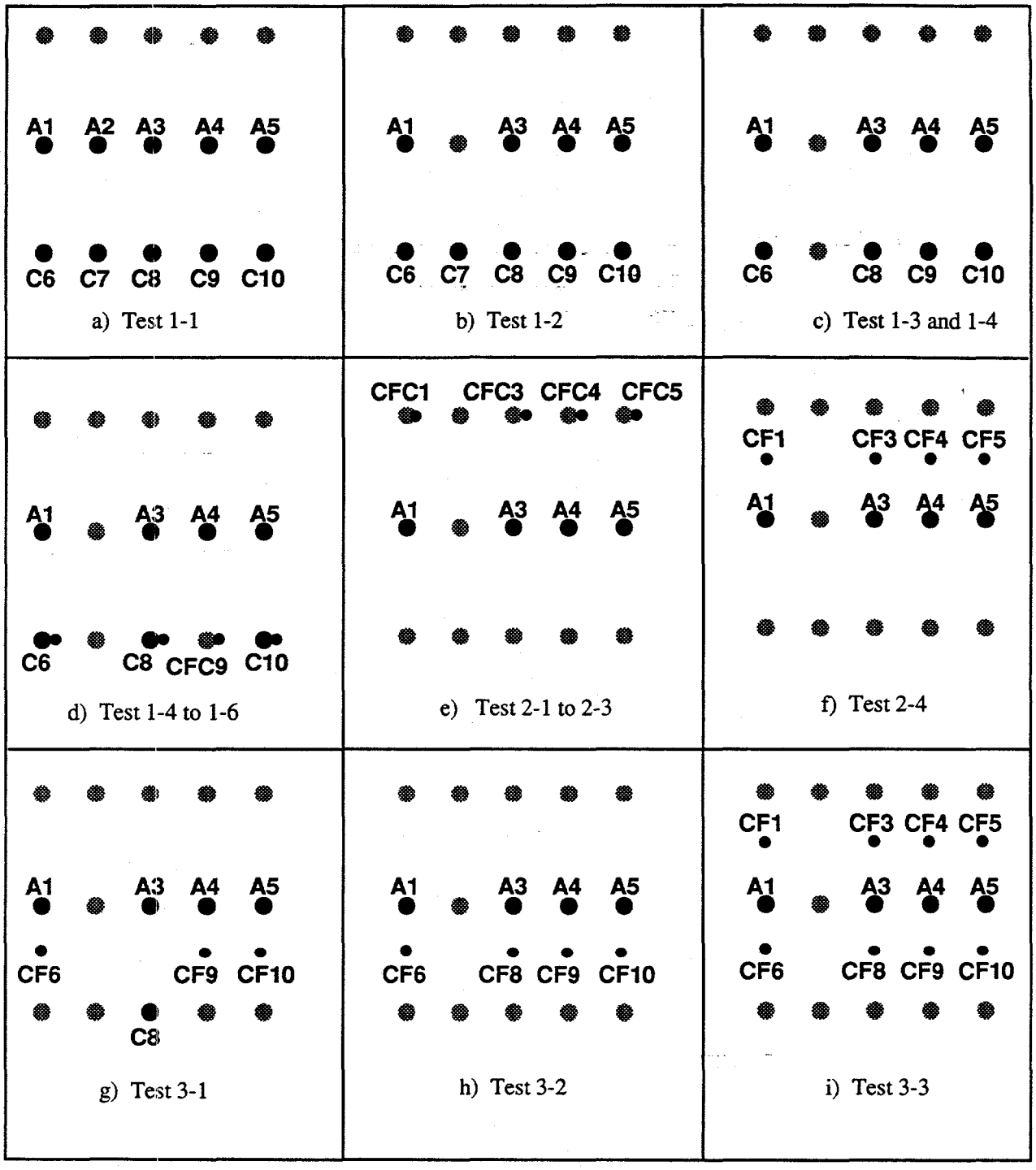

Figure 5-1. Configuration of anodes and cathodes that were active for each test.

Table 5-2. Power Distribution Configuration

Date	Counter Reading	Figure 5-1	Power Distribution Configuration
5/15/96	0	a	Start of Test 1-1. Parallel Interface Controller (PIC) used to maintain constant voltage potential at all paired electrodes (i.e., A1/C6, A2/C7, A3/C8, A4/C9, A5/C10)
5/28/96	108	b	Start of Test 1-2. Reconfigured power distribution system to remove A2
6/26/96	485	c	Start of Test 1-3. Reconfigured power distribution system to remove C7
7/08/96	555	c	Reconfigured power distribution system (due to PIC failure) to PS1 to A1/C6 and PS2 to the remaining pairs
7/22/96	774	c	Start of Test 1-4. Reconfigured power distribution system to PS1 to A1/C6, PS2 to A3/C8, PS3 to A4/C9, and PS4 to A5/C10 to boost the power output
7/27/96	835	d	Switched power application from C9 to CFC9 (air leak in ceramic)
8/06/96	962	d	Paralleled power between C6 and CFC6, C8 and CFC8, and C10 and CFC10 (to stop CF corrosion)
8/09/96	1030	d	Start of Test 1-5
8/12/96	1065	d	Start of Test 1-6
8/22/96	1246	e	Start of Test 2-1. Reconfigured power distribution system to PS1 to A1/CFC1, PS2 to A3/CFC3, PS3 to A4/CFC4, and PS4 to A5/CFC5
8/26/96	1322	e	Start of Test 2-2
8/30/96	1411	e	Start of Test 2-3
9/26/96	1744	f	Start of Test 2-4. Reconfigured power distribution system to PS1 to A1/CF1, PS2 to A3/CF3, PS3 to A4/CF4, and PS4 to A5/CF5
10/10/96	1920	g	Start of Test 3-1. Reconfigured power distribution system to PS1 to A1/CF6, PS2 to A3/C8, PS3 to A4/CF9, and PS4 to A5/CF10
10/11/96	1940	h	Start of Test 3-2. Reconfigured power distribution system to PS1 to A1/CF6, PS2 to A3/CF8, PS3 to A4/CF9, and PS4 to A5/CF10
10/18/96	2051	i	Start of Test 3-3. Reconfigured power distribution system to PS1 to A1/CF1&CF6, PS2 to A3/CF3&CF8, PS3 to A4/CF4&CF9, and PS4 to A5/CF5&CF10.
11/24/96	2757		End of Demonstration.

Note: PS = power supply; Ax = anode x; Cx = cathode x; and CF = Cold Finger

Table 5-3. Summary of the Testing Parameters

Run No.	Run Time (hr)	Average Applied Current (A)	Average Applied Voltage (V)	Average Applied Power (kW)	Cumulative Effluent Flow Rate (L/h)	Volume of Effluent Removed (L)
1-1	108	18	67	1.2	1.7	186
1-2	377	23	80	1.8	0.9	344
1-3	289	20	88	1.7	0.9	259
1-4	256	37	146	5.1	2.3	596
1-5	35	48	141	6.6	3.5	123
1-6	181	39	114	4.3	3.9	714
2-1	76	34	142	4.9	3.3	250
2-2	89	22	88	2.0	1.6	144
2-3	333	21	88	1.9	2.3	787
2-4	176	32	88	2.9	2.1	373
3-1	20	36	76	2.6	2.0	40
3-2	111	41	76	3.0	2.3	251
3-3	706	38	59	2.2	2.2	1552
Total	**2757**					

Table 5-4. Test Matrix Details

Test Area	Test #	Average Current Applied to Each Electrode (A)					Average Voltage per Electrode (V)					Average Power Applied to Each Electrode (kW)					Average Effluent Rate from Electrode (L/hr)				
		A1	A2	A3	A4	A5	A1	A2	A3	A4	A5	A1	A2	A3	A4	A5	A1	A2	A3	A4	A5
Southern Zone	1-1	4.2	7.5	1.8	1.4	3.0	67	67	67	67	67	0.28	0.49	0.22	0.09	0.19	0.40	0.43	0.30	0.25	0.34
	1-2	11.9		5.5	1.9	3.8	80		80	80	80	0.95		0.44	0.15	0.30	0.22		0.26	0.17	0.26
	1-3	11.8		3.5	1.5	2.9	88		88	88	88	1.04		0.31	0.14	0.26	0.21		0.26	0.18	0.24
	1-4	13.0		7.5	8.1	8.4	79		167	170	170	1.04		1.25	1.38	1.43	1.24		0.44	0.31	0.33
	1-5	12.9		10.7	12.7	11.3	65		160	170	170	0.84		1.71	2.16	1.92	1.15		0.97	0.63	0.77
	1-6	11.3		11.5	8.8	7.3	65		130	130	130	0.73		1.49	1.14	0.94	1.28		1.07	0.83	0.77
Northern Zone	2-1	8.3		10.2	7.2	8.6	104		155	155	155	0.88		1.58	1.12	1.33	1.04		0.97	0.68	0.60
	2-2	4.0		7.4	4.8	5.8	50		100	100	100	0.20		0.74	0.48	0.58	0.33		0.46	0.52	0.27
	2-3	4.1		6.6	4.6	5.5	50		100	100	100	0.20		0.66	0.46	0.55	0.55		0.52	0.45	0.76
South 1/2 of Northern Zone	2-4	6.7		8.2	8.0	9.2	50		100	100	100	0.34		0.82	0.80	0.92	0.52		0.63	0.46	0.52
Southern Zone	3-1	13.2		6.6	6.4	9.3	50		85	85	85	0.66		0.56	0.54	0.79	0.48		0.57	0.57	0.38
North 1/2 of Southern Zone	3-3	13.7		7.7	8.1	11.3	50		85	85	85	0.69		0.66	0.69	0.96	0.56		0.55	0.42	0.73
Mid Portion	3-3	9.9		9.3	8.2	10.3	40		65	65	65	0.40		0.60	0.54	0.67	0.57		0.64	0.44	0.55

5.2.2 Test 1-2: Removal of Inefficient Anodes

The results of Test 1-1 showed that A2 was performing below the average of all of the electrodes. Therefore, in order to increase the chromium removal efficiency of the overall system, A2 (the anode with the lowest chromate removal rate) was disconnected from the power grid in an attempt to redirect the current to zones which exhibited higher extraction efficiencies of chromium removal. Figure 5-1 illustrates the configuration of the four anodes and the five cathodes for Test 1-2.

In addition, the effluent in A2 was emptied into the effluent collection barrel, and no soil cooling was maintained for this electrode location for the remainder of the demonstration. However, the applied vacuum within this electrode was maintained allowing A2 to hydraulically extract water from the soil. Soil pore water in the vicinity of A2 with soil water potentials above the applied vacuum would be hydraulically transported into the A2 porous casing.

The cathode operating system was not modified from Test 1-1.

5.2.3 Test 1-3: Removal of Inefficient Cathode

During Test 1-2, C7 supplied over 60% of the current. Removing this conductive electrode was expected to result in a more equal distribution of the current; therefore, C7 was disconnected from the power supplies. Unfortunately, seventy hours into Test 1-3 the parallel interface controller (PIC) for the 4 power supplies failed. This failure allowed little time for a steady- state comparison of Tests 1-2 and 1-3 with the same power distribution system.

Due to the uncertainty of the length of time for repairs to the PIC and a tight time schedule, the power distribution system was redesigned. The redesigned power distribution system created a system similar to that with the PIC but with a slight modification and incorporated only two of the existing four power supplies. The first power supply, identified as PS1 in Table 5-2, was connected to A1 and C6. The second power supply supplied power to A3, A4, and A5 in parallel, with the returns from C8, C9, and C10 also in parallel. The main difference between the new power distribution system and the PIC system is the current between C6 and A1 was isolated from the other set of cathodes and anodes where current could flow between any cathode/anode combination. Although the power distribution system was modified, the results of this test were not considered to be affected greatly.

5.2.4 Test 1-4: Increase in the Applied Voltage/Power

Test 1-4 examined the effect of increasing the power on the overall efficiency of chromium extraction. By increasing the voltage, the overall current and, hence, the applied power to the demonstration increased. The voltage to the pairs A3/C8, A4/C9, and A5/C10 was approximately doubled. However, due to the apparently high electrical conductivity between A1 and C6, the voltage applied to A1/C6 remained the same.

To increase the power, the power distribution system had to be modified from Test 1-3. Individual power supplies were connected to single anode/cathode pairs (see Table 5-2). The remainder of the demonstration was conducted by manually adjusting the voltage gradient between each anode/cathode pair, allowing individual control for each pair (as was the case with A1/C6 for Test 1-3).

In addition to the modification to the power distribution system, the application of current was switched from C9 to the simpler cold finger (CFC9) at the same location approximately 61 hours into the test. The ceramic casing for C9 developed an air leak, causing false high water alarm shutdowns. Unlike the termination of A2, the fluid in C9 was allowed to continue to circulate through the heat exchanger, thereby continuing to cool the soil in the area.

Also during this test, it was speculated that the cold fingers attached to the outside of the cathode ceramic casings were electrically corroding due to the applied current. Near the end of Test 1-4, the internal electrodes of the remaining operating electrodes C6, C8, and C10 were connected to the associated cathode cold finger to keep the cold fingers from deteriorating further. Energizing the cold fingers associated with the cathodes was not expected to affect significantly the chromate extraction results at the anodes.

5.2.5 Test 1-5: Increase in the Effluent Extraction Rate

Test 1-5 examined the possibility of ion back diffusion out of the anode due to concentration gradients. The effluent extraction rates were increased in an attempt to lower the chromium concentrations in the anodes to study this hypothesis. However, Test 1-5 was terminated after 35 hours of operation due to increasing soil temperatures and provided little information for comparison.

5.2.6 Test 1-6: Decrease in the Applied Voltage/Power

Due to increased voltage/power in Tests 1-4 and 1-5, the temperature of the soil between the electrodes increased. Test 1-6 continued the high effluent extraction rates of Test 1-5, but the applied voltage (hence power) was lowered to keep the soil temperatures within acceptable ranges. The voltage was reduced to 130 volts for electrodes A3-A5. A1 remained at 65 volts, approximately ½ the voltage applied to the rest of the anodes (Table 5-4).

5.3 Tests Conducted in the Northern Zone

Although power to the remediation area was decreased, the soil temperatures did not drop in the Southern Zone; therefore, the remediation area was moved to the Northern Zone of the demonstration site. While operating in the Northern Zone, designated Phase 2 of the demonstration, the Southern Zone soil temperatures were monitored as the soil cooled.

Furthermore, the success of using the cathode cold fingers paralleled with the internal cathodes in Tests 1-4 through 1-6 led to abandoning the complex cathode extraction electrodes in favor of the simpler cathode cold-finger design (see Section 3.2.4.7). No liquid from the soil was removed or exchanged in the cold finger design. No pH control was applied to the cold finger design.

5.3.1 Test 2-1: Initial Baseline Testing in the Northern Zone

Test 2-1 was conducted to provide a baseline of measurements for the Northern Zone of the demonstration. The four anodes (A1, A3-5) were used in the same manner as previously discussed, but the four corresponding cathodes were the cold fingers attached to the C1, C3-5 ceramic electrode casings (Figure 5.1.e). The anodes were pumped out prior to the start of Test 2-1 and refilled with non-contaminated water.

The electrode power distribution configuration continued as two sets during Phase 2, the A1/CFC1 pair and the A3-A5/CFC3-CFC5 pairs. The power supply set voltage was the same for the three eastern pairs throughout Phases 2 and 3. The western anode/cathode pair was operated independently due to the apparently high electrical conductivity in that area. The applied power was approximately 4 kilowatts.

5.3.2 Test 2-2: Decrease in the Applied Voltage and Effluent Extraction Rate

Test 2-2 continued to use the same cathode/anode pairs as in Test 2-1, but the power was reduced by approximately half (4.1 to 1.9 kW). The power was reduced to minimize the effect of soil heating between the anodes and the cathodes. The same cathode-anode configuration was maintained. The effluent extraction rate was also reduced.

5.3.3 Test 2-3: Infiltration of Water to Zones of Low Soil Electrical Conductivity

Water was added to a series of infiltration wells, spaced between the anodes and the northern cathodes, in an attempt to redirect the current pathway through zones of higher contamination. It was speculated that the current was traveling through the upper portion of the demonstration area where the soil exhibited a higher electrical conductivity than the lower portion.

Water was injected though the infiltration wells at ten run times for Test 2-3 (Table 5-5). The first two injections included wells that were between adjacent cathodes or anodes (i.e., well I1-4 and I19-22) (see Figure 3-16). The remaining eight injections used only the wells between the northern set of cathodes and the anodes (i.e. I5-18). In general, all the injection wells received 600 ml of water per injection except I8 and I9. These two filled up with only 350 to 500 ml, possibly indicating lower permeable soil in this area.

Table 5-5. Location and Amount of Water Injected

Date	Counter Reading	Wells and Amounts	Comments
8/30	1410	I1-I22 @ 0.6 L each	
9/4	1439	I1-I22 @ 0.6 L each	
9/5	1462	I5-I18 @ 0.6 L each	
9/6	1484	I5-I18 @ 0.6 L each	
9/9	1550	I5-I18 @ 0.6 L each	except I8 @ 0.4 L
9/10	1557	I5-I18 @ 0.6 L each	except I8 @ 0.4 L, and I9 @ 0.5 L
9/11	1583	I5-I18 @ 0.6 L each	except I8 @ 0.35 L, and I9 @ 0.5 L
9/12	1606	I5-I18 @ 0.6 L each	except I8 @ 0.35 L, and I9 @ 0.5 L
9/13	1627	I5-I18 @ 0.6 L each	except I8 @ 0.35 L, and I9 @ 0.5 L
9/16	1698	I5-I18 @ 0.6 L each	except I8 @ 0.4 L, and I9 @ 0.55 L

5.3.4 Test 2-4: Reducing the Distance Between Anodes and Cathodes

For Test 2-4, the cathode location was moved to the set of cold fingers placed midway between the anodes and the previous set of cathodes (Figure 5-1f). This test was designed to determine if it is efficient to add new sets of cold fingers to the system in an attempt to "herd" the contaminants towards the anodes. These field cold fingers, designated as CF1-5 in Figure 3-21, were shorter and smaller than those attached to the electrode casings (see Section 3.2.4.7).

5.4 Revised Southern Zone Testing

While tests were performed in the Northern Zone of the demonstration, the Southern-Zone soil temperatures cooled to a sufficient level to restart the testing. These tests are designated Phase 3.

5.4.1 Test 3-1: Collecting Cathode Exhaust Gas and Effluent Samples

Test 3-1 was operated with the same anode set as in Phase 2, but the cathode locations were changed to three cold fingers (CF6, CF9, and CF10) and the C8 extraction electrode (Figure 5-1g). The sole purpose of Test 3-1 was to collect a gas and effluent sample from the C8 electrode (a permit regulatory requirement).

5.4.2 Test 3-2: Testing the Cold Fingers in Southern Zone

The C8 electrode was changed to the cold finger CF8 for Test 3-2 (Figure 5-1h) so that the anode/cathode geometry would be similar to that in Test 2-4.

5.4.3 Test 3-3: Long-Term Testing of Electrokinetic Remediation

Two sets of cathodes, one on either side of the anodes, were powered in parallel for Test 3-3. The cathodes were those used in Test 2-4 (CF1, CF3-5) and in Test 3-2 (CF6, CF8-10) (Figure 5-1i). A full size remediation process would most likely incorporate this type of geometry and cathode system.

This test operated the longest of any of the electrokinetic tests, 706 hours, approximately 25% of the total operation time.

6. DISCUSSION

Many parameters of the EK demonstration were modified to explore the principles and efficiencies of operation. Section 6.1 details the results of the various tests discussed in Section 5 and considers the effects on removal rates and extraction and energy efficiencies. Section 6.2 details the post-test soil sampling results by examining the soil electrical conductivity, pH, moisture content, and chromium content, and by comparing the post-test results to the pretest results. In addition, a look at post-test soil acetate concentrations as a tracer for the current pathways is discussed. The next several sections discuss transference number predictions, soil heating ramifications, voltage gradient distributions, buried metal problems, and organic compound concentrations.

6.1 Electrokinetic Testing

A summary of the EK testing results and the effects of modifications are given below. First, an overview of all of the tests including the run times, the power applied, and the removal rates and efficiencies are summarized. The initial results of applying current to the remediation zone confirmed that chromium was transported away from the cathodes and towards the anodes. The extraction efficiencies were seen to vary from one electrode to another, most likely the result of varying transference numbers in the soil. Increasing power densities resulted in increasing chromium removal rates; however, the cost considerations are also important. Variations in the extraction removal rates, the soil moisture contents, and the electrode configurations are also discussed.

6.1.1 Overview of Electrokinetic Testing

Tables 6-1 and 6-2 list calculated operating conditions and removal rates for the thirteen tests described in Section 5. The rates are defined as removal rate, extraction efficiency, and energy efficiency, respectively (see Section 2 for definitions and theoretical discussions). Overall totals for these variables are listed in Table 6-1, whereas Table 6-2 lists the operating conditions and rates for each anode. The amount of applied charge (amp-hrs) and energy (kw-hrs) were calculated from data collected by the CR7 data logger. The amount of charge distributed at each electrode was calculated by summing the measured current for each operational hour to obtain amp-hours. Kilowatt-hours were calculated in a similar manner by summing the product of the voltage and amps for each hour of operation.

Table 6-1. Summary of Testing Results

Run No.	Run Time (hr)	Total Amount of Charge Applied (A-hrs)	Total Amount of Energy Applied (kW-hrs)	Ave. Soil Temp. N. Zone (°C)	Ave. Soil Temp. S. Zone (°C)	Cr(VI) Removed (g)	Cr(VI) Removal Rate (g/hr)	Cr(VI) Extraction Efficiency (g/A-hr)	Cr(VI) Energy Efficiency (g/kW-hr)
1-1	108	1897	127		15	7.8	0.072	.0041	0.061
1-2	377	8487	676		16	35.7	0.095	.0042	0.053
1-3	289	5586	493		17	22.5	0.078	.0040	0.046
1-4	256	9044	1245		30	56.0	0.219	.0062	0.045
1-5	35	1663	232		48	11.5	0.329	.0069	0.050
1-6	181	7556	839		43	38.9	0.215	.0051	0.046
2-1	76	2574	369	25	39	11.1	0.146	.0043	0.030
2-2	89	1999	182	30	33	9.0	0.101	.0045	0.049
2-3	333	6943	626	28	26	61.6	0.176	.0089	0.098
2-4	176	5665	507	25	25	36.0	0.204	.0064	0.071
3-1	20	745	54	21	30	4.7	0.235	.0063	0.087
3-2	111	4525	331	19	42	25.4	0.229	.0056	0.077
3-3	706	26781	1572	21	35	203.7	0.289	.0076	0.130
Total	**2757**					**523.9**			

Table 6-2. Chromium Data

Test Area	Test #	Average Concentration in Electrodes (mg/L)					Total Mass Removed from Electrodes (g)					Regressed Extraction Efficiency of Electrodes (mg/A-hr)					Regressed Energy Efficiency of Electrodes (mg/kW-hr)				
		A1	A2	A3	A4	A5	A1	A2	A3	A4	A5	A1	A2	A3	A4	A5	A1	A2	A3	A4	A5
Southern Zone	1-1	43.1	13.9	46.2	63.4	57.2	1.9	0.6	1.5	1.7	2.1	2.7	0.5	5.3	9.9	5.1	41.0	9.7	79.7	147.6	75.8
	1-2	52.2		97.0	127.3	55.2	6.6		12.8	11.4	7.5	1.7		5.5	17.1	5.9	21.1		69.8	215.2	74.3
	1-3	31.9		19.8	62.0	17.6	6.0		4.1	8.8	3.6	1.8		4.2	20.1	4.3	21.4		47.6	228.9	48.4
	1-4	61.5		68.9	448.0	71.0	18		6.9	32.1	5.5	3.7		3.9	18.3	2.8	46		23.0	107.9	16.3
	1-5	23.4		27.7	272.2	64.5	1.2		1.1	7.2	2.0	2.8		2.9	16.4	5.1	43.2		18.2	96.7	30.2
	1-6	21.4		24.4	146.5	51.0	5.6		5.1	21.3	6.9	2.5		2.2	12.2	4.8	38.2		17.3	93.5	37.2
Northern Zone	2-1	13.9		21.4	87.8	45.4	1.3		2.1	5.0	2.8	2.0		3.3	9.2	4.4	19.3		17.5	59.7	28.3
	2-2	39.4		47.6	75.1	119.9	1.2		2.0	3.0	2.9	3.2		3.0	6.6	5.2	64.1		30.5	66.2	52.3
	2-3	46.0		77.7	133.7	71.8	8.3		13.6	21.8	17.9	6.2		5.8	12.5	8.4	123.9		58.5	124.8	84.3
South 1/2 of Northern Zone	2-4	46.0		83.0	150.6	86.9	4.6		9.7	13.5	8.2	3.9		6.6	9.5	5.2	78.2		65.8	95.4	52.4
Southern Zone	3-1	81.9		113.9	172.9	53.6	0.6		1.3	2.2	0.6	2.3		9.4	16.2	3.0	46.8		110.6	190.1	35.9
North 1/2 of Southern Zone	3-2	72.2		93.9	211.4	83.9	4.5		5.3	10.3	5.4	2.8		6.0	11.8	4.2	56.3		70.3	138.8	49.4
Mid Portion	3-3	76.0		98.3	241.8	168.2	29.6		41.5	76.2	56.4	4.1		6.2	13.2	7.8	103.2		95.3	202.8	119.7

The mass of chromium removed from each electrode was calculated by two methods. To evaluate the chromate removal from each anode as a function of time, coulombs, and energy, anode electrolyte fluid samples were collected for chemical analysis, and the effluent volume in each of the effluent collection barrels was recorded approximately daily. The electrolyte samples were analyzed by an in-house colorimetric method for chromate (note that all water-soluble chromium is assumed to be chromate, Cr(VI)) and the results given as ppm chromium. The mass of chromium removed from each electrode during each time interval was calculated from the volume of effluent removed from the electrode since the last sampling event and the electrolyte chromium concentration. These masses were correlated to run hours, applied charge, and energy at each electrode and are reported in Tables 6-1 and 6-2.

Secondly, to determine the total amount of chromium removed by the electrokinetic demonstration, and as a check on the accuracy of the first method, an effluent sample was collected from each anode collection barrel. The sample was collected and the barrel volume was recorded when it was moved to the waste storage area. These samples were analyzed for total chromium concentrations by EPA method 6010 by Quanterra Laboratories, Denver, Colorado.

To evaluate chromate removal efficiencies, the first method of determining the chromium mass has the advantage of obtaining more data points as a function of time; however, the second mass calculation method is considered to be more accurate. The volume used to calculate the chromium mass for the first method is less accurate than the second method due to the smaller liquid volumes. A typical volume of water extracted from the anode would be on the order of 3 gallons (~12 L) with an estimated uncertainty of approximately 0.5 gallon. Conversely, a typical waste barrel contained approximately 50 to 55 gallons, allowing for a more accurate measurement of the effluent volume. In addition, the second method conforms to standard EPA methods and protocols for sample collection and analysis.

Results of calculating the chromium mass for the electrokinetic demonstration by the above described methods indicate that the mass of chromium removed by the first method underestimates the considered true mass, as determined by the second method, by approximately 13%. The total amount of chromium removed by the EPA total chromium analyses is 600.3 g Cr compared to 524 g Cr by the colorimetric method.

To determine the removal rates, the chromium mass data were calculated by the first mass calculation method. These mass data points were plotted as a function of hours, charge, and energy and linearly regressed to obtain a slope (i.e., removal rate) for each dependent variable. The rates listed in Tables 6-1 ands 6-2 are considered to be conservative estimates of the true rates for the reasons described above.

6.1.2 Initial Testing

Chromium concentration changes in the ceramic electrodes during the initial application of power to the electrodes imply that chromate was electrically transported from the cathode to the anode. During this time, no electrolyte fluid was removed from the electrodes except small samples for analysis. Figures 6-1 and 6-2 illustrate the chromium concentrations in the anodes and cathodes as a function of applied charge during the first 16 hours of testing. Prior to applying power to the electrodes within the porous ceramic casings, the initial concentrations of chromium in the electrolyte fluid ranged from 5 to 35 ppm. This chromium was the result of hydraulic flow of contaminated pore water into the electrode due to the applied vacuum in the ceramic casing to remove water present after installation (see Section 3.2.4.1). However, after the application of power, the chromium concentrations in the anodes increased (Figure 6-1) while the concentrations in the cathodes decreased (Figure 6-2). Anode chromium concentrations increased linearly (Figure 6-1) during this initial testing phase due to the electromigration of chromate ions into the anode casing. Cathode chromium concentrations, on the other hand, decreased in an exponential decay towards zero (Figure 6-2).

Both the rate of accumulation and the rate of depletion of chromate are related to the transference number of the chromate. The rate of chromate accumulation in the anode is based on the chromate transference number in the surrounding soil, whereas the rate of chromium depletion in the cathode is based on the electrolyte fluid composition in the cathode's porous ceramic casing. In other words, the rate of chromate transport is dependent on the transference number in the medium from which the chromate is moving (i.e., from the soil for the anodes and from the electrolyte fluid for the cathodes).

In addition, the shapes of the chromium accumulation/depletion curves (Figures 6-1 and 6-2) further support the locations at which transference numbers should be calculated. The transference number for each anode appears to be constant, as noted by the linear correlation between concentration and applied charge (Figure 6-1). At the anodes, the migration of chromate into the anode casings appears to be a function of the ionic composition of the pore water in the soil where there was an unlimited supply of chromate ions during this time period. In this case, chromate ions were continuously being added to the anode in relation to the transference number of the soil pore water independent of the transference number of the electrolyte fluid. In contrast, the transference numbers at the cathodes decrease with time, as seen by the exponential decay of the chromate concentration in Figure 6-2. Within the cathode electrode, the number of chromate ions was continuously becoming less while the number of other ions in the electrolyte fluid was increasing due to electrolysis reactions. Therefore, less and less of the current within the electrode was being transported by chromate ions as the EK process continued.

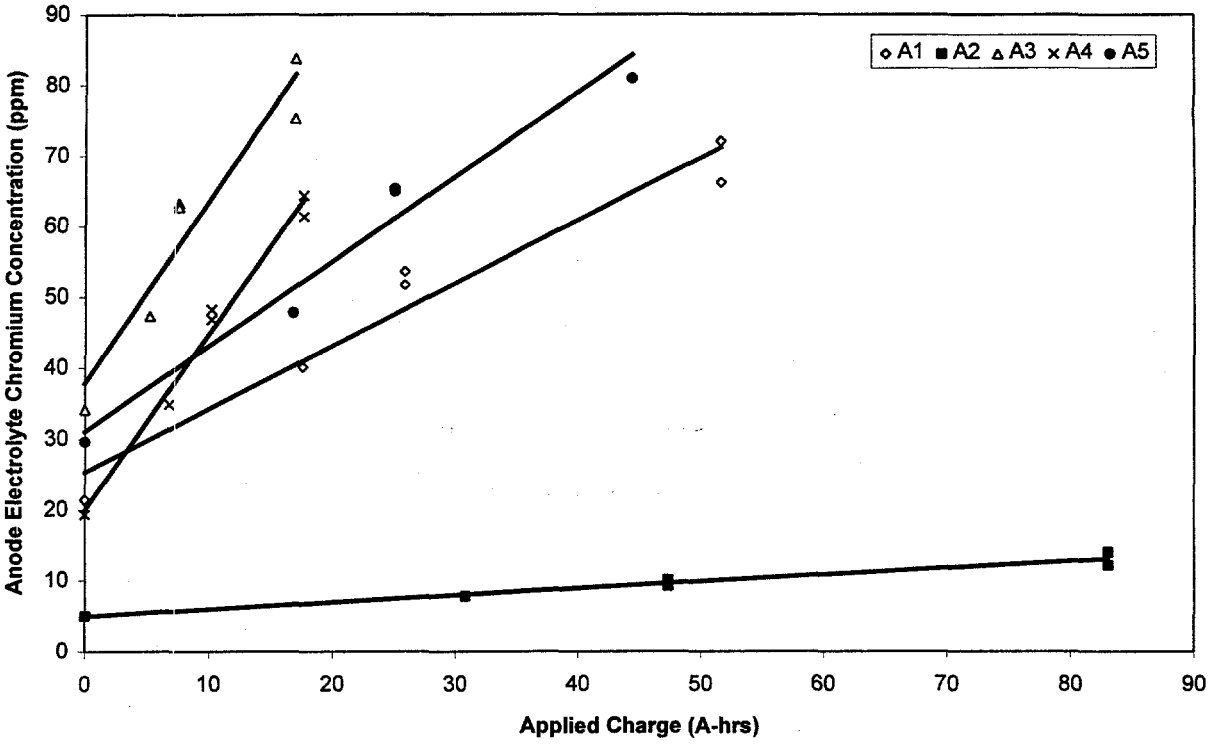

Figure 6-1. Chromate concentrations in anodes as a function of applied charge.

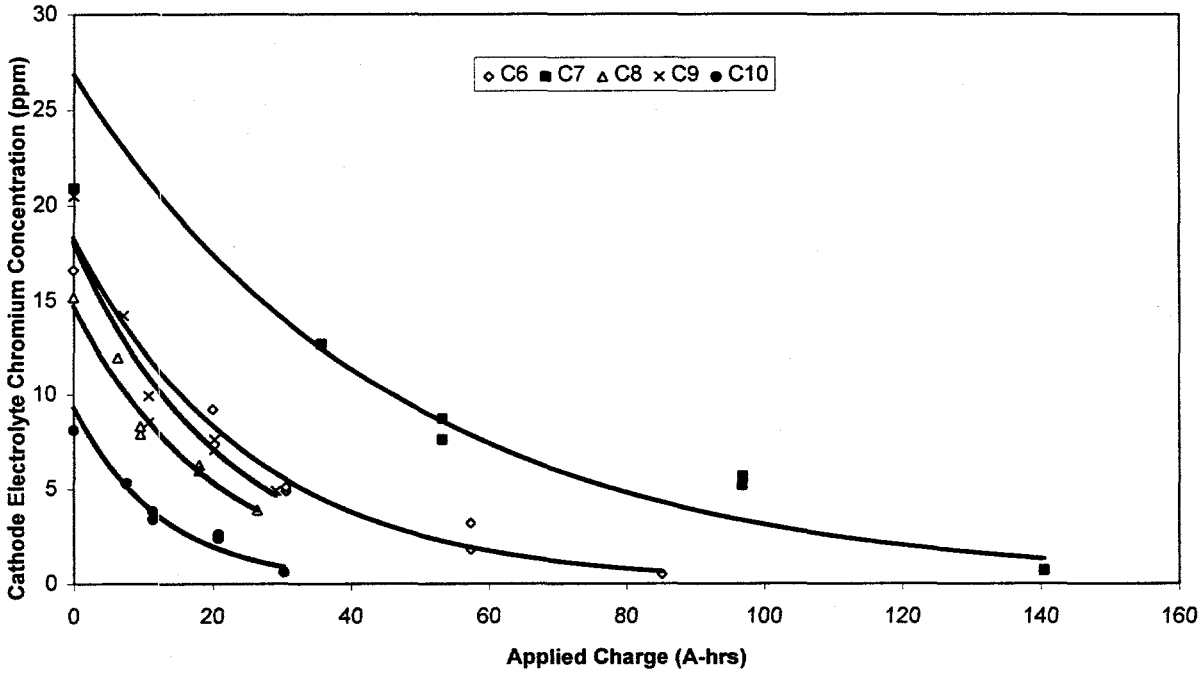

Figure 6-2. Chromate concentrations in cathodes as a function of applied charge.

6.1.3 EK Extraction Efficiency

As discussed in Section 2.3, the extraction efficiency describes the amount of chromate removed by the EK system per amount of current applied over some period of time. This section describes the overall efficiency of the electrokinetic demonstration and of the individual anodes.

Overall, the extraction efficiency did not change significantly throughout the 13 electrokinetic tests. Figure 6-3 illustrates the amount of chromate as grams of chromium removed from the soil as a function of applied charge. A quadratic line ($y = 2E\text{-}8x2 + 0.0045x$) was best fitted to the data set with a R^2 of 0.999; however, a linear regression ($y = 0.0058x$) also fit well with a R^2 of 0.987. The quadratic line indicated a weak increasing slope as a function of applied charge. In other words, the extraction efficiency increased slightly the longer the demonstration was operated. Although the relationship between extracted chromate and applied charge is expected to be linear, the slight change in slope may be due to spatial variability in the chromium distribution and/or temporal increases in the transference numbers due to injection of water (Test 2-3), as discussed in Section 6.1.6 below.

Chromium extraction efficiencies varied significantly between electrodes throughout the demonstration. Experimental data for the extracted chromate as a function of applied charge for each anode is plotted in Figure 6-4. As indicated by the slopes of the data sets, the extraction efficiency (the amount of chromium removed per amp-hour) varied greatly between electrodes and is likely related to differing chromium transference numbers in the soil (discussed in Section 6.3).

Although not readily apparent in Figure 6-4, the chromium extraction efficiencies do vary slightly between electrokinetic tests. Figure 6-5 illustrates the extraction efficiency of the four anodes (A1, A3-A5) as a function of the electrokinetic test. Most noticeable in Figure 6-5 is the domination of A4 for the removal of chromate. Secondly, the variations of the extraction efficiencies can also be seen between tests. Some of this variation can be explained by experimental changes discussed in the following sections, whereas other variations may be due to spatial variability or experimental measurement errors.

6.1.4 EK Energy Efficiency

Not surprisingly, application of increased power to the EK demonstration resulted in higher Cr removal rates (i.e., mg Cr per hour, Tables 5-3 and 6-1); however, the electrical cost per mass of chromium removed increased. As discussed in Section 2.4, care must be taken when examining EK efficiencies in terms of power and energy.

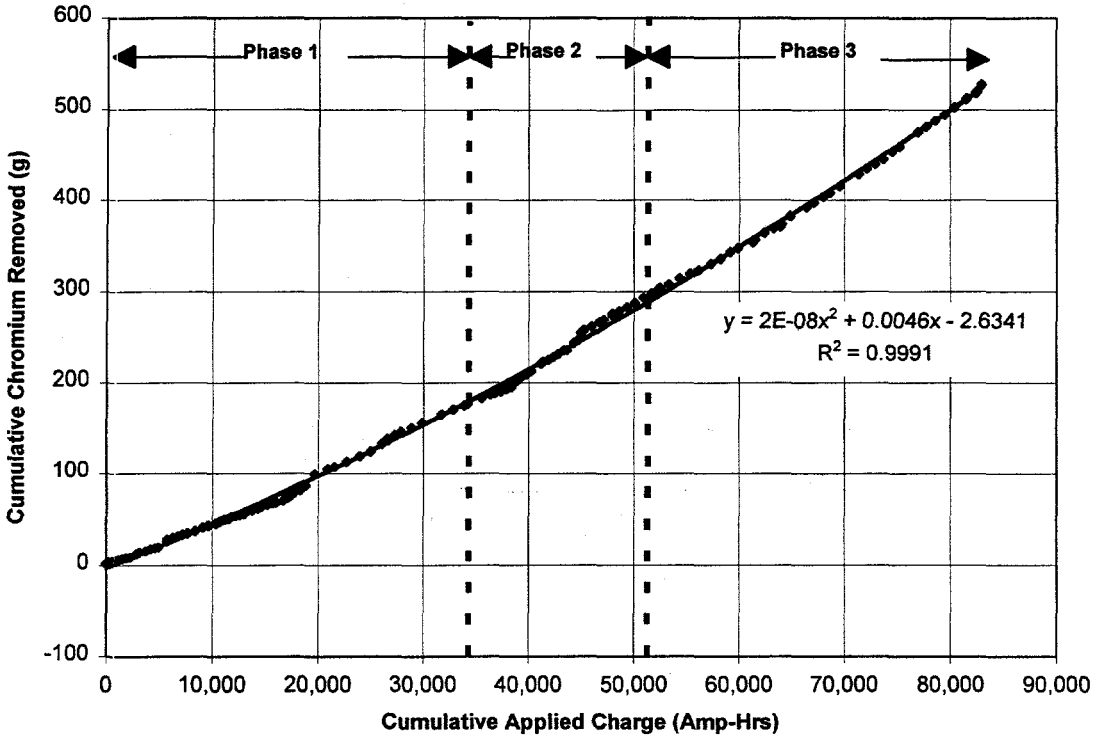

Figure 6-3. Cumulative chromium removal as a function of applied charge.

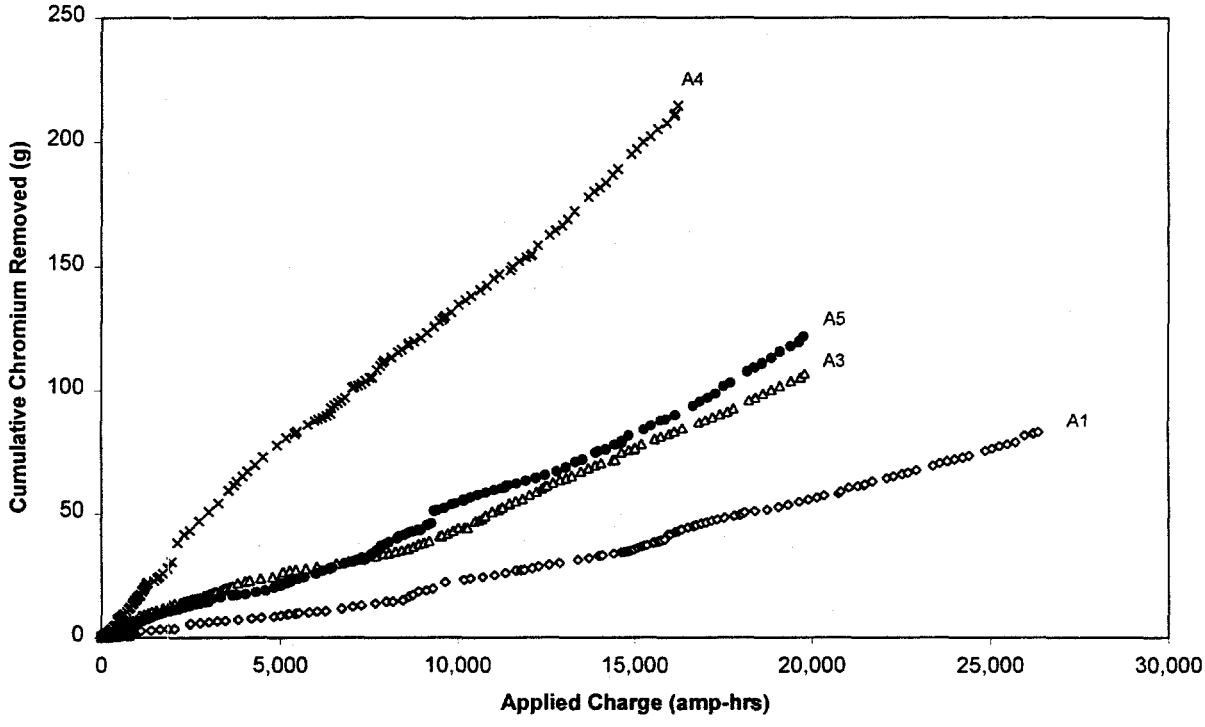

Figure 6-4. Cumulative chromium removal as a function of applied charge per anode.

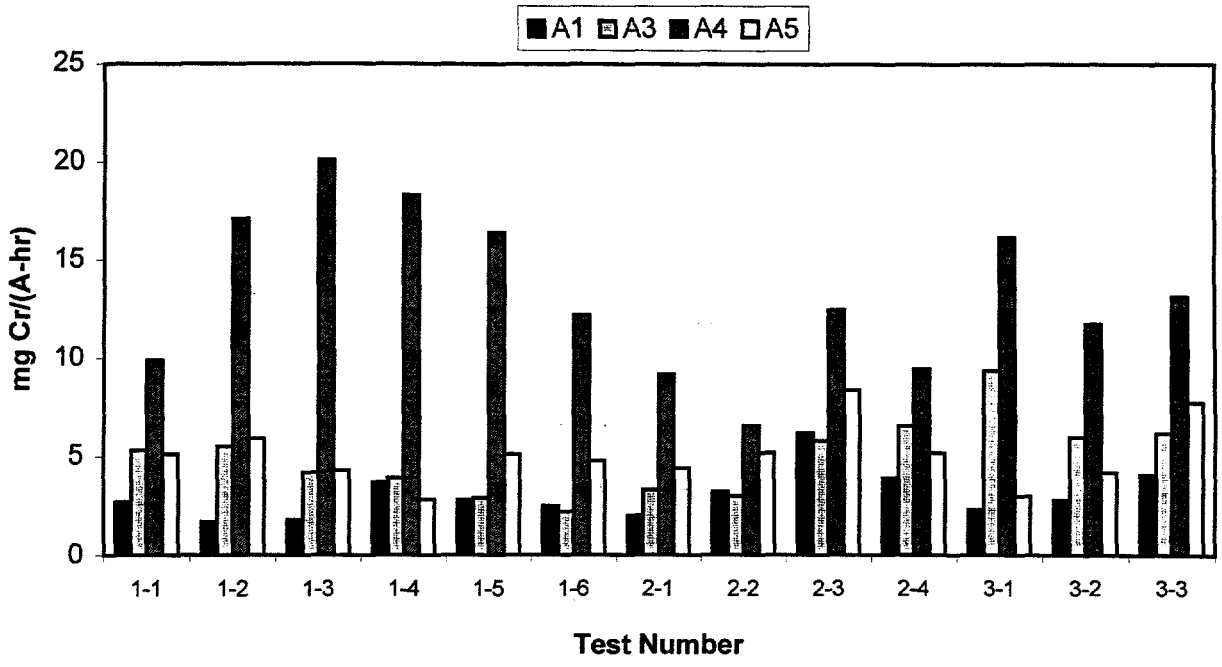

Figure 6-5. Removal efficiency of four anodes used continuously.

The distribution of power, the rate of energy application, to the soil can be modified in two ways. First, as illustrated in Table 5-1, the amount of power applied to the electrodes was changed during Tests 1-4, 1-6, and 2-2. Test 1-4 examined the effects of increasing the applied current to the electrodes, i.e., an increase in applied power to the system, whereas Tests 1-6 and 2-2 decreased the applied power to the system in an effort to limit the soil temperature in the EK remediation zone.

The second method to change the power distribution to the soil is to change the electrode configuration as was done in numerous tests (Table 5-1). The applied power density was changed either by removing electrodes (Tests 1-2 and 1-3) or by changing the locations of the cathodes (Tests 2-4, 3-2, and 3-3). For example, the connection of an additional set of cathodes to the north of the anode row for Test 3-3 resulted in a significant power density decrease from Test 3-2 with the application of nearly the same amount of current (Table 5-3).

Power density is a convenient way to examine the distribution of power because it takes into account both the amount of power applied to the EK system and the electrode geometry configuration. This allows tests of varying electrode configurations to be compared. In addition, power density is directly related to the heating of the soil (Section 6.4).

In an effort to examine the effects of changing the applied power density to the EK demonstration site, an effective volume was assumed for each electrode pair. This volume was assumed to have the following dimensions: 6-ft height (the height of the electrode), 3-ft width (the spacing between similar electrodes), and a length equal to the distance between the cathodes

and the anodes. Although this volume likely under-represents the actual volume that the current travels through, it was established to maintain consistency between tests.

In general, there exists an inverse relationship between the energy efficiency of chromium removal and the rate at which the energy is applied. Figure 6-6 illustrates the relationship between energy efficiency and the applied power density for the four continuously active electrodes (for Tests 1-3 through 1-6) for the EK demonstration. The energy efficiency was much higher when the applied power density was low than when the applied power density was high. In other words, the electrical costs are higher per gram of chromium the faster you try to remove it from the soil.

In addition, higher applied power densities will result in greater soil temperatures in the EK remediation zone. This secondary effect will be discussed more in Section 6.4.

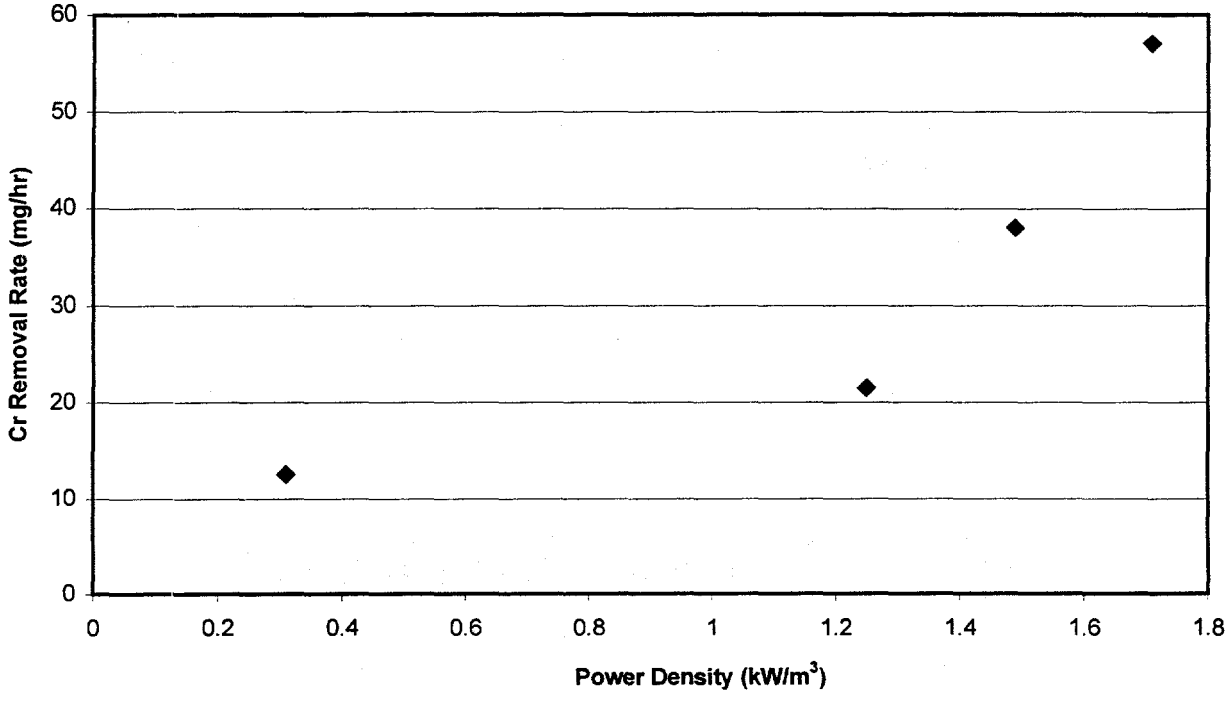

Figure 6-6. Energy efficiency as a function of applied power density for four electrodes.

6.1.5 Effluent Extraction Rates

One possible negative effect of high chromium concentrations in the anodes is diffusion of the chromate ions from the anodes back into the soil, thereby decreasing the extraction efficiency. The effluent removal rate should decrease the concentration of the chromate in the anode and decrease the diffusion potential gradient. Test 1-5 examined this possibility by increasing the rate at which the effluent was removed from the anodes from 2.3 L/hr for Test 1-4 to 3.5 L/hr (Table 5-3).

Results from Test 1-5 do not indicate a diffusion effect for chromate from the electrode to the soil. Anodes 3 and 4 showed an approximate halving of the average chromate concentration from Test 1-4 to Test 1-5, whereas electrode A5 exhibited only an approximately 10% decrease (see Table 6-2 which shows the average chromium concentrations of A3 and A4 dropping from 68.9 to 27.7 and from 448.0 to 272.2, respectively, and of A5 dropping from 71.0 to 64.5). However, the extraction efficiencies did not show a consistent trend in relation to these concentration changes. Anodes 3 and 4 showed a decrease in the extraction efficiency (from 3.9 to 2.9 and from 18.3 to 16.4 mg/A-hr, respectively), whereas A5 almost doubled its extraction efficiency (from 2.8 to 5.1 mg/A-hr). Possible explanations include either that the duration of Test 1-5 (35 hours) was not long enough to provide sufficient data or that the concentration of chromate in the electrodes did not reach significantly high levels in Test 1-4 to exhibit a reduction in the extraction efficiencies.

6.1.6 Water Injection

During Test 2-3, tap water was injected between the anodes and cathodes of the Northern Zone in an attempt to increase the soil electrical conductivity in an area that exhibited low pretest electrical conductivities and moisture contents and higher water-soluble chromium concentrations (Figure 6-7). As discussed in Section 3.2.1.1 and shown in Equation 3.2, the soil electrical conductivity is approximately proportional to the square of the volumetric moisture content. Therefore, the addition of water to areas of low electrical conductivity directly between the electrodes should redirect the current through these areas, thereby increasing the chromium removal rate.

Most of the locations for water injected into the soil were between the anodes and cathodes. However, the first two injections included the addition of water to the soil between adjacent cathodes through injection wells I1 to I4 and between adjacent anodes through injection wells I19 to I22 (Figure 3-16). The remaining 8 injections were only to the soil between the anodes and the cathodes (Table 5-5).

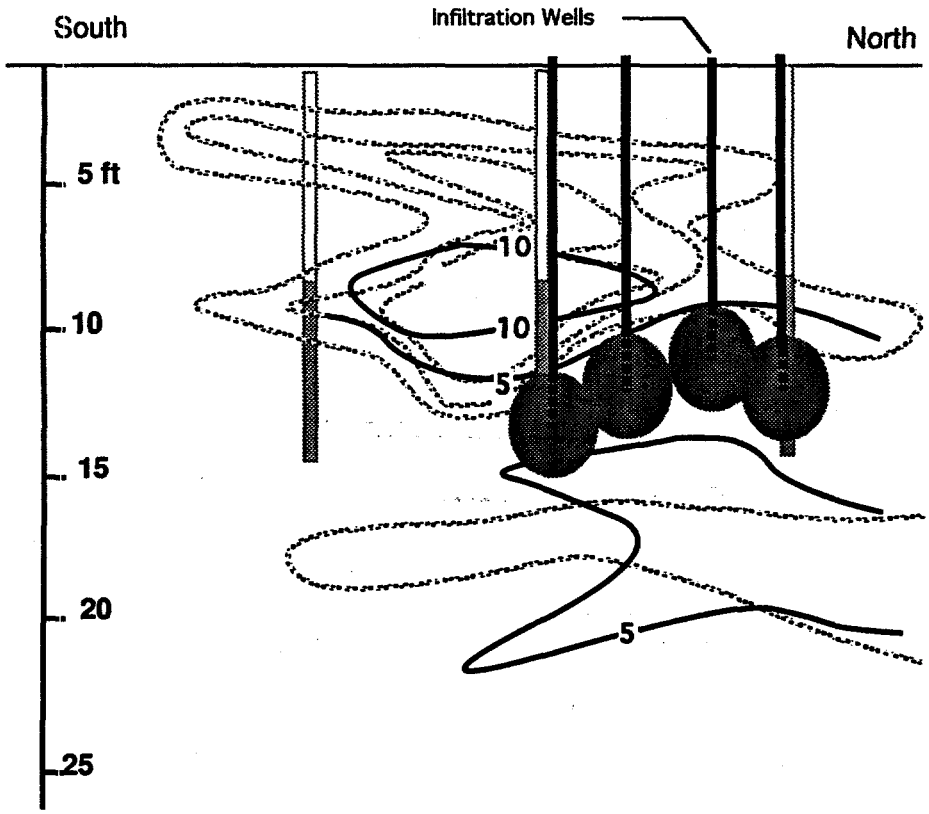

Figure 6-7. Zone of water injected into soil through the infiltration wells.
Light contours represent pretest electrical conductivity profiles as illustrated in Figure 3-7; whereas, dark contour intervals represent initial soil moisture contents.

The amount of injected water should have increased the soil moisture in this zone by approximately 20 to 40% over the initial moisture content. Each of the injection wells between the anodes and the cathodes received 10 injections of 0.6 liters (except as noted in Section 5.3.3) of water over an interval of approximately 2½ weeks. Assuming that each well influenced a soil volume of approximately 16 cubic feet (2 feet by 2 feet in area by 4 feet in depth), the ten injections would have increased the soil moisture by approximately 1.3% by volume (~0.7% by weight), i.e., from 2-5 weight percent to 3-6 weight percent soil moisture.

The chromium extraction efficiency during Test 2-3 was approximately double that of Test 2-2 (from 0.045 to 0.089 g Cr per amp-hr; Table 6-1), indicating that approximately twice as much chromium was being removed per applied charge. At first glance, it appears that the injection of water was able to redirect the current pathways through areas of higher contamination. However, the extraction efficiency was high and nearly constant throughout Test 2-3 (Figure 6-8) with a possible extraction efficiency increase in the last 5 data points. Since the water was injected over a 2½-week period of time, the chromium extraction efficiency was expected to increase throughout the test (which would have been indicated by constantly increasing slopes in Figure 6-8) rather than remain fairly steady.

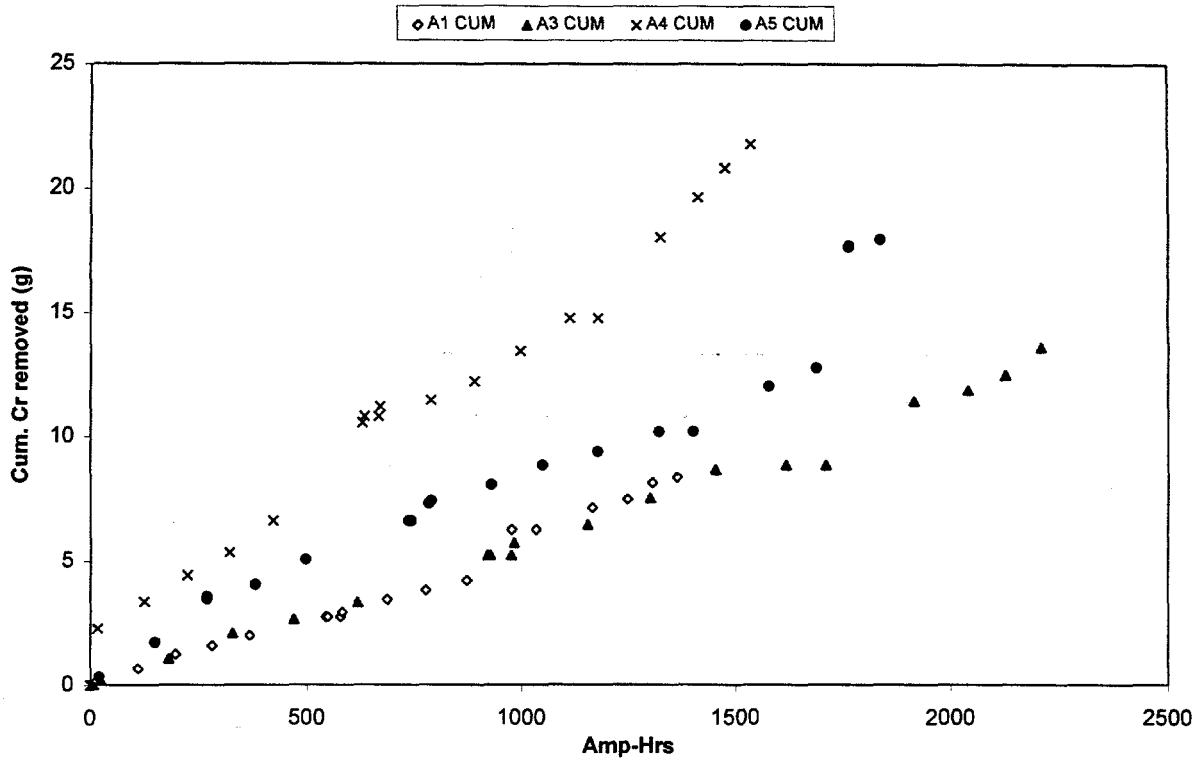

Figure 6-8. Extraction efficiency (as calculated from the slope of the data sets) during Test 2-3.

An alternate explanation for the increase in chromium extraction efficiency could be the dissolution of precipitated chromate in the soil adjacent to the anodes. In this scenario, the injected water dissolved a calcium chromate precipitate, thereby increasing the amount of chromium in the pore-water solution. The first two injections included locations between the anodes (infiltration wells I19 to I22). These injections, as well as subsequent injections near the anodes or unintentional additions of water due to chiller leaks (see Section 6.2.3.1), could be responsible for the chromate extraction efficiency increase. Which of the above described scenarios was responsible for doubling the chromate extraction efficiency cannot be resolved. It is likely that both hypotheses had some effect.

6.1.7 Electrode Configuration

Many of the demonstration tests involved changing the electrode power distribution configuration to evaluate extraction efficiencies. These tests can be separated into the three categories discussed in the following sections.

6.1.7.1 Removal of Inefficient Anodes

Anode 2 was removed from service during Test 1-2. This anode exhibited a chromium extraction efficiency of only 0.5 mg Cr per amp-hr, approximately $1/5^{th}$ that of the next least efficient anode (Table 6-2). The resulting overall extraction efficiency remained approximately the same with the removal of A2; however, the performance of each electrode varied. Anode 1 became less efficient, most likely due to the spreading of current flow pathways to less contaminated zones when A2 was disconnected. While the efficiencies of A3 and A5 did not change significantly, the extraction efficiencies of A4 almost doubled from what they were in Test 1-1. The reason for the increase in the extraction efficiency of A4 is speculated to be due to the spatial variability of chromium concentrations in the soil and not due to the removal of A2. Looking at the overall energy efficiency (Table 6-1) and especially the A1 energy efficiency (Table 6-2) rather than the overall or A1 extraction efficiencies, a decrease was noted with the removal of the A2 electrode (from 0.061 to 0.053 overall and from 41.0 to 21.1 mg/kW-hr). This was anticipated due to the reduced number of active anodes and the increase in power input.

6.1.7.2 Removal of Cathodes

The removal of C7, which had been paired with A2 (Test 1-3), did not have a significant effect on the total chromium extraction efficiency (Table 6-1); but, did exhibit a decrease in the energy efficiency comparable to that when A2 was removed. Since less electrode area was available for electron transfer with the removal of C7 during Test 1-3, the energy efficiency would be expected to decrease.

6.1.7.3 Reducing Distance Between Anodes and Cathodes

After Test 2-3, the distance between the anodes and cathodes was halved by changing the cathodes from the cold finger locations on the electrodes to those in the soil (see Figure 5-1) for Test 2-4. Comparing the extraction and the energy efficiencies of these two sets of tests indicates the initially counterintuitive result that both types of efficiencies decreased when the distance between the anodes and cathodes was decreased. However, the decreased efficiencies are due to increased power densities resulting from the reduction of the distance between the anodes and cathodes.

By keeping the applied voltage between the electrodes the same as it was during Test 2-3 and reducing the electrode spacing by one half the previous distance, the power density was increased by a factor of three. As seen in Section 6.1.4, an inverse relationship exists between energy efficiency (in mass of chromium per kilowatt-hour) and applied power. Although more chromium was removed per hour in Test 2-4 than in 2-3, a more efficient operational parameter would have been to decrease the applied voltage to maintain the same power density through the system.

Overall, both the chromium extraction and energy efficiencies increased during Test 3-3 when compared to Test 3-2 or 2-4 (Table 6-1). These increasing efficiencies indicate that an electrode geometry with cathodes on each side of an anode row may be the preferred electrode geometry to operate electrokinetic remediation.

6.2 Post-test Sampling

A plethora of soil electrical conductivity surveys and soil samples were taken before and after the electrokinetic demonstration to examine the effects of applying direct currents to the soil. The following sections discuss the various parameters studied.

6.2.1 Soil Electrical Conductivity

In general, the soil electrical conductivity, as determined by the Geoprobe® method (Section 3.2.1.1), did not change significantly before and after the electrokinetic demonstration. Figures 6-9 and 6-10 illustrate the north-south and the east-west cross sections of soil conductivity in milliSiemens per meter. The light gray contour lines are the 10, 20, and 30 mS/m isometric lines before the demonstration, whereas the black lines represent the electrical conductivity after the demonstration was completed. Although slight variations can be seen between the two contour sets, the general shapes and values appear to be the same.

The 10 mS/m contour may be slightly lower in the Northern Zone of the demonstration site due to the injection of water during Test 2-3. However, there was not enough data from this area to better quantify the effect of infiltrating water into the soil to increase its electrical conductivity.

Soils with the highest electrical conductivities exhibit the greatest current densities. As illustrated in Figures 6-9 and 6-10, soil electrical conductivity in the 8 to 10 feet BLS horizon is over three times more conductive than other soil in the EK. This soil zone likely conducted the majority of the current from the cathodes to the anodes resulting in a non-uniform distribution of the current in the EK remediation zone.

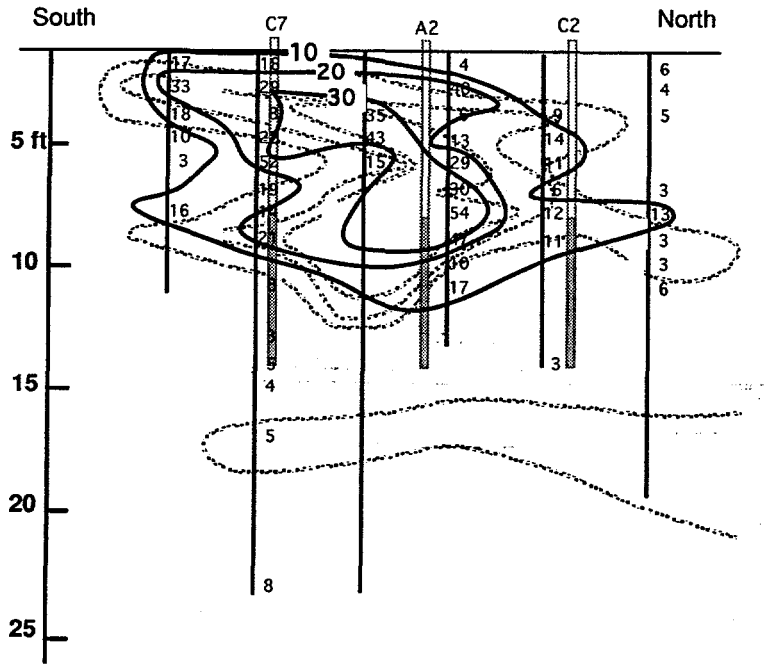

Figure 6-9. North-south cross sections of soil conductivities (mS/m).
(Pretest values are represented by light gray contours and post-test values by dark contours.)

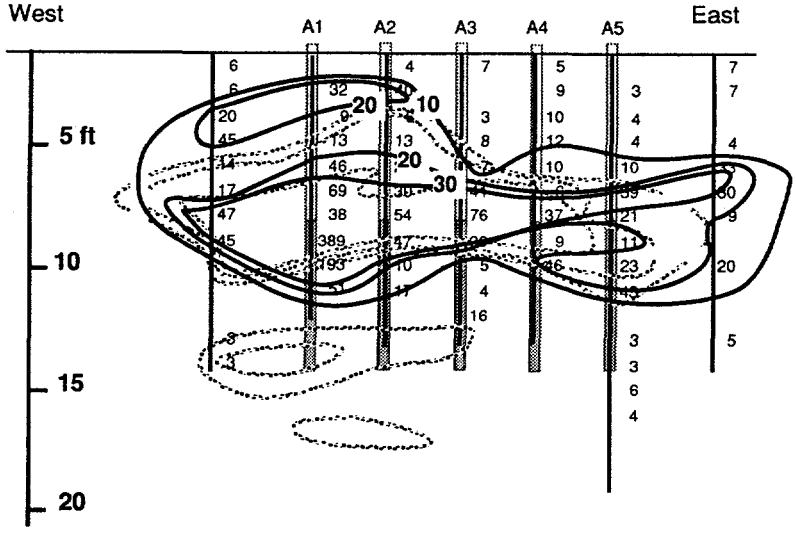

Figure 6-10. East-west cross sections of soil conductivities (mS/m).
(Pretest values are represented by light gray contours and post-test values by dark contours.)

6.2.2 Soil pH

Soil pH, as determined by measuring the pH of 2:1 water-to-soil extracts, did not change significantly across the entire demonstration site; however, localized pH increases were noted in the vicinity of the cold finger cathodes. During the first phase of testing, the more complex porous-ceramic casing electrode system that included pH conditioning of the electrolyte fluid in the cathode casing was used at the cathodes. In contrast, during Phase 2 and 3 of the demonstration, the cold finger cathodes were used, which did not condition the pH at the cathodes. These cold finger cathodes produced hydroxyl ions due to the transfer of electrons from the cathodes to the soil pore water by electrolysis reactions (Equation 4.1). As illustrated in Table 6-3, the pH of the soil increased in the active area of the cold finger by approximately 1 pH unit due to the production of the hydroxyl ions. The soil pH above and below this active cathode area did not change significantly.

Table 6-3. Comparison of the pH of Soil/Water Extracts Before and After the Demonstration for One Anode and One Cold-Finger Cathode

		Cold Finger CFC3		Anode 4	
	Depth (ft)	Pretest pH	Post-test pH	Pretest pH	Post-test pH
	6	8.2	7.8	8.1	8.5
Active Electrode Area	8	8.3	9.1	7.7	7.6
	10	8.2	9.5	7.8	7.4
	12	8.2	9.0	7.8	7.6
	14	7.7	NA	NA	7.5
	16	7.9	7.9	7.7	8.3

In areas away from the cathodes, no significant pH changes were noted in the soil. Anodes were pH conditioned throughout the entire electrokinetic demonstration. Post-test soil pH values remained at approximately the same values as the pretest values in areas located near the anodes (Table 6-3). Examination of soil pH values in the central area of the demonstration site did not show any net change due to the electrokinetic demonstration.

6.2.3 Soil Moisture Content

Changes in the subsurface soil moisture content were evaluated by three methods: water balance by logging water added and removed from the electrokinetic demonstration, destructive soil sampling and drying, and monitoring the soil profile by neutron activation through a series of neutron access tubes. All of these analysis method results indicated that no significant changes in soil moisture were caused by the electrokinetic demonstration that would adversely affect the remediation of chromate. Each method is discussed in the sections below.

6.2.3.1 Water Balance Analysis

A water balance determination made by monitoring the amount of water input to the electrokinetic demonstration and the amount of water removed yields a net gain of approximately 20 gallons. Water was intentionally added to the electrokinetic system through the input of makeup water, acids, and bases to the ceramic electrokinetic electrodes, as well as the injection of water directly into the soil through the series of injection wells. A small amount of water was also unintentionally added to the soil through defective electrode heat exchangers and cold fingers that allowed leakage of chiller water. Water was extracted from the electrokinetic system by pumping water from the ceramic electrodes to the effluent barrels.

Table 6-4 lists the numerical values for each of the above processes. Values for the make-up water, acid/base additions, injected water, and effluent water were documented accurately in the field log books. However, no formal documentation was maintained on the amount of de-ionized water added to the chillers. The chillers typically showed approximately a one-gallon loss in the chiller reservoir per week. During heat exchanger or cold finger failures, an additional 5 to 7 gallons of water were added to the chillers. It is estimated that approximately 35 gallons of de-ionized water could have been added to the soil profile through these unintentional losses. Therefore, a net of approximately 20 (+/- 10) gallons of water were added to the soil from activities conducted at the electrokinetic demonstration.

Table 6-4. Summary of Water Balance Calculations

Item	Cathodes (gal)	Anodes (gal)	Total (gal)
Make-up Water to Electrodes	661	1404	2065
Acid Additions	74	-	74
Base Additions	-	134	134
Water Injections	25	25	50
Chiller Water Additions	5	30	35 (+/-10)
Total Additions	765	1593	2358
Effluent Water Extractions	(831)	(1506)	(2337)
Total	(66)	87	**21** (+/-10)

6.2.3.2 Soil Sample Moisture Content Analysis

A comparison of the moisture contents from pretest and post-test soil samples indicates that there was no significant moisture redistribution nor were there significant increases resulting from the electrokinetic demonstration. Pretest soil sample analysis results are given in Table A-3 of Appendix A. Post-test soil samples were collected from December 1996 through January 1997 for subsequent soil moisture and chemical analyses. These results are given in Table A-5 of Appendix A.

Statistical comparisons were made between paired pretest and post-test samples to evaluate if the soil moisture had increased as a result of the electrokinetic demonstration activities. One way to evaluate the data is to analyze the variance of both the pretest and post-test samples and then perform an F test, a statistical analysis tool, on this data set. The F test can determine if it is statistically probable that two data sets, such as pretest and post-test moisture content samples, could have been drawn for a sample population of equal means. In other words, is there a statistical difference between the pretest and post-test moisture contents?

Pretest and post-test soil moisture content sampling pairs were statistically evaluated by the F test procedures at the 0.05 significant levels from within the EK remediation area. Results of the F test analyses suggest that no soil moisture content changes occurred in the remediation area due to the EK demonstration.

6.2.3.3 Neutron Probe Monitoring

To monitor moisture content profiles, a CPN® 503 DR HYDROPROBE® was employed at ten locations within the electrokinetic demonstration. The neutron probe has an americium beryllium source which emits fast neutrons into the surrounding soil and a counter which sums the number of thermalized neutrons detected by the probe in a specified time interval. The number of thermalized neutrons is normally considered to be proportional to the amount of water in the surrounding soil. At the electrokinetic demonstration site, the probe was lowered through the soil profile in 2.5-inch PVC access pipes (described in Section 3.2.4.2). Thermalized neutron counts were recorded at one to two foot intervals to a depth of 40 feet on a weekly basis.

In an attempt to calibrate the neutron probe, soil samples were taken adjacent to the neutron access tubes during the post-test sampling. Results of this calibration exhibited a poor coefficient of correlation ($R^2 = 0.29$) between the neutron probe count and the measured moisture contents. This poor correlation was attributed to the material of the neutron access tubes and the installation method used. Neither the recommended pipe material nor method of installation could be used at the electrokinetic demonstration site. The recommended method of installing neutron access tubes is pushing an aluminum pipe into a slightly undersized hole. Aluminum pipe was not an acceptable material to use at the electrokinetic demonstration because of its electrical conductivity properties. Therefore, the access tubes were made of PVC pipe which is nonconductive. However, PVC has the disadvantage of being a hydrocarbon material that will thermalize neutrons, causing the neutron probe to lose some of its sensitivity. The pipe was also installed in holes drilled with 8-inch hollow stem augers and backfilled with soil cuttings. The backfill material would further decrease the neutron probe precision by thermalizing the fast neutrons in the backfill and not in the native soil.

No significant changes were noted in the neutron probe counts once the borehole backfill soil reached equilibrium with the surrounding soil. Although the quantitative calibration of neutron probe counts to soil sample moisture contents was poor, there existed a qualitative positive correlation between the number of neutron probe counts and the increased moisture

contents. An increase of neutron probe counts at any specific depth during the EK demonstration would indicate an increase in the soil moisture contents at that location and none was found.

6.2.4 Soil Chemistry

Soil samples were collected at various locations throughout the electrokinetic demonstration site for chemical analyses. Pretests samples, those taken during the installation of the electrokinetic demonstration equipment, were collected to determine the amount and distribution of chromium initially in the soil. Results of the pretest investigation were presented in Section 2.3.6 of this report. Post-test samples were collected to evaluate the chromium distribution in the soil after the application of electrical current during the EK demonstration. This section compares the results of the pretest and post-test chemical analyses. Table 6-5 lists the types of chemical analyses and the number of samples analyzed for each type. Additional pretest and post-test samples were taken for analyses by EPA oversight personnel as part of the EPA Superfund Innovative Technology Evaluation (SITE) program. Appendix A contains tables with the horizontal coordinates, vertical depths, and results of each analysis.

Table 6-5. Number of Samples Obtained during Pretest and Post-test Sampling Events for Chemical Analyses

Type of Sample	Pretest	Post-test
In-house XRF	47	0
In-house water extraction	96	121
TCLP for permit	117	109
Total Cr	4	0
EPA SITE TCLP	10	0
EPA SITE Total Cr	50	84
EPA SITE Cr(IV)	50	84
Total number of samples	187	208
Number of locations	34	26

The aspect of electrokinetics to be evaluated determines the type of chromium analysis to be conducted on the soil sample. Water-soluble extractions followed by ion chromatography (IC) analyses are best to evaluate the ions in the pore water solution (i.e., ions that are able to be moved by electrokinetic remediation). Soil samples analyzed for chromium by EPA method 7196 (chromium(VI)) will better estimate the amount of soluble chromium ions contained in the soil profile. TCLP (EPA method 1311/6010) will best determine if the soil would be considered hazardous for disposal in a landfill, and finally, XRF and total chromium analyses best estimate the total amount of chromium in all of its oxidation states. Therefore, each of these chromium concentration analysis techniques will be examined in more detail in the following sections.

6.2.4.1 Chromium(VI) Geochemistry at the EK Site

Chromium distribution beneath the unlined chromic acid pit in SNL's CWL has been evaluated in numerous studies from 1981 through this demonstration. All of the studies agree that elevated levels of chromate exist in the soil beneath the original pit boundaries. See Section 3 for more details.

Beneath the electrokinetic demonstration site, chromium(VI) may exist in both a dissolved anionic form with oxygen (chromate) or as a precipitated solid with calcium. Although chromate does not typically sorb strongly to soil surfaces and is normally thought of as an ion in pore water solutions, a recent report submitted to SNL suggests that chromate may form a solid phase in arid alkaline soils. Stein (1994) has suggested that significant amounts of Cr(VI) can coexist with gypsum ($CaSO_4*2H_2O$), a black crystalline material, through substitution of CrO_4^{2-} for SO_4^{2-} and as anhydrous chromatite ($CaCrO_4$), noted as a yellowish material in her study. Soil samples retrieved from the electrokinetic site contained both of these colored materials suggesting that some chromate may be in the precipitated form at the electrokinetic site.

Pretest water extracts of the soil samples have likely underestimated the chromium concentrations in the soil. If a significant amount of chromate is precipitated with calcium in the form of chromatite or gypsum, equilibrium conditions may not be reached during the water extraction procedure due to the kinetics of dissolution of these compounds. Stein (1994) reported that the steady-state solubility value of chromatite was not reached until after 168 hours at a pH of 8.46. This data suggests that the two-hour extraction time used during the pretest in-house water extraction method was not sufficient to estimate steady-state values.

As a further verification that chromate containing solids are present in the UCAP soils, a laboratory experiment was initiated to examine solidified chromate dissolution with time in the water extraction process. A soil sample from the UCAP 3 hole was mixed with 200 mL of deionized water for 5 minutes. The solution was next allowed to quiescently separate into the supernatant and solid portions. The supernatant was then decanted and analyzed for chromate concentrations using a colorimetric procedure. The soil sample washing was repeated several times a day over a 7 day span. Results indicate a reduction of the supernatant chromate concentration over each day, but an approximate doubling of the chromate concentration from the previous day's last wash to the next day's first wash. This consistent increase in the chromate concentration while the sample sat overnight supports the view that these UCAP soils contain slowly dissolving chromate solids.

Furthermore, the pretest extraction procedure was performed on oven-dried soils that could exacerbate the precipitation of chromium. Oven drying the soil samples prior to performing the water extraction procedure may have co-precipitated some of the chromate into a fairly insoluble gypsum/plaster-of-paris matrix. This drying-induced precipitation of the chromate would thus underestimate the true water-soluble chromium in the soil water for the pretest samples.

6.2.4.2 Comparisons of Pretest and Post-test Chromium Analyses

The pretest and post-test data was evaluated by two different methods: statistical analysis of paired data, and comparison of chromium concentrations in north-south cross sections. For the statistical comparison, pretest and post-test data were considered to be a pair if they were located within one foot of each other horizontally and one-half foot vertically.

North-south cross sections of pretest and post-test chromium profiles were developed to compare the effects of applying the electrokinetic current to the contaminated soil. Figure 6-11 illustrates the locations of the chromium concentration profiles. These locations were chosen because there were enough data to develop a suitable cross section and this area of the demonstration was operated in the most similar manner allowing for comparisons between cross sections.

Water-Soluble Chromate Comparison

Comparisons of pretest and post-test water extractions and IC analyses of chromate soil samples are not possible for the electrokinetic demonstration due to a change in the water extraction procedure. Pretest soil samples were oven dried prior to preparing the soil water extract, whereas post-test extraction procedures were performed on moist soil samples. These two varying sample preparation procedures make it impossible to quantitatively compare the pretest and post-test IC chromate samples.

Although the pretest and post-test chromate data is not directly comparable, the post-test chromate analyses can be compared to the pretest TCLP results corrected to equivalent IC chromate concentrations. For the post-test data, a well-defined second order polynomial (R^2 = 0.95) was obtained between the TCLP and the in-house water-soluble chromium extraction IC concentrations. This correlation was developed so that pretest TCLP concentrations could be converted to equivalent pretest IC chromate concentrations thereby allowing a comparison of the water-soluble chromium distribution in the soil profile before and after the electrokinetic demonstration.

Fifty-one paired post-test in-house IC and contract lab TCLP analyses were obtained and fitted with a polynomial regression (Figure 6-12). At low chromium concentrations, the slope of the regressed line is 16.54. A theoretical correlation would have a slope of 20 since the TCLP concentrations are for the extracted liquid (the TCLP extraction is 20 parts liquid to 1 part soil), whereas the IC chromium results are reported a soil concentrations in ppm.

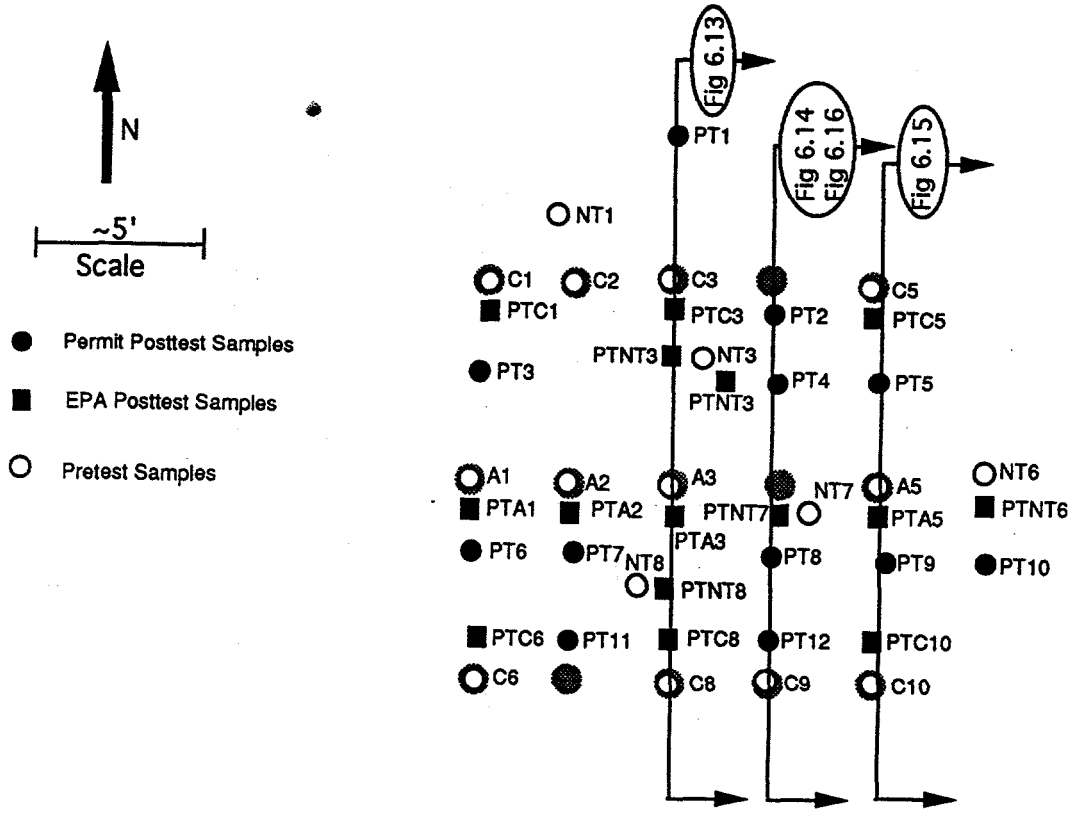

Figure 6-11. Locations of the chromium concentration profiles.

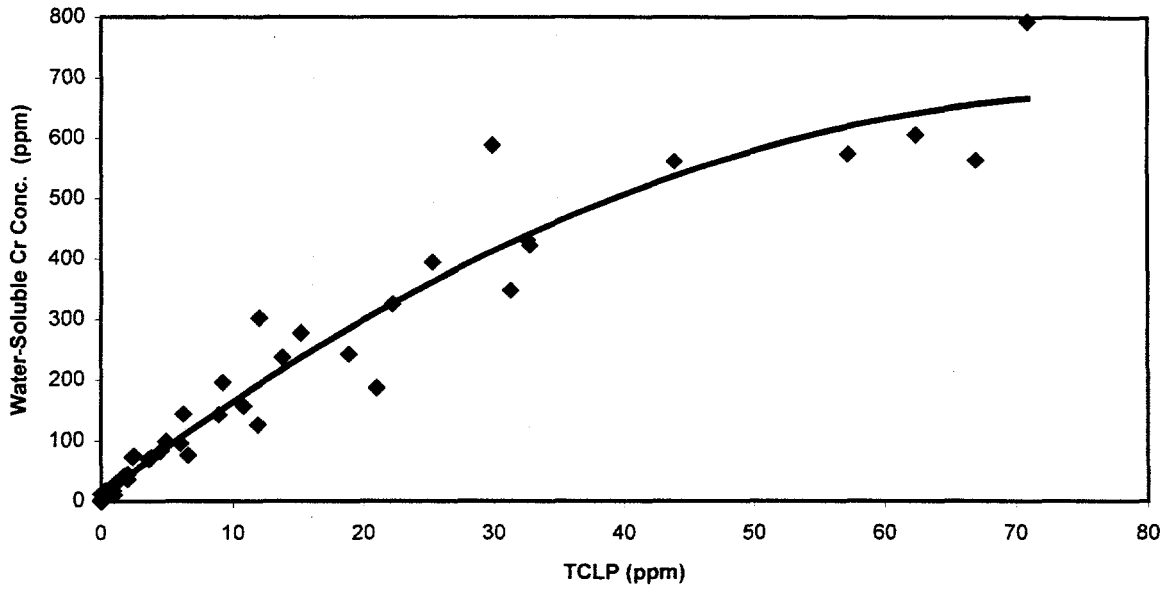

Figure 6-12. Polynomial regression of post-test in-house IC and TCLP analyses.

At higher chromium concentrations, the regressed line exhibits a slightly decreasing slope indicating a lower extraction efficiency of the in-house method as the concentration increases. The decreasing efficiency may be due to the fact that the solubility limit of gypsum is reached in the in-house extracts and not in the TCLP extracts. The in-house extraction method uses a 2-to-1 liquid-to-soil ratio, whereas the TCLP extraction method uses a 20-to-1 ratio. The greater amount of liquid for the TCLP analysis would tend to have a lower concentration of soluble ions in the extract which could allow more of the precipitated gypsum/chromate solids to dissolve. A second reason for the decreasing efficiency may be the greater solubility of the gypsum/chromate solids in the weak acid as the extraction liquid for TCLP analyses.

Figures 6-13 to 6-15 illustrate the equivalent pretest IC chromium concentrations and post-test IC concentrations for three cross sections. All three cross sections illustrate similar trends and are similar to the cross section developed for the TCLP analyses (discussed below). The area of soil adjacent to the cathodes exhibited a significant reduction in the chromium concentrations, whereas an increase in chromium concentrations was noted in areas away from the cathodes and near the anodes. In addition, soil horizons above the "treatment zone" also appeared to exhibit lower chromium concentrations suggesting the current travel paths were short circuited through these upper soil horizons (see Section 6.2.1).

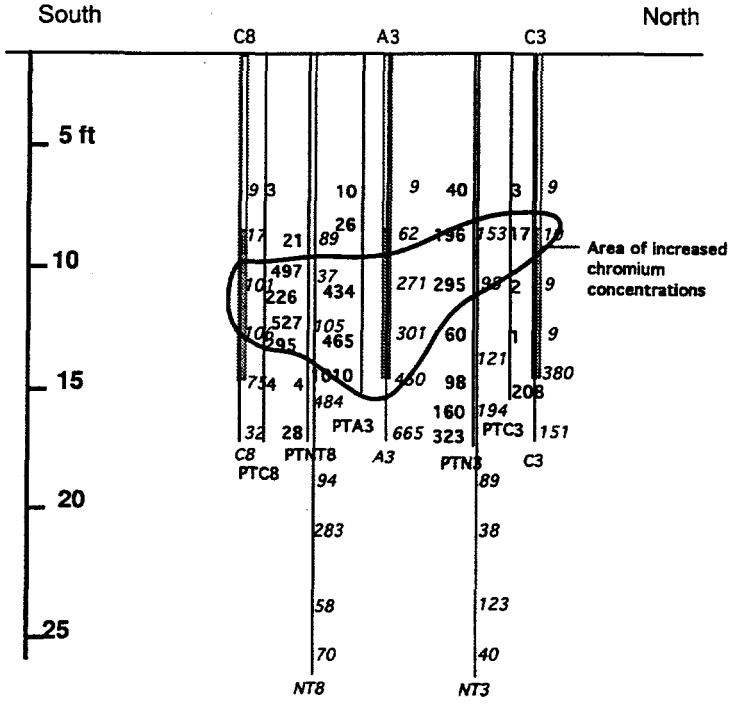

Figure 6-13. Pretest and post-test chromium concentrations in soil for cross section C8 to C3.
Equivalent pretest IC Cr concentrations in ppm are in italics. Post-test IC Cr concentrations are in bold. The contour line represents the boundary between net increases and decreases of IC concentrations.

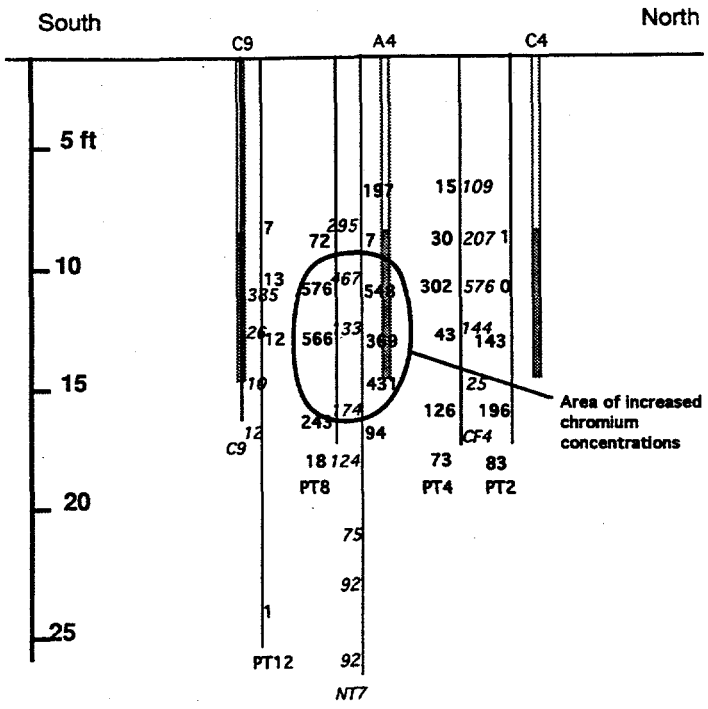

Figure 6-14. Pretest and post-test IC chromium concentrations for cross section C9 to C4.
Equivalent pretest IC Cr concentrations in ppm are in italics. Post-test IC Cr concentrations are in bold. The contour line represents the boundary between net increases and decreases of IC concentrations.

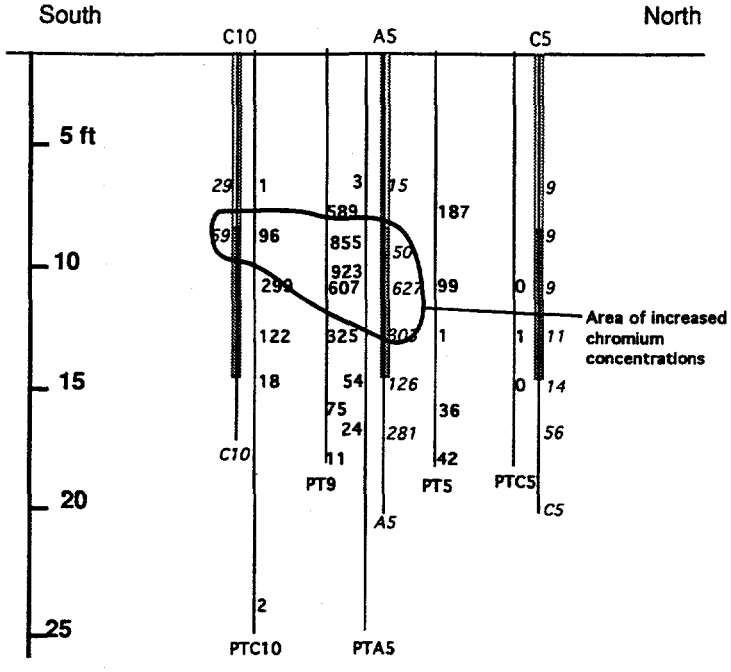

Figure 6-15. Pretest and post-test IC chromium concentrations for cross section C10 to C5.
Equivalent pretest IC Cr concentrations in ppm are in italics. Post-test IC Cr concentrations are in bold. The contour line represents the boundary between net increases and decreases of IC concentrations.

Chromium(VI) Comparison

Forty paired samples were collected and analyzed for chromate by EPA method 7196. Overall the average chromate concentration increased very slightly (652 to 658 ppm soil; Table 6-6) from the pretest to the post-test. However, the standard deviation is high for both the pretest and the post-test chromate analyses, indicating that the slight increase in the post-test average is not statistically significant. The data is highly variable for location and depth with little correlation between data points. It is likely that since the demonstration was terminated prior to complete soil remediation, not enough chromium was removed to show significant decreases in the chromium(VI) concentrations by this statistical analysis. Other possible factors that may preclude paired statistical analyses of all the data includes: 1) introduction of additional chromium to the soil from outside the electrokinetic demonstration zone, 2) breaking of containers containing chromate during sampling, 3) dissolution of co-precipitated calcium chromate sulfate species, or 4) inadequate distribution of Cr(VI) samples to adequately describe the site.

Table 6-6. Chromate Paired Data Summary

	Number of Pairs	Pretest Average Concentration (ppm soil)	Pretest Standard Deviation	Post-test Average Concentration (ppm soil)	Post-test Standard Deviation
All Pairs	40	652	991	658	1057
@ Cathodes	9	402	846	72	93
@ Anodes	9	1085	1630	1287	1249

A more enlightening way to examine the data is to look separately at paired data at the cathodes and at the anodes in the active zone (i.e., 8 to 14 ft BLS). In this way, the effects of electrokinetic remediation within similar EK remediation zones can be compared. Table 6-6 lists the average pretest and post-test Cr(VI) concentrations and their respective standard deviations for samples located near the cathodes and near the anodes. As expected, a significant reduction for the average chromate concentration was noted at the cathodes (402 to 72 ppm in soil), whereas the post-test average chromate concentration at the anodes increased from the average concentration of the samples taken prior to the application of the current. Not enough data was available to develop a cross section from the Cr(VI) analyses.

Within these two unique treatment zones, it appeared that the soil near the cathodes was becoming cleaner and that the chromium was being accumulated near the anodes. Therefore, it follows that the application of current from the electrokinetic remediation moved the chromate from the soil near the cathodes toward the anodes. Since the demonstration was terminated prior to compete soil remediation, elevated chromium concentrations still exist in the soil near the anodes.

TCLP Chromium Comparison

There were an insufficient number of TCLP pairs for statistical analysis; however, enough TCLP data was available to develop a cross section between C9 and C4. Figure 6-16 illustrates the TCLP chromium concentrations for the soil samples taken before and after the electrokinetic demonstration. The contour separates areas of TCLP concentration decreases and increases.

The upper portion of the demonstration (6 to 10 ft) and the areas near the cathodes showed marked decreases in the TCLP chromium concentrations. These zones were less than 5 ppm, indicating that the soil would be considered non-hazardous if excavated and subsequently tested. Prior to conducting the electrokinetic demonstration, pretest TCLP chromium concentrations were as high as 28 ppm in this same area (Figure 6-16).

The area between C9 and A4 exhibited higher post-test TCLP chromium concentrations after the electrokinetic demonstration. These higher concentrations were likely due to the electromigration of chromium from the cathodes towards the anodes or possible inherent spatial variability of the chromium distribution.

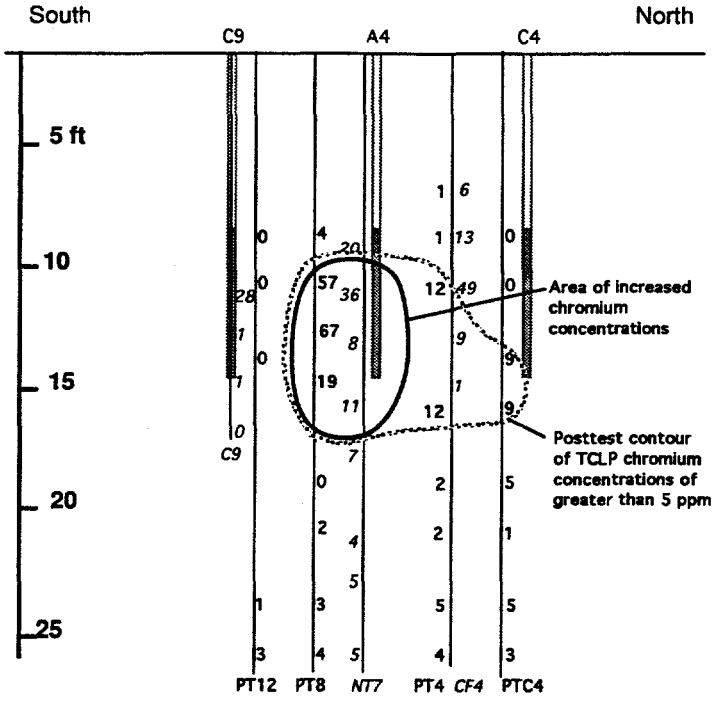

Figure 6-16. Pretest and post-test TCLP chromium concentrations for cross section C9 to C4.
Equivalent pretest IC Cr concentrations in ppm are in italics. Post-test IC Cr concentrations are in bold. The inner contour line encloses the area of increased TCLP Cr concentrations near the anodes. The area outside the outer contour line has TCLP concentrations of ≤5 ppm Cr.

Total Chromium Comparison

Paired analyses of soil samples analyzed for total chromium exhibited qualitatively similar, but not as well-defined, behavior as the paired Cr(VI) comparison, which indicated increases at the anodes and decreases at the cathodes. Total chromium analyses were made at the request of the EPA SITE Program contractor, and the results are shown in Table 6-7. Insufficient data exist to develop a total chromium cross section.

Table 6-7. Total Chromium Paired Data Analyses

	Number of Pairs	Pretest Average Concentration (ppm soil)	Pretest Standard Deviation	Post-test Average Concentration (ppm soil)	Post-test Standard Deviation
All Pairs	42	1592	1970	2522	3391
@ Cathodes	10	1209	2600	905	908
@ Anodes	9	2442	2157	4600	4426

Electrokinetic methods will remediate only contaminants that are dissolved in the soil pore water and therefore are not likely to remediate the trivalent chromium in the soil. The total chromium concentrations included the mobile Cr(IV) and the immobile Cr(III) species concentrations. It is not likely that the application of current through the soil pore water would remediate any of the Cr(III) species. The trivalent chromium most likely would be strongly bound to the soil and would be immobile without significantly lowering the soil pH.

6.2.4.3 Acetate Results

Acetate ions, as chemical tracers, can delineate the zones of electrokinetic remediation. Cathodes produce hydroxyl ions by electrolysis (Section 4.2.1); therefore, acetic acid was added to the electrolyte to maintain a pH of approximately 8 during the first phase of the electrokinetic demonstration. The by-product of the neutralization reaction is an acetate ion that was transported across the demonstration site towards the anodes by electromigration; therefore, it makes an ideal tracer of the current pathways through the soil.

Amount of Acetic Acid Added

A total of 1070 moles of acetic acid were added to the southern cathodes to control the pH in the electrolyte solutions. Table 6-8 lists the calculated amounts of acetic acid added to each of the southern cathodes. During Phase 1, C6, C8, and C10 continuously received acetic acid. In addition, C8 also received a slight amount of acetic acid for Test 3-1. Cathode 7 received acetic acid for Tests 1-1 and 1-2 and then was shut down for the remainder of the demonstration due to its high current demand.

Table 6-8. Acetic Acid Additions to the Southern Cathodes

Cathode	Total Coulombs Applied While Conditioning the pH ($C \times 10^6$)	Calculated Moles of Acetic Acid Added to Neutralize Base Generation (moles)	Total Coulombs Applied ($C \times 10^6$)
C6	44	450	44
C7	19	200	19
C8	15	150	15
C9	7	70	22
C10	19	200	19

Cathode 9 had a more complex operational history. This cathode received acetic acid only for the first portion of Phase 1 testing in the Southern Zone although current was applied for the entire Phase 1 testing from the C9 location. Cathode 9 developed a leak in the ceramic during Test 1-4 causing erratic readings in the float level system. Due to this air leak, the interior electrode was disconnected, and power was applied to the cold finger electrode attached to the outside of the C9 ceramic casing. No pH conditioning was used after moving the applied power to the C9 cold finger for this electrode.

Distribution of Acetate

Post-test soil samples were analyzed for acetate concentrations by an in-house ion chromatography method. Detection limits were approximately 1 ppm acetate in soil. Figure 6-17 illustrates the plan view of the distribution of acetate across the electrokinetic demonstration site. Sampling locations which had a detectable level of acetate in one of its samples are illustrated in black, whereas sampling locations which exhibited no acetate detection at any depth are depicted by the open circles. Figure 6-17 illustrates that all of the post-test sampling locations adjacent to the southern cathodes (C6-C10, the bottom row of electrodes) with the exception of C9 had detectable concentration of acetate. Furthermore, post-test sampling locations adjacent to A1 and A2 also had acetate in the soil samples.

There appears to be a continuum of acetate between C6 and A1. Cathode 6 received more than twice the amount of acetic acid than any other cathode. Acetate was detected in post-test sample location PT6 (Figure 6-17) as well as in samples from A1 and A2. It is likely that acetate from C6 migrated completely across the southern half of the demonstration site to A1.

The reason acetate is found at A2 is not completely clear. Anode 2 was disconnected from the power source after Test 1-1. After this time a vacuum was maintained in A2, effectively making A2 a porous cup sampler. Liquid did accumulate in the A2 porous ceramic casing and was removed periodically. It is possible that acetate from near A1 was hydraulically transported to the A2 location.

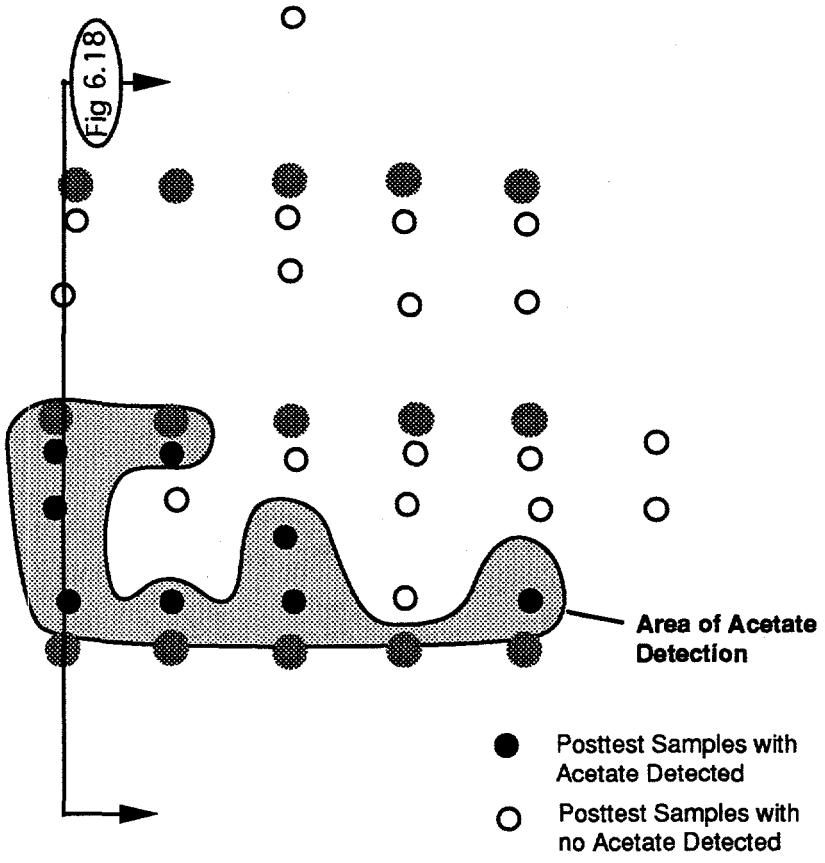

Figure 6-17. Distribution of acetate across the electrokinetic demonstration site.

A second possible transport mechanism that would allow acetate to be adjacent to A2 is that the current path from cathode C6 to A1 was not a direct line between the two electrodes but rather doglegged in the vicinity of A2. Anode 2 was drawing 42% of the current during Test 1-1, implying that the soil near A2 was more conductive than that near the other electrodes. After discontinuing the operation of A2, A1 greatly increased its current consumption. This increase may imply that the current that normally would have terminated at the A2 electrode maintained a similar pathway but was detoured to A1 when A2 was terminated.

The acetate-free soil near C9 also can be explained. First, C9 received the least amount of acetic acid during Phase 1 of the electrokinetic demonstration (Table 6-8). Furthermore, C9 received an additional 15 million moles of charge, most likely as hydroxyl ions, after the pH conditioning with acetic acid was discontinued at this electrode during Test 1-4. Any acetate in the soil near the C9 location would have migrated away during the application of the additional current. This acetate likely lies between post-test sampling holes PT8 and PT12.

Unlike C9, no additional current was applied to C7 when its operation was terminated. The acetate in this location likely was stagnant and exhibited little or no migration.

When viewed in a cross section profile between C6 and A1 (Figure 6-18), the acetate appears to be confined to the upper layer of the demonstration zone. Acetate was detected at 8 to 12 feet at both the anode and cathode and only between 6 to 8 feet at the approximate midpoint. This is the same soil horizon in which pretest elevated moisture contents existed, also shown in Figure 6-18. Since soil electrical conductivity is highly correlated with soil moisture, the detection of acetate in these layers would be expected. A similar correlation exists in the C8-A3 cross section where elevated moisture contents at NT8 at 8 ft (19.24%) also had acetate detected in the soil sample.

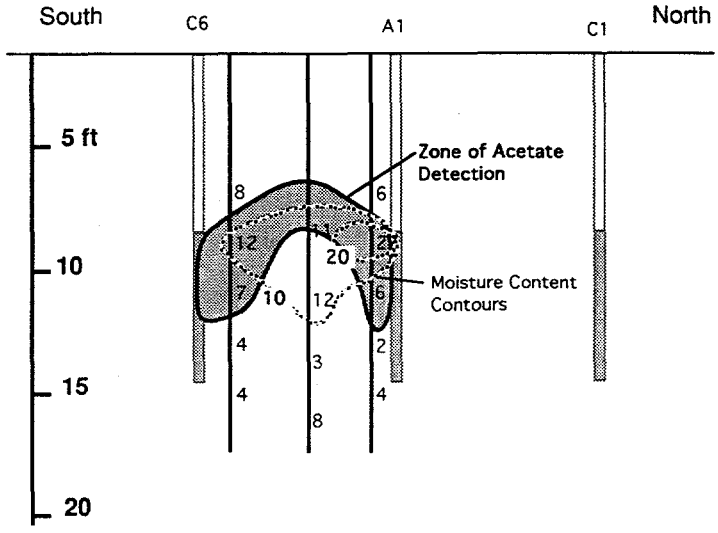

Figure 6-18. Zone of acetate detection and moisture content contours for cross section C6 to C1.

6.3 Transference Number Prediction

Long-term performance of the electrokinetic extraction efficiency can be predicted from soil sample analyses. Pre-test soil extract conductivity-based transference numbers were calculated from the analysis of soil samples collected during the installation of the five anodes. The average transference number for soil samples collected in the 8 to 14 foot zone for each anode are listed in column one of Table 6-9. Soil water extracts were analyzed for electrical conductivity by a bench top conductivity meter, and chromate concentrations were determined spectrophotometrically by the selective diphenylcarbazide method described by Marczenko (1986). Transference numbers were then calculated using Equation 2.7 after the mobility had been corrected for the effects of ionic strength.

As discussed in Section 6.1.3 and illustrated in Figure 6-4, extraction efficiencies varied significantly between anodes during the electrokinetic test; however, the relationship between chromium mass extracted (as measured in anode effluents) and applied charge appears to be linear (both overall and for each anode). Chromate transference numbers (as %) can be calculated for each data set using equation 2.13 and multiplying by 100 to get a percent. Values of the effluent current-based transference number for the initial and long-term operation of the anodes generally agreed. Current-based transference numbers were calculated initially for the first 108 hours (Test 1-1) and then for the entire demonstration for each anode. Values for each anode are listed in Table 6-9, columns two and three. Anode 2 was terminated after Test 1-1 and therefore is not listed in column three. The general agreement of values listed in columns two and three of Table 6-9 indicates that long-term performance can be predicted from initial testing results. Furthermore, the rankings of the electrodes generally agree between the effluent current-based and soil extract conductivity-based transference numbers. Both methods predicted A2 to have the worst efficiency, yet there is some discrepency between the top two performers. Variations in the numeric values are likely indicative of spatial variability of the chromium concentration with respect to the other ions in the soil profile.

Table 6-9. Transference Numbers Calculated by Conductivity-Based and Current-Based Methods

Anode	Pretest Soil Extract–Conductivity-Based Transference Numbers (%)	Initial Anode Effluent–Current-Based Transference Numbers (%)	Long-Term Anode Effluent–Current-Based Transference Numbers (%)
A1	0.42	0.28	0.28
A2	0.05	0.07	-
A3	1.16	0.30	0.52
A4	1.20	1.02	1.39
A5	1.90	0.53	0.57

Besides a qualitative agreement between the conductivity-based and the current-based transference number, an estimate of the current-based transference number can be made from the soil extract conductivity method. Conductivity-based transference numbers generally overestimate the current-based transference number even after adjusting the electric mobility of the contaminant ion for concentration effects in Equation 2.7. The conductivity-based transference numbers will predict the current-based transference numbers as long as the current pathways are through the soil zones where the samples for the conductivity-based transference numbers were taken. As discussed in previous sections, at the EK demonstration site much of the current was likely "short-circuited" through the upper remediation zone rather than being uniformly distributed throughout the demonstration area. However, despite this abnormality, the conductivity-based transference numbers are fairly close to their respective current-based values.

Evaluating a site to determine the length of time to complete remediation by the EK process requires knowledge of the mass of the contaminant in the remediation zone and the contaminant transference number. First, the amount of contaminant to be removed can be converted to an equivalent electrical charge and then the number of coulombs needed by use of Equations 2.6 and 2.5 (Section 2.2). Finally, if a rate of charge application (electrical current as amperage) is decided upon, the remediation time can be calculated. However, choosing the amperage is not a trivial matter. Amperage is related to electrical power (Section 2.4), and power is related to soil heating (Section 2.5). In addition, soil electrical conductivity, distance between the electrodes, electrode configuration, and thermal properties of the soil all affect the process. In general, the amount of soil heating that can be tolerated is typically the determining factor for the upper limit of current application and hence determines the time of remediation.

6.4 Soil Temperature/Heating

Due to the relatively dry conditions that existed at the electrokinetic site, dissipating the heat generated in the soil was a potential problem. If temperatures in the EK remediation zone were sufficient to induce fluid flow out of the remediation zone, the soil could eventually dry out, stopping the electrokinetic process. To evaluate the potential soil-heating problem, simple heat transfer models were examined. During testing, the amount of energy applied to each electrode was monitored, as well as the soil temperature profile throughout the EK remediation zone.

Numerical modeling results prior to conducting the EK demonstration indicated that the amount of energy input to the soil for electrokinetic remediation would require active cooling of the electrodes to maintain an acceptable temperature in the soil. For this reason, the active electrodes and cold fingers were designed as heat sinks to remove excess heat from the remediation zone. A one-dimensional steady-state heat conduction heat transfer model with volumetric heat generation and constant temperature boundary conditions on each end was solved analytically. This calculation represented the "best case" of electrokinetic remediation with the electrodes that are planar and actively cooled. Results indicated that even with the active cooling of the electrodes, the soil temperature midway between the anodes and cathodes could become unacceptably high. For example, for electrodes spaced 6 feet apart, the distance in the EK demonstration, a peak soil temperature of 50 °C would be reached at a power density of 147 watts per cubic meter at a soil moisture of approximately 12% by weight. The 147 watts per cubic meter could be accomplished by supplying a current density of approximately 2.7 amps per square meter and a voltage potential of approximately 100 volts between the electrodes.

To examine if actively cooling the electrode fluid would be sufficient to maintain soil temperatures at acceptable levels, two-dimensional modeling was also conducted. This model examined the effects of the varying current densities across the EK remediation demonstration area due to line electrodes rather than planar electrodes. For the EK demonstration, the electrodes were constructed of pipe material. The current density would be the highest adjacent to the electrodes since the cross-sectional area was the smallest in this zone. Since soil heating is proportional to the applied power density, the soil temperatures would rise most rapidly in this zone. Modeling results indicated that actively cooling the electrodes would be sufficient in this area to maintain the soil/electrode temperature at acceptable levels; therefore, the fluid in the

electrode casings was actively cooled (Section 4.2.2). Modeling results also predicted the maximum soil temperatures expected midway between the anodes and the cathodes.

The soil temperature profile measured during the demonstration generally agreed with the predicted two-dimensional modeling results. Figure 6-19 illustrates the soil temperature profile for C8 to C3 near the end of Test 1-6. During this testing period, power was being applied between the middle row of anodes and the southern row of cathodes (Figure 5-1 [d]). The highest temperature was located at temperature probe T12 midway between the anode and the cathode (see Table 3-3 and Figure 3-19), which qualitatively agreed with the two-dimensional modeling results.

Soil temperature contours are shifted slightly towards the anodes in Figure 6-19, suggesting that the use of the cathode cold fingers in parallel with the internal electrode is not as efficient in cooling the surrounding soil as the internal electrode by itself. When the cold fingers were energized in parallel with the internal electrodes in Test 1-4 to stop further corrosion of the copper pipe, a portion of the applied current was transmitted from the cold finger to the soil. The cold fingers themselves were not actively cooled during Test 1-4 through 1-6 resulting in an adjacent soil temperature of approximately 26 °C even though the fluid in the cathode cases was maintained at approximately 8 to 10 °C. Heat generated in the vicinity of the cold finger was not dissipated as easily as when the electrode was immersed in the cooled fluid itself (i.e., such as at the anodes).

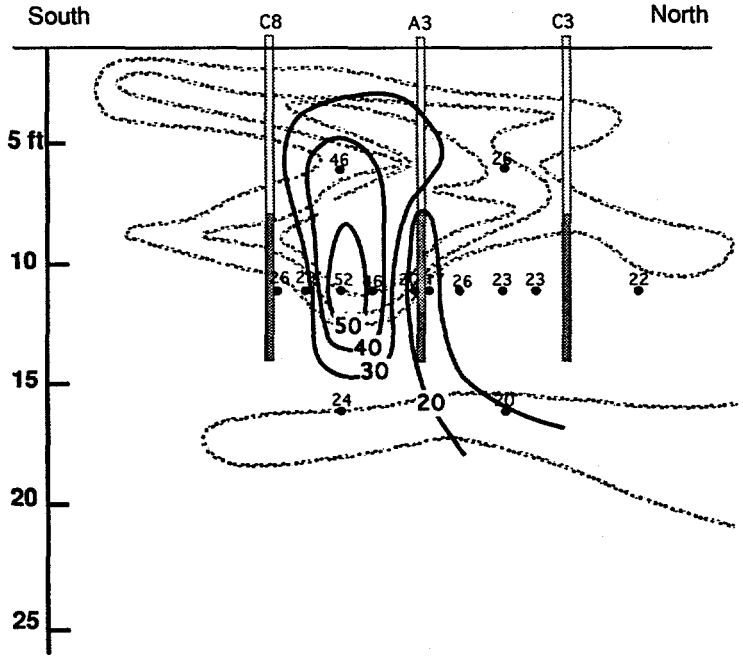

Figure 6-19. Soil temperature profile for cross section C8 to C3.

In general, soil outside the "active remediation zone" was in the 20 to 25 degree range, except for temperature probe T11. This temperature probe, located two feet above the remediation zone, measured soil temperatures much closer to those between the anode and cathode. The increased temperature in this location supports the hypothesis that current was being short circuited though the layer of higher electrical soil conductivity (Figure 6-10) that was located above the active-electrode zone.

6.5 Voltage Gradients

Voltage gradients were examined by measuring voltages at a network of passive electrodes across the EK demonstration site. The voltage potentials were recorded by the CR7 data logger with a 1-gigaohm-resistor voltage-splitter device for electrical isolation. Passive electrodes were placed both in the soil and on the anode and cathode casings (Section 4.2.5).

Analysis of the voltage gradients indicates that there was a significant loss of electrical power due to the electrode geometry. For example, during Test 1-6 approximately 25% of the applied voltage was lost within the anodes and cathodes. Of the 130 volts applied between A3 and C8, a 100 volt difference was recorded by the passive electrodes placed on the outside of the two casings. The 30 volt drop was due to the transfer of the electrical current from the electrode through the fluid in the electrode casing and through the porous ceramic.

The majority of the voltage loss was due to the decreasing area as the current approached the electrode. This reduction of area was caused by using pipes as the electrodes. The surface area of the electrodes was fairly small (approximately 0.3 square feet) when compared to the approximately 18 square feet of soil for the current to travel through midway between the electrodes. Ohm's law dictates that as the cross-sectional area becomes less, the voltage drop will become proportionally higher. Large planar electrodes would overcome this voltage loss at the electrodes.

Within the soil, the voltage gradient varied between the anodes and cathodes. Figure 6-20 illustrates the voltage gradient between A3 and C8 during Test 1-6. The largest voltage drop was seen near C8 where a calculated voltage drop of 37 volts per foot was measured between P11 and PC8 (see Table 3-3 and Figure 3-20). Although a similar argument to the one above could explain this large voltage drop, a similar voltage drop was not seen in the vicinity of the anode. This voltage drop in the soil near C8 was likely due to hydroxyl ions produced at the CFC8 electrode precipitating calcium hydroxide thus lowering the electrical conductivity of the pore water solution. The low voltage drop near the anode (7 volts per foot) was likely due to a slight acidification of the soil. The other variations between the measured soil voltage gradients (9 to 17 volts per foot) were likely due to spatial variability of the soil electrical conductivity or measurement error of the voltage gradients.

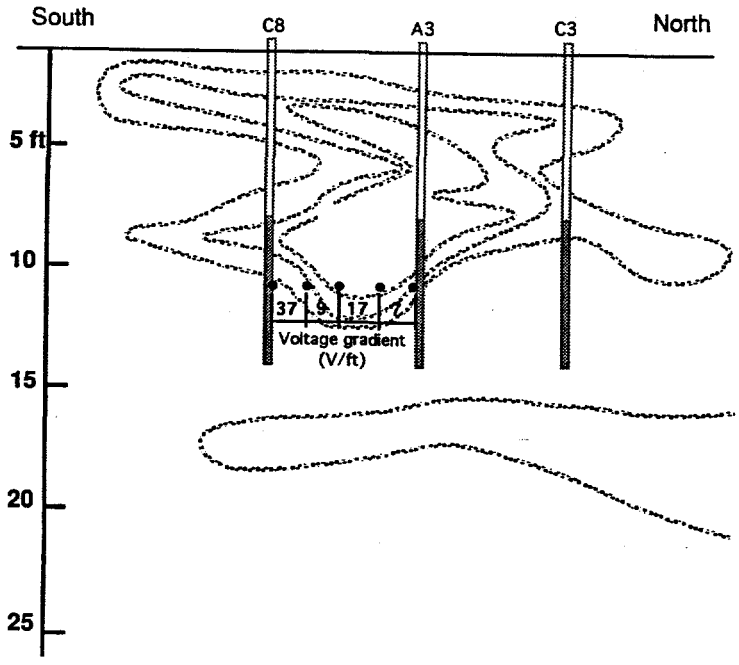

Figure 6-20. Voltage gradient between A3 and C8 during Test 1-6.

6.6 Metal in the Remediation Zone

Buried metallic objects are much more electrically conductive than soil. Copper, for example, is a trillion times more conductive than the soil at the EK demonstration site. Because of their high electrical conductivity, metallic objects will tend to readily conduct electrical current through them. The portion of the metallic object near the anode will become reduced, whereas the opposite end will be oxidized. This oxidization of the metal will eventually destroy any metal in the remediation zone. Lageman (1993) suggested that metallic objects of greater than 10 cm diameter be removed from the soil prior to electrokinetic remediation.

Although the surface geophysical surveys and soil sampling did not indicate any metallic debris in the electrokinetic remediation area, copper cold fingers were installed prior to the application of current as backup electrodes. These cold fingers were thought to be safe from electrical oxidation due to their small diameter (1 inch OD) and the fact that they were placed parallel to the voltage gradient. High copper concentrations were detected in the cathodes during

the first phase of testing. After Test 1-4, when the CFC9 external cold finger would not hold water, the source of copper was confirmed to be the cold fingers attached to the cathode casings which corroded due to the high voltage gradient in those areas at the cathodes. Subsequent pressure testing of the cold fingers located between the anodes and cathodes (CF1-CF10 in Figure 3-21) prior to Test 3-1 indicated small leaks in these cold finger assemblies as well, despite their being located within fairly low voltage gradients as compared to gradients near the cold fingers attached to the cathode assemblies (see Section 6.5).

It appears that all metal, regardless of size and location, in the EK remediation zone is subject to galvanic corrosion. Pre-investigations of potential EK remediation sites should include geophysical surveys to evaluate sites for the potential of buried metal. Care should be taken when selecting monitoring equipment and materials. In addition, EK remediation sites under buildings where structural steel, water pipes, electrical conduits, and reinforced concrete are present will have to be electrically insulated or placed at the same electrical potential as the cathodes to prevent galvanic deterioration of these items.

6.7 Organic Analyses

If present, aqueous-phase, chlorinated volatile organic compounds (CVOCs) could be electroosmotically transported into the cathode casings and exit in the liquid effluent or be stripped out of the water and exit through the vacuum. In addition, if any liquid organic phase VOCs are present in the zone of influence, the resistive heating could result in increases in the measured concentrations of VOCs in the soil gas. Both liquid and gaseous CVOCs were suspected to be present in the UCAP. Therefore, soil samples were collected at 7.5 and 12.5 feet, from two boreholes, NT3 and NT7 (Fig. 3.15) for organic analyses to assess what type of VOCs were present in the EK demonstration area. Two additional types of samples (cathode liquid effluent and cathode gaseous exhaust) were collected to determine whether the transport of VOCs to the cathodes by electroosmosis was significant. Finally, soil gas samples were collected from a sampling port within the demonstration area to assess the affects of soil heating on the VOC soil gas concentrations.

Liquid effluent samples were collected from the middle cathode effluent stream (C8) directly into 40-milliliter volatile organic analysis (VOA) vials. The exhaust from all of the cathodes was directed into one exhaust port, and this exhaust was sampled directly into evacuated SUMMA™[32] canisters. The cathode effluent stream and vacuum system exhaust were collected together at two times during the demonstration, within Test 1-3 and between Tests 3-1 and 3-2.

Soil gases were also collected directly into evacuated SUMMA™ canisters. The soil gas sample port was located at the T5 location (see Table 3-3 and Fig. 3-19) 9 feet below the ground surface. The port was simply a 200 mesh steel screen about 3 inches long, rolled up and clamped to the end of a ¼ inch polyethylene tube. The tubing was purged with a vacuum pump prior to

[32] SUMMA™ is a trademark of B R C/Rasmussen

sampling. Soil gas samples were collected 2 months prior to the application of current for the EK demonstration, approximately mid-way through the demonstration (Test 3-1), and about two weeks after the end of the demonstration.

TCLP extracts of soil and liquid samples were conducted by an outside contract laboratory (EPA Method 1311). Soil samples were analyzed for volatile organic compounds (VOCs) by EPA Method 8240, semi-volatile organic compounds (SVOCs) by EPA Method 8270, and poly-chlorinated biphenyls (PCBs) by EPA Method 8080. Effluent samples were analyzed for VOCs by Method 8240, and cathode exhaust gas and soil gas samples were analyzed for VOCs by Method TO-14.

For the soil samples and cathode effluent and exhaust gas samples, most analytes were not detected at all, and those that were had very low concentrations. The results of the sample analyses for only those organics detected are listed in Table 6-10. In general, organics were not driven out of the EK demonstration area through the cathode effluents or cathode exhausts. Tests 3-2 and 3-3 utilized the simpler cold finger electrodes which mitigate the release of VOCs by not extracting liquid or gas to the ground surface. The complex ceramic cathodes would be needed only if the contaminants are in a cationic state.

The soil gas sampling showed a slight increase in VOC concentrations in the samples after the EK demonstration was completed. Although no soil samples showed high organic concentrations to indicate the presence of liquid phase VOCs, the increased soil temperatures from the soil heating induced by the EK remediation process could have led to the slightly higher levels detected.

Table 6-10. Results of Sample Analysis for Detected Organics

Sample	NT-3	NT-3	NT-3	NT-7	NT-7	Cathode Effluent	Cathode Exhaust	Cathode Effluent	Cathode Exhaust	Soil Gas North	Soil Gas North	Soil Gas North
Location	7.5	7.5	12.5	7.5	12.5							
Date	Pretest	Pretest	Pretest	Pretest	Pretest	7/10/96	7/10/96	10/11/96	10/11/96	3/8/96	9/13/96	12/9/96
Sample I.D.	026991	026991 DUP	026993	027012	027014	30533	30532	52060	31699	27717	31524	32269
	mg/kg	mg/kg	mg/kg	mg/kg	mg/kg	(mg/L)	(ppmv)	(mg/L)	(ppmv)	(ppmv)	(ppmv)	(ppmv)
ANALYTES:												
Acetone	0.022	0.030	0.0042 J	0.016	0.012	25 B		64				
Benzene							0.001 J					
2-Butanone (MEK)						44		150				
Chloroform								5.5				1.6 E
Chloromethane								18				
1,2-Dibromoethane												0.47
1,2-Dichlorobenzene												0.35
1,1-Dichloroethane												0.14
1,2-Dichloroethane						4.8 J		11				0.36
Dichlorodifluoromethane												0.38
bis(2-Ethylhexyl)phthalate			0.038 J									
Methylene chloride						2.4 J,B	0.004 B,J	3.9 J	0.42			0.36
Nitrobenzene	0.35	0.38	0.20 J	0.40	0.56							
PCB: Aroclor 1260	0.17	0.16	0.67	0.16								
PCB: Aroclor 1242					1.4							
Tetrachloroethene								4.8 J				2.4 E
Toluene							0.001 J	7.5				
1,2,4-Trichlorobenzene	0.34	0.39	0.16 J	3.4	0.74		0.002 J			0.94		5.3 E
1,1,1-Trichloroethane								4.5 J			0.45 E	4.2 E
Trichloroethene						4.1 J	0.002 J	69		3.3	1.6 E	19.0 E
Trichlorofluoromethane											0.41 E	1.2 E
1,1,2-Trichloro-1,2,2-trifluoroethane							0.001 J				0.82 E	2.1 E
m-Xylene & p-Xylene							0.002 J					
o-Xylene							0.0008 J					
total Xylenes												0.076 J

J is below the quantitation limit but above the method detection limit.
E is above the calibration range; therefore, the result is estimated.
B denotes the analyte was detected in the associated method blank.

7. SUMMARY

The SNL EK demonstration successfully removed anionic contamination from unsaturated soil at the field scale without significantly changing the soil moisture content. After 2700 hours of operation, 600 grams of chromium(VI) were extracted from the soil beneath the SNL CWL in a series of thirteen tests. The contaminant was removed from soil which had moisture contents ranging from 2 to 12 weight percent. This demonstration was the first EK field trial to successfully remove contaminant ions from arid soil at the field scale.

The success of the demonstration is attributed to the patented EK extraction electrodes (Lindgren and Mattson, 1995). These electrodes allow the transfer of contaminant ions from water contained in the soil pores to liquid contained in the electrode casing. The electrode system is constructed of a porous-ceramic outer casing and an inner iridium-coated titanium electrode. A vacuum applied to the interior of the electrode allows liquid to circulate freely within the electrode casing without being transferred to the surrounding soil. A voltage potential is applied between electrodes resulting in a current that provides the transport mechanism for the contaminant ions through the soil and into the electrode casing. Over time, the contaminant concentrations will build up in the electrode casing liquid. The contaminants are removed from the electrode casings by pumping the electrode liquid to the ground surface for subsequent treatment or disposal.

A special feature of the patented electrode system is its ability to control the amount of water added to the soil in the EK demonstration. The anode casings were treated prior to placement in the ground with a coating which mitigated the water loss to the soil by electroosmosis, as was noted in previous field testing of the electrode system (Mattson, 1994). Water mass-balance calculations indicate that a net of approximately 20 gallons of water was added to the soil during the EK demonstration. However, three times that amount of water was transported in the soil-water system from the anodes to the cathodes due to electroosmosis. No significant changes in the soil moisture content profiles were noted when compared to the pre-demonstration values. In addition, no significant changes in electrical conductivity and only minor changes in soil pH were noted during the EK demonstration.

The EK demonstration was terminated prior to complete cleanup of the soil beneath the UCAP site. During the demonstration, chromium extraction efficiencies (grams Cr(VI) removed per amp-hr) did not deteriorate, indicating that the EK process is stable over long periods of time. The EK demonstration was stopped due to budget constraints and to time constraints since the SNL Environmental Restoration Program had scheduled a Voluntary Corrective Action at the site.

Post-test soil sample chemical results in the EK remediation zone indicate a cleaning of the soil near the cathodes and an accumulation of chromate in the area near the anodes. No significant changes in chromium concentrations were noted outside of the remediation zone. Soil samples adjacent to the cathodes would pass the TCLP criteria of 5 ppm, indicating that soil in this area would not be considered hazardous waste if excavated and removed to the surface. Soil samples taken in the area of the cathodes had TCLP chromium concentrations as high as 28 ppm

prior to conducting the EK demonstration. It is expected that all of the soil in the of remediation area would have passed TCLP criteria if the EK demonstration had run to completion.

Electrokinetic remediation can transport only contaminants that are dissolved in the soil water. Contaminants that are in a precipitated solid phase or sorbed onto the soil particles will not be transported until they are brought into the liquid phase. At the EK demonstration site, some of the chromium(VI) has likely co-precipitated with gypsum as $CaCrO_4 \cdot 2H_2O$ or has precipitated as anhydrous chromatite ($CaCrO_4$). Both of these solid forms of chromate have slow dissolution rates. In soil zones where the chromate ions have been removed by electromigration, these slowly dissolving solid forms of chromate may recontaminate the water contained in the soil pores after some period of time. This dissolution of chromate would extend the time to complete a remediation effort.

Transference numbers compare the fraction of the current carried by the contaminant ions to the total amount of current applied. Calculating contaminant transference numbers from soil samples collected prior to conducting EK remediation permits an estimate of the EK extraction performance. Transference numbers calculated from pretest soil samples closely correlated with EK extraction efficiencies. Using these numbers, an estimate of the amount of chromium removed per applied charge can be made for individual electrodes. If the total mass of contaminant is known in the remediation zone, the amount of electricity needed to remediate the site can also be estimated.

The EK performance can be qualitatively predicted by the electrical conductivity profile surveys. These surveys give a vertical profile of the soil electrical conductivity. At the EK demonstration site, the electrical conductivity survey indicated a more electrically conductive layer above the EK remediation zone. This more conductive zone was expected to carry a more significant portion of the applied current than the less electrically conductive zones directly between the anodes and the cathodes, and subsequent tests confirmed this hypothesis.

Acetate, a byproduct of the neutralization reaction at the cathode, was used as a chemical tracer to identify current pathways through the soil at the EK demonstration. Acetate was detected in the upper zone of the demonstration site, which supported the theory that much of current was transported in the upper more electrically conductive soil layer.

Analysis of soil temperature profiles during an EK operation can also indicate areas of electrokinetic remediation. Temperature increases from pretest values are indicative of the amount of power passing through the soil. Heat generation is a function of the thermal capacity of the soil and the power density. Power can be described by the square of the current times the soil resistivity. In general, soil temperature increases are directly related to the amount of current passing through the soil. At the EK demonstration site, the soil horizon immediately above the electrode zone exhibited substantial temperature increases and infers the passage of significant amounts of electrical current in this area.

The application of increased power to the EK remediation zone has a two-fold effect on EK remediation. First, although the soil should be remediated in less time by increasing the

applied electrical power, the electrical cost per mass of contaminant removed will increase substantially. Increasing the electrical power, increases the driving force of electromigration, thereby hastening the time to remediate the soil. Typically, less time spent remediating a site will result in an overall remediation cost savings. However, increased power density to the soil also results in more electrical energy being expended to remove a certain mass of contaminant. The time savings by increasing the electrical power would have to be weighed against the lower energy efficiency of contaminant extraction.

Besides a cost consideration of applying more power, perhaps more importantly are the secondary transport effects of heating the soil. Although some benefits are realized by limited soil heating, overall excess soil heating is likely detrimental to the EK process. Electrical currents may concentrate in certain areas of the soil profile bypassing other contaminated soil zones. Soil pore water could be diminished by thermally induced gradients or be evaporated from soil zones to effectively stop the EK process. Indigenous biological organisms may be killed. Release of VOCs into the soil gas may be significantly increased by an increase in organic vapor pressures. Although the EK demonstration did not exhibit all of these effects, it is reasonable to assume that they were taking place to some extent.

Theoretically, the current travel pathways should be controllable in unsaturated soils by the addition of water to soil zones where higher electrical current density is desired. Electrical conductivity of unsaturated soil is a strong function of moisture content. During one series of testing, water was added to the soil in the lower portion of the EK demonstration in an attempt to increase the soil electrical conductivity. Chromium extraction efficiencies almost doubled during this test, indicating that the current pathways were redirected through these wetted soil zones. However, it is also possible that additional chromate was dissolved by the water added to the soil profile causing increased removal efficiencies.

Using the simpler designed cathodes (i.e., cold fingers) proved to be as effective in the removal of chromate as the more complex extraction cathodes. Tests using the cold finger cathodes exhibited no loss in extraction efficiency when compared to the tests using the more complex cathode system. Due to electrolysis reactions between the copper electrode and the soil water, minor pH increases were noted in the soil adjacent to the cold finger electrodes.

Any metal in the EK remediation area should be avoided. Metal is much more electrically conductive than soil and therefore, can create a current "short circuit" through the soil. Electrical current in soil that contains significant amounts of metallic objects could effectively bypass zones of contaminated soil. In addition, metallic objects would be oxidized to the extent that they would contribute to dissolved ions in the soil water. Proposed EK remediation under buildings that contain structural steel, metallic pipelines, and other electrically conductive accessories deserve special consideration.

Operation of electrokinetics can increase soil temperatures to the extent that organic vapor concentrations in the soil gas can become significant if organic liquids are present in the remediation zone. Soil gas concentrations in the EK remediation area increased slightly likely due to an increase of the soil temperature. No significant concentrations of VOCs were noted in

the cathode effluent or in the cathode vacuum exhaust. If liquid organics are present, it may be advantageous to combine EK remediation with soil vapor extraction for the removal of both organic and inorganic contaminants.

Although the newly patented electrode system was successful in removing an anionic contaminant (i.e., chromate) from unsaturated sandy soil, the electrode system was a prototype and has not been specifically engineered for commercialization. A redesign of the electrode system to improve operation and reliability and to reduce maintenance and cost is suggested for future EK field trials.

This demonstration has also led to the initiation of an innovative electrode system to remove chromium that will substantially reduce the cost of EK remediation. The new system uses a solid matrix chromate capture system, thus eliminating the need for a liquid control system and a vacuum system. In addition, the new electrodes will be planar in design to better transfer the electrical power to the soil. Electrical costs will be reduced to one-half the present values by operating the system at a lower power, thereby avoiding the expense of actively cooling the EK electrode system. SNL and Sat-Unsat, Inc. have tested a laboratory-scale prototype of this electrode for removing chromate from unsaturated soil. Additional funding is being sought to further develop this new electrode system.

8. REFERENCES

Acar, Y.B., R.J. Gale, G. Putnam, and J. Hamed, 1989. "Electrochemical Processing of Soils: Its Potential Use in Environmental Geotechnology and Significance of pH Gradients." *2nd International Symposium on Environmental Geotechnology*, Shanghai, China, May 14–17. Envo Publishing, Bethlehem, PA, Vol. 1, pp. 25–38.

Acar, Y.B., R.J. Gale, and G. Putnam, 1990. "Electrochemical Processing of Soils: Theory of pH Gradient Development by Diffusion and Liner Convection." *Journal of Environmental Science and Health, Part (a); Environmental Science and Engineering*, Vol. 25, No. 6, pp. 687–714.

Archie, G.E., 1942. "The electrical resistivity logs as an aid in determining some reservoir characteristics." Trans. *AIME* 146, pp. 54–62.

Bard, A.J., and Faulkner, L.R., 1980. *Electrochemical Methods Fundamentals and Applications*. John Wiley and Sons, New York.

CRC (The Chemical Rubber Company), 1971. *Handbook of Chemistry and Physics - 1970-1971*. Section 4, p. D82.

Griffin, R.A., and J.J. Jurinak, 1978. "Estimation of activity coefficients from the electrical conductivity of natural aquatic systems and soil extracts." *Soil Science*, (116): 26–30.

Hillel, D., 1980. *Fundamentals of Soil Physics*. Academic Press, New York, NY.

Hunter, R.L., 1981. *Zeta Potential In Colloid Science*. Academic Press, New York.

Hyndman, D.A., 1995. "Magnetic and Electromagnetic Investigations at the Unlined Chromic Acid Pit." Unpublished report by Sunbelt Geophysics prepared for Sandia National Laboratories, Albuquerque, NM.

IT (International Technologies), 1992. "Unlined Chromic Acid Pit (UCAP) Site Investigation." Report submitted to Sandia National Laboratories, October, 1992.

Lageman, R., 1993. "Electroreclamation : Application in the Netherlands." *Environ. Sci. Technology*, Vol. 2, No. 13, 2648.

Lindgren, E.R., and E.D. Mattson, 1995. "Electrokinetic System for Extraction of Soil Contaminants from Unsaturated Soils." United States patent # 5,435,895, July 25, 1995.

Marczenko, Z., 1986. *Separation Spectrophotometric Determination of Elements*. Ellis Horwood Limited, Chichester, England.

Mattson, E.D., 1995. "Borehole Effects on Unsaturated Electrokinetic Remediation." Presented at the *Fifth Annual WERC Technology Development Conference*, April 18-20, 1995, Las Cruces, NM.

Mattson, E.D. and Lindgren E.R., 1993. "Electrokinetic Extraction of Chromate from Unsaturated Soils", in *Emerging Technologies in Hazardous Waste Management IV*, ACS Symposium Series, WA.

Mattson, E.D. and Lindgren, E.R., 1994. "Electrokinetics: An Innovative Technology for In-situ Remediation of Heavy Metals." Presented at *the 8th Annual Outdoor Action Conference* of the National Ground Water Association, May, 1994.

McCorkle, R. Wayne, and Thomas A. King, 1997. "Radio Imaging Method Survey Analysis for the Electrokinetic Remediation Project at the SNL UCAP Site, Final Report." Unpublished report by New Mexico State University Physical Science Laboratory prepared for Sandia National Laboratories, Albuquerque, NM.

Persaud, N. and Wierenga, 1982. "Solute Interactions and Transport in Soils from Waste Disposal Sites at Sandia Laboratories." Report submitted to Sandia National Laboratories by Dept. of Agronomy, New Mexico State University, June, 1982.

Shapiro, A.J., Dissertation submitted to the Massachusetts Institute of Technology, 1990.

SNL (Sandia National Laboratories), 1991. "Chemical Waste Landfill Final Closure Plan and Post-Closure Permit Application." Prepared by SNL Environmental Impact and Restoration Division 7723, December, 1991.

Stanier, R.Y., Ingraham, J.L., Wheelis, M.L., and Painter, P.R., 1986. *The Microbial World.* Prentice Hall, New Jersey.

Stein, C.L., 1994. "Chromium Geochemistry in Calcareous Soils." Report submitted to Sandia National Laboratories Mixed-Waste Landfill Integrated Demonstration, December 8, 1994.

APPENDIX A: RESULTS OF SITE INVESTIGATIONS

Further investigations of the proposed EK remediation site were performed to identify more accurately the areas of high water-soluble chromium in order to choose the actual site and to estimate the initial chromium mass concentrations at the site. The first level of activity was to take geoprobed ("GP") samples with the Hurricane Sampling System®. These samples were quickly analyzed for total chromium by XRF, for gravimetric moisture content, and then for water-soluble chromium by a quick in-house water-extraction method (Method A) with subsequent analysis by flame or graphite furnace atomic absorption spectroscopy. The pH and conductivities of the extracts was also determined. The method and results are described in Section A.1.

Secondly, while drilling the boreholes for the electrode casings and the neutron tube access holes, pretest samples were taken to further characterize the actual site chosen. A portion of these samples was oven-dried for gravimetric moisture content. A second portion was extracted by a refined, in-house water-extraction method (Method B) and analyzed by graphite furnace atomic absorption spectroscopy. In addition, the extracts were measured for pH and conductivity at a later time period. A third portion was sent to an off-site laboratory for analysis by the EPA Approved Toxicity Characteristic Leaching Procedure (TCLP) (Method 1311 of EPA Publication SW-846) which extracts metals with a 20:1 weak acid to soil ratio. This work is described in Section A.2.

After the EK remediation effort was ended, post-test soil samples were taken to determine changes in the moisture and chromium contents. Because the pretest in-house sample results exhibited some inconsistencies, a further refined, water-extraction method was developed (Method C). In addition, pH and conductivity of the water extracts were measured, and acetate, chloride, nitrate, and sulfate as well as the chromate concentrations were determined by ion chromatography. Again, samples were sent out for TCLP analysis. Section A.3 describes these results.

A summary of the three in-house methods of water-extraction is given below.

GP Samples (Method A)	Pre-Test Samples (Method B)	Post-Test Samples (Method C)
Some samples a mixture of dried & original soil; others original soil	Samples all dried soils	Samples all original soils
Water : soil ratio 2:1	Water : soil ratio 2:1	Water : soil ratio 2:1
Shake 30 sec. by hand	Orbital shaker 1.1 hours	Hematology mixer 2.0 hours
Centrifuge 1 min	Sit undisturbed 1 hour	Sit undisturbed 15-20 hours
Filter w/ 0.45 μm filter with a syringe	Vacum filter through 2.5 μm filter circles	Centrifuge 1 hour
If filtrate not clear, add 25 mL glacial acetic acid, let sit, refilter	Filter w/ 0.45μm filter with a syringe	No filtration

Finally, additional samples were taken for the EPA Superfund Innovative Technology Evaluation (SITE) program for the oversight personnel. The samples were analyzed for TCLP chromium (pretest only), total chromium, and chromium(VI). These results are in Section 4.

A.1. "GP" Soil Samples

OBJECTIVE

Soil samples were taken around UCAP 3 to survey the high chromium contamination levels in order to make a decision about placement of the EK Extraction System Demonstration. Samples were called GPxx-dd (xx is hole number, dd is the depth) and dated, were collected in October of 1995 and analyzed for several properties.

SAMPLING METHOD

Samples were collected with the Geoprobe® and Hurricane Sampling System®. Two-foot samples were taken in the 6- to 20-foot range BLS with a plastic sleeve inside a sampler that was pneumatically-pounded into the soil. The sampler had a tip that was stationary while being pounded to depth and then retracted into the sampler while pounded two feet to obtain the sample. A portion of the soil sample was poured into a can for oven drying for moisture analysis, and a second portion poured into a bottle for chemical analysis (later samples were stirred prior to taking splits).

PROCEDURE

A portion of the bottled sample (about 100 g) was then microwave-oven dried, passed through a 10-mesh seive, and analyzed by energy-dispersive XFR. The extra dried soil was poured back into the bottle for the first set of samples. Another portion of the bottled sample was mixed with water, and the water-soluble chromate analyzed by either graphite furnace or flame atomic absorption spectroscopy for total chromium. The later decision to do a water-soluble extraction resulted in the test being performed on the mixture of dried and original soil for that set. The water extracts were also measured for pH and conductivity.

WATER-EXTRACTION METHOD A

Extractions for water-soluble chromium were performed according to a quick and easy in-house method described below:

1. Stir soil sample to homogenize.
2. Determine soil moisture content (oven dry a sample).
3. Weigh out 10 g of the original soil into a centrifuge tube.
4. Calculate the appropriate amount of water to add to make a 2:1 ratio of water to dry soil.
   For example, 15% moisture content (water/dry soil) is 1.5g water in 10g soil or in 8.5g dry soil; therefore, for a 2:1 ratio, a total of 17g water or 15.5g of added water is needed.
5. Add (by weight) the calculated amount of water needed by syringe directly into the centrifuge tube.
6. Shake by hand 30 seconds.
7. Place into centrifuge for 1 min. at full speed.
8. Decant supernatant directly into a syringe.
9. Filter through 0.45micron syringe filter into sample bottle.
10. If small particles are not removed by filtration, add 25 microliters of glacial acetic acid, allow to precipitate out, and refilter.

The total elapsed time (from the time the water was added until the filtering was done) was usually 15 - 25 minutes (the longer times were for sets with samples that were hard to filter).

RESULTS

Results for total chromium by XRF, moisture content, and water-soluble Cr (reported as ppm in soil) for the "GP" samples are given in Table A-1. In addition, the pH and conductivity of the water extracts is given.

TABLE A-1: XRF, Moisture Content, and Water-Soluble (Method A) Chromate Results for "GP" Soil Samples Taken from the CWL

Hole	Date	XRF ppm Cr	Moisture (wt%)	Water-soluble Cr * (ppm in soil)	Extract pH	Extract Conductivity (mS/cm)
GP01-15	100695	80		3.12		
GP02-15	100795	32478	4.44			
GP03-13	100795	25141	3.88			
GP04-14	100795	3540	5.09			
GP05-15	100795	40	1.54			
GP08-11A	101495	21	2.49			
GP08-11B	101495	102	2.01			
GP11-07	101795	60	9.17	0.5	5.22	10.83
GP11-09	101795	2584	24.55	1520.5	7.93	19.71
GP11-11	101795	7615	9.36	127.2	7.83	6.73
GP11-13	101795	22692	4.39	288.8	7.74	4.60
GP11-14	101795	19063	3.72	357.7	7.80	4.98
GP13-03	102795	222	8.44	13.5	8.07	0.63
GP13-05	102795	159	3.67	19.9	8.20	0.88
GP13-07	102795	65	4.92	9.5	7.75	1.51
GP13-09	102795	42	4.08	12.7	7.59	2.85
GP13-11	102795	35	4.39	4.2	7.77	1.69
GP13-13	102795	30	1.66	1.8	7.82	0.78
GP13-15	102795	79	2.40	5.3	8.01	0.78
GP13-17	102795	112	7.05	44.6	8.05	1.21
GP13-19	102795	42	2.07	3.3	7.83	0.63
GP14-17	110495	2312	2.76	171.4	7.84	3.26
GP14-19	110495	126	1.96	29.8	7.91	0.82
GP14-21	110496	575	5.35	73.0	8.17	1.32
GP15-09	111195	15	4.38	3.0	8.72	0.41
GP15-11	111195	20	6.47	1.5	8.09	0.70
GP15-13	111195	26	4.88	1.2	8.23	0.56
GP15-15	111195	6435	2.77	59.5	7.87	2.55
GP15-17	111195	335	7.38	36.5	8.09	1.16
GP15-19	111195	113	9.96	47.1	8.03	1.40
GP15-21	111195	85	2.18	6.0	8.14	0.30
GP16-09	111195	93	8.52	0.1	9.00	1.08
GP16-11	111195	25	1.82	1.0	8.32	0.43
GP16-13	111195	5275	2.01	36.2	8.10	1.63
GP16-19	111195	193	8.42	97.1	8.33	1.33
GP16-21	111195	175	2.85	18.1	8.60	0.65
GP17-17	111195	4515	3.63	48.3	7.89	1.98
GP17-19	111195	79	2.07	2.9	8.30	0.36
GP17-21	111195	142	1.69	2.3	9.10	0.45
GP20-07	111795	125	6.97	20.9	8.36	0.91
GP20-09	111795	26770	12.41	605.4	7.97	2.75
GP20-11	111795	8965	8.28	155.8	7.71	3.11
GP20-13	111795	13383	2.25	114.7	7.84	2.64
GP21-07	111795	146	6.31	19.0	8.81	3.61
GP21-09	111795	1219	11.24	2.5	9.17	4.95
GP21-11	111795	80	4.94	2.6	8.82	1.25
GP21-13	111795	12316	2.09	119.3	8.04	3.99

*GP11-7—14-21 by flame AA; GP 15-9—21-13 by furnace AA

A.2. Pretest Soil Samples

OBJECTIVE

To further characterize the EK site, soils samples from the electrode casing boreholes were extracted with water, and the extracts were analyzed for chromate. The in-house water extraction method was refined to extract more of the water-soluble chromium. The pH and conductivities of the extracts were also determined. In addition, the moisture content of a set of these pretest soils samples (electrode casing boreholes and others) was determined and a set of soil samples were set to an off-site laboratory for TCLP Cr content.

WATER-EXTRACTION METHOD B

REAGENTS, APPARATUS, AND INSTRUMENTATION

Sodium dichromate (99.5%) was used in the preparation of standards. Deionized water for the extractions and the preparation of standards and eluents was polished to greater than 18 MΩ with a Barnstead® Nanopure® system (Barnstead® model 04741).

The extracts were pre-filtered with 2.5 μm glass fiber filter circles (Fisherbrand®, Fisher P/N 09-804-42D) in a Büchner funnel. Subsequent filtrations were done with 0.45 μm Gelman® polyethersulfone syringe filters (Fisher P/N 09-730-264D). Chromate concentrations were determined with a Dionex® model 4000i using a Dionex® AS11 anion column and hydroxide eluents.

METHOD

Samples were received dry (except for sample IDs C2-6, C2-10, and C2-12). The three samples which had not been previously dried were dried in an oven at 110 °C for 48 hours.

The soils were coned and quartered, and a section with a mass between 9 and 12 grams was placed in a tarred 50-mL disposable weighing beaker. The soil was accurately weighed in the beaker and placed into a 250- or 125-mL Erlenmeyer flask.

Enough deionized water was added to the flask so that a 2:1 ratio of water to soil was used for the extraction. The flask was sealed immediately with Parafilm M® and placed on an orbital shaker at 250 rpm for 1.1 hours. After mixing was complete, the samples sat undisturbed for 1 hour before filtration was initiated.

The extractions were performed in sets of twelve samples each. For a given run, between 45 and 60 minutes were required to complete the pre-filtration step. Thus, some samples were given a longer sitting period than other samples. The supernatant was vacuum filtered through 2.5-μm glass filter circles in Büchner funnels, and the filtrate was collected in 20-mL polypropylene scintillation vials. A final filtration was completed by pushing the extracts through 0.45-μm syringe filters. This filtrate was collected in a second set of plastic scintillation vials. Extract pH and conductivity was determined.

The filtered extracts were initially diluted 2-fold before the analysis was performed by ion chromatography. Subsequent dilutions of 5-fold, 10-fold, or 20-fold were prepared for those samples that were out of range of the standards. Three standards were prepared having concentrations of 0.100, 0.200, and 0.400 mM. A quadratic regression function was used to establish the calibration curve. The curve was forced through the origin. The chromatographic separation was done with an AS11 Dionex® column using hydroxide eluents. An isocratic separation was performed with an eluent strength of 24 mM NaOH. Conductivity detection was utilized.

RESULTS AND DISCUSSION

The in-house water-extraction chromate concentration of each soil sample (reported as parts per million in the original soil sample) is presented in tabular form in Table A-2. This represents the portion of soil that contains chromium that can be extracted in the form of chromate with deionized water. Sample A3-16 was highest in extractable chromate. Many samples had no chromate or too little chromate to detect by this method, which permitted the detection of as little as 0.1 ppm chromate in the diluted extracts (sample C5-14). The pH and conductivity of the extracts given in this table.

The moisture contents (in-house gravimetric method) and off-site laboratory TCLP results of a set of pretest soil samples is given in Table A-3. The TCLP Cr concentration is that for the extract (the extract is from a 20:1 weak acid to soil extraction), not calculated back to the soil sample.

Table A-2. DI Water Extracts (Method B) of EK Casing Borehole Samples

Sample ID	Extractable Cr in form of CrO_4^{2-} (ppm/soil)	Extract Conductivity (mS/cm)	Extract pH
A1-6			
A1-8			
A1-10	73.38	5.76	7.26
A1-12			
A1-17			
A2-7.5	0.00	4.98	7.49
A2-10	19.51	6.46	6.82
A2-12.5			
A2-15			
A2-17.5			
A2-20			
A2-22.5			
A2-25			
A2-30	27.33	0.86	8.11
A3-10	93.18	3.69	7.48
A3-12	95.52	2.90	7.70
A3-16	620.21	3.67	7.83
A4-6	8.40	1.29	8.10
A4-8	60.54	4.27	7.68
A4-10	199.82	3.42	7.75
A4-12	55.20	2.90	7.79
A4-16	246.57	3.73	7.67
A5-6			
A5-10	232.84	4.14	7.49
A5-12	115.12	2.78	7.73
A5-16	140.29	3.14	7.56
C1-6	0.00	1.93	8.20
C1-10	0.00	0.44	8.39
C1-12	1.19	0.35	8.27
C1-14	229.72	3.76	7.72
C2-6	0.00	1.73	8.00
C2-8	0.00	0.61	8.34
C2-10	0.00	0.42	8.09
C2-12	5.59	0.69	7.60
C3-6	0.00	1.30	8.24
C3-8	0.00	0.81	8.30
C3-10	0.00	0.50	8.22
C3-12	0.00	0.36	8.21
C3-14	146.94	2.99	7.70

Sample ID	Extractable Cr in form of CrO_4^{2-} (ppm/soil)	Extract Conductivity (mS/cm)	Extract pH
C3-16	151.10	1.71	7.89
C5-6	0.00	0.57	8.27
C5-8	0.00	0.39	8.38
C5-10	6.47	0.55	8.07
C5-12	2.23	0.35	8.11
C5-14	0.35	0.31	8.13
C5-16	43.76	1.09	7.68
C6-16	4.95	0.57	8.11
C7-6	0.00	5.13	9.36
C7-8	60.29	10.40	6.96
C7-10	12.71	4.24	7.88
C7-12	230.76	4.44	7.52
C7-12'	85.85	4.14	7.59
C7-14	12.00	1.25	8.02
C7-16	36.42	1.80	7.80
C8-10	30.70	1.81	7.81
C8-12	50.48	2.82	7.75
C8-14	34.30	1.45	7.82
C8-16	17.33	0.80	7.88
C9-6	0.79	1.13	8.89
C9-8	68.72	3.07	7.44
C9-10	147.98	3.02	7.75
C9-12	14.48	0.60	8.00
C9-14	13.02	0.62	7.98
C9-16	1.52	0.42	8.15
C10-6			
C10-10	258.63	3.73	7.82
C10-12	49.21	1.19	8.03
C10-16	21.61	0.69	8.14

Table A-3. Pretest Soil Moisture Contents and Chromium Concentrations of TCLP Extracts of Pretest Soil Samples

Sample I.D.		Contract Lab	In-House Analysis
Location	Depth	TCLP Cr (ppm)	wt% moisture
NT-1	7.5	ND	7.17
NT-1	10	ND	4.93
NT-1	12.5	ND	3.22
NT-1	15	1.7	3.5
NT-1	15	1.7	----
NT-1	17.5	1.2	----
NT-1	20	2.1	5.97
NT-1	22.5	0.47	9.08
NT-1	25	0.26	5.83
NT-1	30	0.096	7.34
C1	6	0.012 J	6.92
C1	8	ND	
C1	10	ND	3.29
C1	12	ND	1.9
C1	14	30.6	4.85
C2	8	ND	6.28
C3	6	ND	5.99
C3	8	0.031 J	6.88
C3	10	ND	2.92
C3	10	ND	-----
C3	12	ND	1.43
C3	14	26.9	2.81
C3	16	9.1	8.48
C5	6	ND	8.34
C5	8	ND	4.8
C5	10	ND	2.68
C5	12	0.14 J	1.93
C5	14	0.31 J	2.06
C5	16	2.9	5.6
NT-3	7.5	9.2	9.27
NT-3	10	5.6	4.18
NT-3	12.5	7.1	4.73
NT-3	15	12.1	3.15
NT-3	17.5	5	4.72
NT-3	20	1.8	2.24
NT-3	22.5	7.2	5.95
NT-3	25	1.9	5.02
NT-3	30	5.8	-----
NT-3	35	2.5	6.03
NT-3	40	5.1	6.32
CF4	6	6.3	-----
CF4	8	13	9.23

Sample I.D.		Contract Lab	In-House Analysis
Location	Depth	TCLP Cr (ppm)	wt% moisture
CF4	10	49.3	12.59
CF4	12	8.5	2.49
CF4	12	8.6	----
CF4	14	1	----
A1	6	0.036 J	----
A1	8	0.64	----
A1	10	20.8	11.4
A1	12	0.52	----
A1	17	12.5	3.36
A2	7.5	0.043 J	8.6
A2	10	3	18.81
A2	12.5	1.8	----
A2	15	1.9	----
A2	17.5	8.1	----
A2	20	1	----
A2	22.5	3	----
A2	22.5	3.2	----
A2	25	0.84	6.92
A2	30	1.5	5.97

A3	6	ND	----
A3	8	3.3	----
A3	10	17.8	12.87
A3	12	20.8	4.01
A3	12	19.5	----
A3	14	33.7	----
A3	16	91.9	6.09
A4	6	----	7.54
A4	8	----	11.83
A4	10	----	10.15
A4	12	----	4.15
A4	16	----	4.13
A5	6	0.38 J	8.27
A5	8	2.5	----
A5	10	103	10.56
A5	12	19.5	3.61
A5	12	20.8	----
A5	14	7.4	----
A5	16	19.2	3.42
NT-6	7.5	56.4	10.62
NT-6	10	8.7	7.8
NT-6	12.5	4	2.64
NT-6	12.5	3.5	----
NT-6	15	2.2	2.52
NT-6	17.5	1.1	3.14
NT-6	20	1.1	2.45

Sample I.D.		Contract Lab	In-House Analysis
Location	Depth	TCLP Cr (ppm)	wt% moisture
NT-6	22.5	4	7.82
NT-6	25	4.4	5.39
NT-6	30	4	6.42
NT-7	7.5	19.7	11.93
NT-7	10	35.5	11.11
NT-7	12.5	7.9	4.7
NT-7	15	10.7	4.82
NT-7	17.5	7.3	3.18
NT-7	20	4.1	4.02
NT-7	22.5	5.2	7.95
NT-7	25	5.2	5.37
NT-7	30	7.5	5.74
NT-7	35	3.8	3.1
NT-7	40	6.8	6.08
NT-8	7.5	3.7	19.01
NT-8	7.5	6.3	-----
NT-8	10	1.7	10.9
NT-8	12.5	6	7.86
NT-8	15	37.3	5.68
NT-8	17.5	5.3	3.95
NT-8	20	18.7	4.56
NT-8	22.5	3	8.08
NT-8	25	3.8	5.87
NT-8	30	3.7	4.08
C6	6	2.1	-----
C6	8	0.37 J	-----
C6	10	0.0066 J	-----
C6	12	ND	-----
C6	14	2	-----
C6	14	2.2	-----
C6	16	0.24	2.4
C7	6	-----	7.58
C7	8	-----	15.83
C7	10	-----	5.69
C7	12	-----	3.94
C7	14	-----	9.07
C7	16	-----	6.11
C8	6	0.0097 J	-----
C8	8	0.49	-----
C8	10	5	5.35
C8	10	6.5	-----
C8	12	6.1	2.89
C8	14	4.1	2.33
C8	16	1.4	3.68
C9	6	-----	9.09

Sample I.D.		Contract Lab	In-House Analysis
Location	Depth	TCLP Cr (ppm)	wt% moisture
C9	8	-----	9.28
C9	10	27.4	7.03
C9	12	1.1	2.33
C9	12	0.92	-----
C9	14	0.7	2.22
C9	16	0.16 J	2.76
C10	6	1.2	7.26
C10	8	3.1	-----
C10	10	-----	9.84
C10	12	-----	8.64
C10	16	-----	7.99
BKG	10	ND	4.28

ND is none detectable
J is below the reporting limit or an estimated concentration

A.3. Post-test Soil Samples

OBJECTIVE

Post-test in-house soil water extracts were evaluated for pH, conductivity, and concentrations of water-soluble chromate, as well as acetate, chloride, nitrate, and sulfate. The method, C, for water extraction was a refined Method B to obtain more consistent results. Soil moisture contents (in-house gravimetric method) and the TCLP chromium concentrations (contract laboratory analysis) were also obtained.

WATER-EXTRACTION METHOD C

REAGENTS, APPARATUS, AND INSTRUMENTATION

Standards for ion chromatography were prepared from the following salts: sodium acetate, sodium chloride, sodium nitrate, sodium sulfate, sodium dichromate (all purchased from Fisher®). Deionized water used for extractions and the preparation of solutions was generated to a purity of 18 MΩ with a Barnstead® Nanopure® system.

The extraction mixtures were placed into centrifuge tubes (50-mL, round-bottom, polycarbonate, 28.5 x 104 mm) and shaken on a Fisher® hematology mixer. The separation of soil and supernatant was done by centrifugation using a Precision Scientific® Universal Centrifuge®. A Dionex® model 4000 ion chromatograph with an AS-11 column was used to determine the concentrations of various anions.

METHOD

The extractions were performed in 50-mL polycarbonate, round-bottom centrifuge tubes. Clean, dry centrifuge tubes were initially labeled and both the top and the tube were weighed together. Non-dried soil (10.0 g) was measured into the centrifuge tube with the exact mass of the soil being recorded. Deionized water was combined with the soil in a 2:1 ratio as determined by soil moisture measurements. Exact quantities of deionized water were measured with an automatic adjustable pipette. These mixtures were capped and shaken on a hematology mixer for 2.0 hours. After shaking, the mixtures were set upright in a test tube stand, overnight (about 15-20 hours). A complete separation of phases was effectuated by centrifuging the mixtures for one hour at 2500 rpm. A 10.00-mL portion of the supernatant was removed from the centrifuge tube using a pipette and placed into a 20-mL polypropylene scintillation vial. The conductivity and pH of the extracts was measured.

DETERMINATION OF ANION CONCENTRATIONS IN THE SUPERNATANT

The determination of acetate, chloride, nitrate, sulfate, and chromate in the supernatants was done by ion chromatography. Combined standards were prepared in the range of 0.10 to 0.40 mM for acetate, chloride, nitrate, and sulfate and in the range of 0.050 to 0.20 mM for chromate. A gradient elution using a sodium hydroxide eluent was performed. The eluent concentration was ramped up from 3 to 28 mM. An initial screen of the different species and their concentrations was done with a 25-fold dilution of the supernatants. A repeat of most samples was performed at a lower or higher ratio of dilution after examination of the initial screen. The most common dilution ratios were: no dilution, 25 fold, and 100 fold.

RESULTS

Table A-4 includes results of the in-house Method C water extraction concentrations of acetate, chloride, nitrate, sulfate, and chromate for the post-test samples. The concentrations of the first four anions were determined with less rigor than the concentration of chromate. Consequently, values of these four anions were listed only when it was clear they were above a concentration of 0.1 mM. The concentrations of chromate, on the other hand, were listed to 0.001 mM. The soil concentration is based on the water-to-soil extraction ratio. This table also includes the pH and conductivity results for the extracts.

Table A-5 gives the soil moisture contents and the TCLP chromium concentrations (of the extract, not back-calculated to soil) for the post-test soil samples.

Table A-4. Data for Anion Concentrations, pH, and Conductivity

Sample ID	Acetate[1] (ppm OAc) in Soil	Chloride1 (ppm Cl) in Soil	Nitrate1 (ppm NO3) in Soil	Sulfate1 (ppm SO4) in Soil	Chromate2 (ppm Cr VI) in Soil	Other Parameters	
						Cond (mS)	pH
PT1-7.5		94.9	14.8	174.7	0.4	720.0	9.1
PT1-10		124.3		56.5		418.0	9.3
PT1-12.5		123.0		40.2		349.0	9.0
PT1-15		97.0		153.3		585.0	9.5
PT1-17.5		161.9	18.2	68.3	0.2	529.0	9.2
PT2-7.5		18.4		514.7	1.4	657.0	8.4
PT2-10		27.0		50.4	0.1	248.0	9.1
PT2-12.5		46.1		3378.6	143.1	2820.0	7.7
PT2-15		80.0		1188.6	195.7	1936.0	8.0
PT2-17.5		103.1		607.3	82.7	1288.0	8.3
PT4-6		47.9	34.5	183.5	15.3	565.0	9.0
PT4-8		13.0		217.7	30.3	4260.0	12.1
PT4-10		19.1		3691.4	301.9	3600.0	10.4
PT4-12		10.2		1188.1	43.4	1445.0	8.3
PT4-15		37.5		1900.9	126.1	2150.0	7.8
PT4-17.5		76.2		293.2	72.7	769.0	8.6
PT5-7.5		13.9		3595.4	187.1	3060.0	7.6
PT5-10		9.0		4240.2	99.2	4120.0	10.8
PT5-12.5				29.2	0.7	532.0	9.8
PT5-15		47.7		774.8	36.2	1389.0	8.3
PT5-17.5		49.3		143.8	41.7	552.0	8.8
PT8-8		31.7		4110.4	72.3	12060.0	12.3
PT8-10		22.1		4354.1	575.8	4620.0	8.1
PT8-12				4337.6	565.5	4710.0	7.9
PT8-15		26.3		3117.8	242.7	2910.0	7.7
PT8-17.5		29.6		234.9	18.2	466.0	8.6
PT9-7.5		424.2		13107.6	589.2	15540.0	8.7
PT9-10		7.8		4177.1	607.5	4410.0	7.5
PT9-12.5		90.0		3789.5	325.1	3600.0	7.9
PT9-15		53.1		737.5	75.3	1135.0	8.3
PT9-17.5		41.2		159.0	10.5	386.0	8.8
PT12-7.5		17.2		381.2	6.5	13020.0	10.4
PT12-10		11.3	17.5	697.8	13.0	1918.0	9.6
PT12-15		6.9		155.0	11.8	568.0	9.2
PTC3-6		30.0		1007.1	3.0	1065.0	7.8
PTC3-8		37.8		355.6	17.1	612.0	9.1
PTC3-10		9.7		108.3	1.5	324.0	9.5
PTC3-12		24.9		214.1	0.7	408.0	9.0
PTC3-16		164.9		2324.2	208.2	2810.0	7.9
PTC5-6		25.8		42.1		203.0	9.1
PTC5-8		15.7		369.5		650.0	9.4
PTC5-10		16.4		81.5	0.4	485.0	10.2
PTC5-12		15.4		108.7	1.1	511.0	10.0
PTC5-14		25.5		26.3	0.3	760.0	10.0
PTC6-6		522.0	791.0	896.9	15.5	10650.0	10.2
PTC6-8	1723.8	412.7	363.3	2489.4	8.2	8630.0	9.5
PTC6-8DUP	165.7	27.0		6796.1	126.4	6730.0	8.4
PTC6-10	165.7	503.6	226.6	6706.5	249.1	7920.0	8.5
PTC6-12		65.1	28.4	5531.5	83.5	5360.0	8.5

Table A-4. Data for Anion Concentrations, pH, and Conductivity

Sample ID	Acetate[1] (ppm OAc) in Soil	Chloride1 (ppm Cl) in Soil	Nitrate1 (ppm NO3) in Soil	Sulfate1 (ppm SO4) in Soil	Chromate2 (ppm Cr VI) in Soil	Other Parameters	
						Cond (mS)	pH
PTC6-14		283.1	109.5	3818.4	235.9	4780.0	8.1
PTC8-6		30.1	23.7	858.0	2.6	1043.0	8.4
PTC8-10	208.5	53.9		3121.9	226.5	3050.0	7.5
PTC8-12		15.4		3083.6	295.4	2890.0	7.6
PTC8-14		41.8		457.6	3.6	596.0	8.6
PTC10-6		21.8		177.3	0.7	503.0	9.4
PTC10-8	66.6	94.4		5769.4	96.5	4430.0	8.1
PTC10-10		9.8		3404.3	298.9	3250.0	7.6
PTC10-12		10.1		2153.6	121.9	2080.0	7.8
PTC10-14		13.6		1332.4	17.7	1300.0	8.3
PTA1-6		957.9	623.5	838.2	1.1	7990.0	10.2
PTA1-8	292.8	4599.5	2157.0	13178.2	118.3	16380.0	7.7
PTA1-10	59.4	423.1	150.3	4921.4	200.1	5200.0	7.8
PTA1-12		267.7	87.5	3661.7	105.3	3780.0	7.8
PTA1-17		554.7	142.2	254.0	56.3	1620.0	8.0
PTA3-6		739.4	154.4	452.7	10.2	1956.0	7.9
PTA3-8		1645.6	249.3	2941.1	25.6	4950.0	7.8
PTA3-10		1353.7	136.6	3671.2	434.1	5950.0	7.8
PTA3-12		295.7		3078.3	464.8	4000.0	7.6
PTA3-14		437.4		3667.0	1010.0	5530.0	7.6
PTA5-6		1299.6		914.1	3.0	3450.0	7.8
PTA5-8		2683.0	198.5	6381.9	855.4	11810.0	7.9
PTA5-10		27.6		4096.8	922.6	4750.0	7.7
PTA5-14		39.3		931.8	53.9	1297.0	8.2
PTA5-16		28.2		220.6	23.4	696.0	9.3
PTNT3-6		78.4		623.2	39.6	967.0	8.2
PTNT3-8		18.1		4755.4	195.5	4590.0	8.1
PTNT3-10				3414.8	295.2	3220.0	7.7
PTNT3-12		11.1		2498.5	59.9	2240.0	7.9
PTNT3-14		58.7		2577.7	97.5	2490.0	7.9
PTNT3-15		42.1		3049.7	160.0	2920.0	7.8
PTNT3-16		91.9		3376.1	322.7	3480.0	7.8
PTNT7-6		166.3	53.9	324.9	196.8	1366.0	8.5
PTNT7-8		14.9		3537.4	7.2	2950.0	7.6
PTNT7-10		10.2		3537.1	548.1	3800.0	7.4
PTNT7-12		15.2		3163.6	369.4	3160.0	7.6
PTNT7-14		47.4		3154.2	430.8	3230.0	7.5
PTNT7-16		56.1		757.0	93.6	1189.0	8.3
PTNT8-6		154.2	68.1	907.1		1379.0	8.3
PTNT8-8	22.1	13.5		5832.4	21.0	4880.0	8.5
PTNT8-10		16.5		3153.3	496.7	3310.0	7.7
PTNT8-12		19.1		3043.2	527.2	3170.0	7.8
PTNT8-14		9.7		546.4	4.0	696.0	8.1
PTNT8-16		26.6		533.0	52.5	826.0	8.2
PTNT8-16DUP		44.3	14.9	84.0	3.6	310.0	8.7
PT3-7.5		89.4		657.6	17.6	6690.0	10.3
PT3-10		7.4		7112.5	95.6	6590.0	8.8
PT3-12.5		21.9		3481.3	422.5	3570.0	7.7
PT3-18		183.9	57.8	199.8	44.9	805.0	8.6
PT6-7.5	197.3	571.1	385.5	827.7	10.6	6860.0	9.7

Table A-4. Data for Anion Concentrations, pH, and Conductivity

Sample ID	Acetate[1] (ppm OAc) in Soil	Chloride1 (ppm Cl) in Soil	Nitrate1 (ppm NO3) in Soil	Sulfate1 (ppm SO4) in Soil	Chromate2 (ppm Cr VI) in Soil	Other Parameters	
						Cond (mS)	pH
PT6-10		159.0		7230.7	277.6	7650.0	8.0
PT6-12.5		182.0	77.3	4273.7	237.6	4590.0	8.2
PT6-16		1106.3	324.5	3452.1	348.0	5440.0	7.7
PT6-17.5		640.5	158.1	3109.7	394.3	4030.0	7.6
PT7-7.5		2611.0	641.5	6585.8		11310.0	8.7
PT7-10		1058.9	160.4	3274.7	75.9	4450.0	7.6
PT7-12.5		726.9	87.1	3050.6	562.7	4420.0	7.4
PT7-15		241.3	30.2	3068.3	793.0	3890.0	7.4
PT10-10		204.4		3550.6	431.5	3800.0	7.7
PT10-14.5		59.7		967.7	144.0	1496.0	8.2
PT10-17.5		61.6	21.1	109.3	3.0	428.0	9.1
PT11-7.5	3183.9	511.3	195.8	6370.8	26.4	9160.0	8.3
PT11-10		81.6	25.2	1840.0	13.7	2500.0	8.4
PT11-12.5		75.8	14.1	1619.7	69.8	2020.0	8.1
PT11-15		380.1	83.3	3303.9	157.1	3560.0	7.8
PT11-17.5		150.1	32.0	187.7	3.1	512.0	8.1
PTC1-6		14.5		2179.2	3.3	2710.0	8.6
PTC1-8		11.1		61.7	3.5	4330.0	10.5
PTC1-12		25.2		3151.6	36.7	3000.0	8.0
PTC1-14		10.2		3876.7	139.6	3510.0	7.9
PTC1-16		371.7	71.6	901.6	129.3	1834.0	7.9
PTA2-6		814.8	265.9	740.1	0.2	3870.0	9.2
PTA2-8	23.9	1627.4	372.1	8094.5	5.7	10710.0	7.7
PTA2-10	31.1	1210.0	207.8	3360.3	26.0	4840.0	7.6
PTA2-12		502.1	92.5	3121.9	77.2	3310.0	7.8
PTA2-12DUP		559.0	101.1	3210.1	100.0	3490.0	7.8
PTNT6-6		1518.9		427.8	435.8	3760.0	8.2
PTNT6-8		1174.2	39.1	4205.1	28.5	5270.0	8.0
PTNT6-10		467.7		4096.2	41.9	4170.0	7.9
PTNT6-12		198.2		3209.9	77.6	3030.0	7.8
PTNT6-14		75.9		825.9	43.3	1241.0	8.1
PTNT6-16		76.3		3203.3	253.5	3220.0	7.8

Footnotes:

1. Only acetate, chloride, nitrate, and sulfate concentrations above a value of 0.1 mM were listed.
2. Only chromate concentrations above a value of 0.001 mM were listed.

TABLE A-5. Post-test Soil Moisture Contents and Chromium Concentrations of TCLP Extracts of Post-test Soil Samples

Sample I.D.		Contract Lab	In-House Analysis
Location	Depth	TCLP Cr (ppm)	wt% moisture
PT-1	7.5	0.0061 J	6.32
PT-1	10	ND	2.33
PT-1	12.5	ND	1.59
PT-1	15	ND	3.18
PT-1	17.5	0.041 J	6.14
PT-1	20	0.0054 J	2.54
PT-1	22.5	0.0046 J	2.77
PT-1	25	0.015 J	5.75
PT-2	7.5	0.078 J	5.85
PT-2	10	ND	2.75
PT-2	10	0.017	
PT-2	12.5	8.9	3.36
PT-2	15	9.2	7.19
PT-2	17.5	4.5	7.32
PT-2	20	1	2.61
PT-2	20	1.2	
PT-2	22.5	4.9	9.05
PT-2	25	2.6	5.29
PT-2	30	1.6	5.51
PT-3	7.5	0.92	16.61
PT-3	10	6	16.09
PT-3	12.5	34.2	5.62
PT-3	12.5	31.3	
PT-3	18	2	3.14
PT-3	20	1.5	2.29
PT-3	22.5	0.38 J	7.33
PT-3	25	0.71 J	
PT-3	30	0.17 J	5.1
PT-4	6	0.52	4.71
PT-4	8	1.1	9.12
PT-4	10	12.2	8.84
PT-4	10	11.7	
PT-4	12	1.9	2.87
PT-4	15	11.9	
PT-4	17.5	2.4	3
PT-4	20	1.5	2.42
PT-4	22.5	5.3	6.95
PT-4	25	4.4	5.89
PT-4	30	4	6.3
PT-4	35	0.73	2.28
PT-4	40	3.9	7.38
PT-5	7.5	21	11.06
PT-5	10	4.9	10.48
PT-5	12.5	0.052 J	2.78
PT-5	15	2	3.55
PT-5	17.5	1.7	3.7
PT-5	20	1.8	2.62
PT-5	22.5	6.1	8.64
PT-5	25	5.2	6.68
PT-5	25	5.4	
PT-5	30	6.6	6.44
PT-6	7.5	0.99	
PT-6	10	15.2	13.94

TABLE A-5. Post-test Soil Moisture Contents and Chromium Concentrations of TCLP Extracts of Post-test Soil Samples

Sample I.D.		Contract Lab	In-House Analysis
Location	Depth	TCLP Cr (ppm)	wt% moisture
PT-6	12.5	13.7	4.13
PT-6	12.5	13.9	
PT-6	16	31.3	8.15
PT-6	17.5	24.6	4.57
PT-6	17.5	26	
PT-6	20	3.6	4.11
PT-6	22.5	3.5	8.34
PT-6	25	1.3	5.8
PT-6	30	2.6	5.01
PT-7	7.5	0.072 J	17.95
PT-7	10	6.6	13.92
PT-7	12.5	45.6	8.26
PT-7	12.5	42.2	
PT-7	15	70.9	6.57
PT-7	17.5	7.9	
PT-7	20	0.54	
PT-7	22.5	1.4	6.77
PT-7	25	4.5	9.18
PT-7	30	5.5	4.77
PT-7	35	7.4	3.82
PT-7	40	8.8	6.63
PT-8	8	3.8	12.14
PT-8	10	57.2	8.29
PT-8	12	67	
PT-8	15	18.9	
PT-8	17.5	0.33 J	2.18
PT-8	20	1.7	2.43
PT-8	22.5	3.2	6.75
PT-8	25	4.1	5.65
PT-8	30	8.9	5.35
PT-8	35	3.5	
PT-8	40	8.1	5.47
PT-9	7.5	29.9	10.36
PT-9	10	62.4	8.1
PT-9	12.5	22.8	4.07
PT-9	12.5	21.6	
PT-9	15	2.5	3.11
PT-9	17.5	0.24 J	2.34
PT-9	20	0.045 J	2.26
PT-9	22.5	1.5	7.08
PT-9	25	4.2	9.92
PT-9	30	5	4.75
PT-10 A	7.5	21	
PT-10	10	32.6	4.65
PT-10	14.5	6.2	3.17
PT-10	17.5	0.052 J	2.72
PT-10	17.5	0.057 J	
PT-10	20	0.089 J	2.71
PT-10	22.5	0.66	6.32
PT-10	25	2.3	6.71
PT-10	30	2.3	5.02
PT11	7.5	0.96	11.35
PT11	10	0.6	4.34
PT11	12.5	3.6	2.44

TABLE A-5. Post-test Soil Moisture Contents and Chromium Concentrations of TCLP Extracts of Post-test Soil Samples

Sample I.D.		Contract Lab	In-House Analysis
Location	Depth	TCLP Cr (ppm)	wt% moisture
PT11	15	10.8	8.54
PT11	17.5	0.043 J	2.95
PT11	20	0.043 J	2.26
PT11	22.5	1.5	5.7
PT11	22.5	1.6	
PT11	25	2.5	6.94
PT11	30	8.4	4.94
PT-12	7.5	0.24 J	12.64
PT-12	10	0.33 J	12.3
PT-12	10	0.36 J	
PT-12	12.5	0.011 J	
PT-12	15		8.63
PT-12	20		2.52
PT-12	22.5	1.1	6.4
PT-12	22.5	1.2	
PT-12	25	3.4	6.16
PT-12	30	7.6	4.87

ND is none detectable
J is below the reporting limit or an estimated concentration

A.4. Additional Analyses of Pretest and Post-test Soil Samples

After the EK demonstration was underway, it was accepted into the EPA SITE program. The oversight personnel requested additional samples be taken and these were analyzed for TCLP chromium concentrations (pretest only), total chromium, and chromium(VI) concentrations. Table A-6 gives the location and depth of these samples and the results of the analyses. In addition, four of the samples for TCLP (given in Table A-3) were split and analyzed for total chromium by the same outside laboratory.

Table A-6. Other Chromium Analyses - Pretest Soil Samples

		Lab	Site		
Sample I.D.		Total Cr	TCLP	Total Cr	Cr (VI)
Location	Depth	(ppm)	(ppm)	(ppm)	(ppm)
NT-1	25			23.9	7.5
C1	10			8.8	0.81
C3	8			11.8	1.2
C3	16		8.2	285	229
C5	8			7.7	0.4
C5	10			11.1	0.65
C5	16		2.6	123	63.6
NT-3	7.5	2775		1580	510
NT-3	10			1920	429
NT-3	12.5	2120		1470	409
NT-3	15			1340	512
NT-3	17.5		5.7	146	135
NT-3	20			62.1	55.7
CF4	6			259	145
CF4	8			1650	526
CF4	10			8440	2590
CF4	12			999	452
A1	10		19.7	4540	1110
A1	12			184	50.9
A1	17			3920	1650
A2	10			824	250
A2	22.5			83.1	69.1
A2	25			32.9	19.7
A3	8			620	156
A3	10		9.4	3450	732
A3	12		14	2990	1050
A3	14			3320	1940
A3	16			11900	5290

		Lab	Site		
Sample I.D.		Total Cr	TCLP	Total Cr	Cr (VI)
Location	Depth	(ppm)	(ppm)	(ppm)	(ppm)
NT-7	7.5	993		891	521
NT-7	10		40.6	6650	5320
NT-7	12.5	1490		1840	577
NT-7	15			2010	764
NT-7	17.5		10.8	1100	497
NT-7	22.5			119	112
NT-7	35			98.8	94.3
NT-6	7.5		44.2	5717	2120
NT-6	10			2360	514
NT-6	12.5			242	127
NT-6	15			189	76.4
NT-6	17.5			48.6	28.3
NT-6	20			67.6	32.9
NT-8	7.5			658	157
NT-8	10		1.2	1150	662
NT-8	12.5			1060	502
NT-8	15			5260	2140
NT-8	17.5			792	358
NT-8	20			1740	861
C6	8			256	44
C6	12			28.2	2.2
C10	8			678	47

Table A-7. Other Chromium Analyses - Post-test Soil Samples

Sample I.D.		Site Total Cr	Site Cr (VI)
Location	Depth	(ppm)	(ppm)
PT-C1	6	20.8	2.3
PT-C1	8	344	9
PT-C1	10	408	47.6
PT-C1	12	660	94.2
PT-C1	14	1230	268
PT-C1	16	223	156
PT-C1	18	84.1	56.5
PT-C1	20	35.3	15.4
PT-C3	8	32.2	12
PT-C3	16	240	203
PT-C5	6	8.2	1.2
PT-C5	8	8.6	ND
PT-C5	10	12.7	1.8
PT-C5	12	11.3	1.3
PT-C5	14	28	1.7
PT-C5	16		
PT-C5	18	72.6	39.6
PT-C5	20	58.2	35.9
PT-NT3	8	4480	1330
PT-NT3	10	4470	1030
PT-NT3	12	1390	219
PT-NT3	14	710	447
PT-NT3	16	2640	961
PT-NT3	18	139	96.9
PT-NT3	20	75.3	44.2
PT-CF4	6	58	7.8
PT-CF4	8	657	55.9
PT-CF4	10	1760	293
PT-CF4	12	273	53.7
PT-CF4	14	1110	322

Sample I.D.		Site Total Cr	Site Cr (VI)
Location	Depth	(ppm)	(ppm)
PT-A1	6	47	2
PT-A1	8	3020	154
PT-A1	10	8340	1070
PT-A1	12	433	174
PT-A1	14	88.3	10.4
PT-A1	16	79.1	54.8
PT-A1	18	600	215
PT-A1	20	252	80.2
PT-A2	8	982	78.1
PT-A2	10	1580	662
PT-A2	12	3480	2520
PT-A3	8	685	69.8
PT-A3	10	8790	2620
PT-A3	12	3970	2270
PT-A3	14	12700	4340
PT-NT7	8	1350	154
PT-NT7	10	13000	3570
PT-NT7	12	3250	992
PT-NT7	14	4660	1410
PT-NT7	16	203	111
PT-NT7	18	22.2	5.9
PT-A5	6	180	0.78
PT-A5	8	3720	ND
PT-A5	10	16200	4730
PT-A5	14	151	64
PT-A5	16	64.2	25.7
PT-NT6	8	4520	597

Sample I.D.		Site Total Cr	Site Cr (VI)
Location	Depth	(ppm)	(ppm)
PT-NT6	10	6350	533
PT-NT6	12	801	159
PT-NT6	14	181	46.4
PT-NT6	16	1360	507
PT-NT6	18	279	53.6
PT-NT6	20	33.5	8.8
PT-NT8	8	1700	214
PT-NT8	10	8330	2700
PT-NT8	12	5470	1830
PT-NT8	14	47.4	11.1
PT-NT8	16	195	74.4
PT-NT8	18	11.8	2.5
PT-NT8	20	10.3	2.1
PT-C6	6	132	22.1
PT-C6	8	2030	43.3
PT-C6	10	5270	1290
PT-C6	12	1590	142
PT-C6	14	1330	390
PT-C6	18	15.8	3.7
PT-C6	20	15.2	2.9
PT-C10	6	125	3.2
PT-C10	8	2280	302
PT-C10	10	5420	1060
PT-C10	12	1450	259
PT-C10	14	78.7	25.5
PT-C10	16	74.1	26.8
PT-C10	18	17.6	2.9
PT-C10	20	43.5	5.5

(This page intentionally left blank)

APPENDIX B: PHOTOGRAPHS

Photograph 1. Aerial View of the EK Demonstration Site in the SNL CWL.

This aerial view shows the facilities that were at the EK Demonstration site. The EK Greenhouse is the rounded structure and the Control Trailer is the truck trailer just below it in the photograph. To the left of the Control Trailer is another smaller trailer for field laboratory analyses and a small workroom. The two smaller sheds between the greenhouse and the trailers (just inside the CWL western edge fence) housed equipment and maintenance supplies, and chemical and sample storage and work areas.

The two round tanks just outside the Greenhouse wall are the cathode and anode influent water storage tanks. The tanker trailer held water for filling the storage tanks, for replenishing the water in the chillers, and for miscellaneous activities. To the top left of the tanker trailer are four sets of effluent barrels removed from the EK remediation area. Between those and the Greenhouse is a round grouping of empty 55 gallon barrels.

Other sheds and items in the photograph were for other projects at the SNL CWL.

Photograph 2. EK Control Panels Housed in the Control Trailer.

The ten control panels, five anode and five cathode, are shown in this photograph. A comparison of this photograph and Figure 4-2 of this report will help identify the major control components (from top to bottom): air purge meters, vacuum meters and regulators, water level indicator lights, influent and effluent meters (and manual on/off switches), recycle meters, conductivity meters, pH controllers, effluent batch controllers, current meters, and 12 volt on/off switches.

In the center panel, at the bottom, the switch and indicator light for the power to the electrodes are also visible. A portion of one of the power supplies is visible under the control panel on the left. The boxes with the power cable connections and the manual power lock out switch can be seen at the far right.

Photograph 3. Interior of the Greenhouse with Some Equipment Installed.

This is a photograph of the interior of the Greenhouse during the equipment installation phase of the EK demonstration. The control and power cables from the Control Trailer were routed above the ground and can be seen hanging down at several points. These cables were connected to the equipment at the electrode heads: the white cylindrical structures which are in place on the five southern cathodes and two eastern anodes; or to the recycle boards (seen in the next photograph). The vacuum and air pressure lines to operate the bladder pumps and to keep the water in the electrode under tension were also connected to the electrode heads. The barrels at the rear of the photograph are for the collection of effluent. The two barrels and the row of chemical feed pumps on the secondary containment pallets to the right were to hold the acid and base electrode electrolyte conditioning solutions. Lying across both pallets is one of the anode electrodes prior to installation. Other visible piping and tubing are for cooling water to the electrodes and for monitoring subsurface conditions.

Photograph 4. Recycle Board for Anode 5.

This is a photograph of the recycle system for Anode 5. A comparison of this photograph and Figures 4-4 and 4-5 will help in the identification of the major components. The electrolyte solution from the electrode to the recycle board flows through the tubing at the left into the top recycle flow sensor. The flow continues to the right into a chamber with a temperature probe (extending up and out of the picture) and then to the back of the board and into the chiller. The chiller water tubing is on the far right and covered with insulation. The electroyte solution then is routed into a chamber with a conductivity probe (inserted into the "T" of the chamber from the left) and a pH probe (inserted into a second "T" from the top). The pH can be read on the transmitter to the right. The solution then continues to the left into a three-way solenoid valve which directs the solution either down, around, and through the effluent flow sensor and out to the effluent barrel (the tubing that goes up over the top of the board) or up into a "T" and back into the electrode assembly. At the "T" is the pH control injection port (a manual on/off valve is at the base of the picture). Cable connections are also visible in the center of the board which leads to/from the control trailer and the sensors.

(This page intentionally left blank)

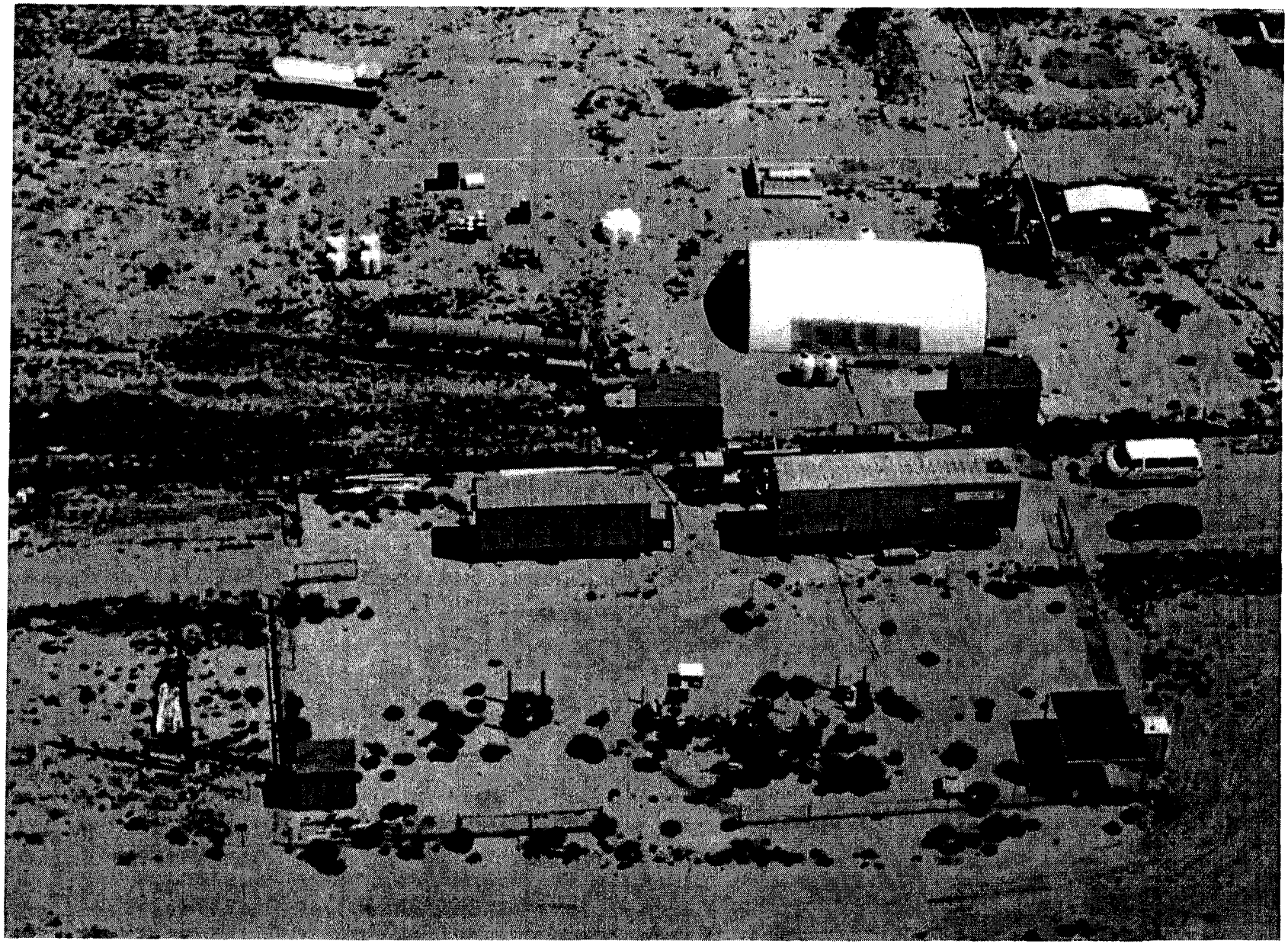

Photograph 1. Aerial View of the EK Demonstration Site in the SNL CWL.

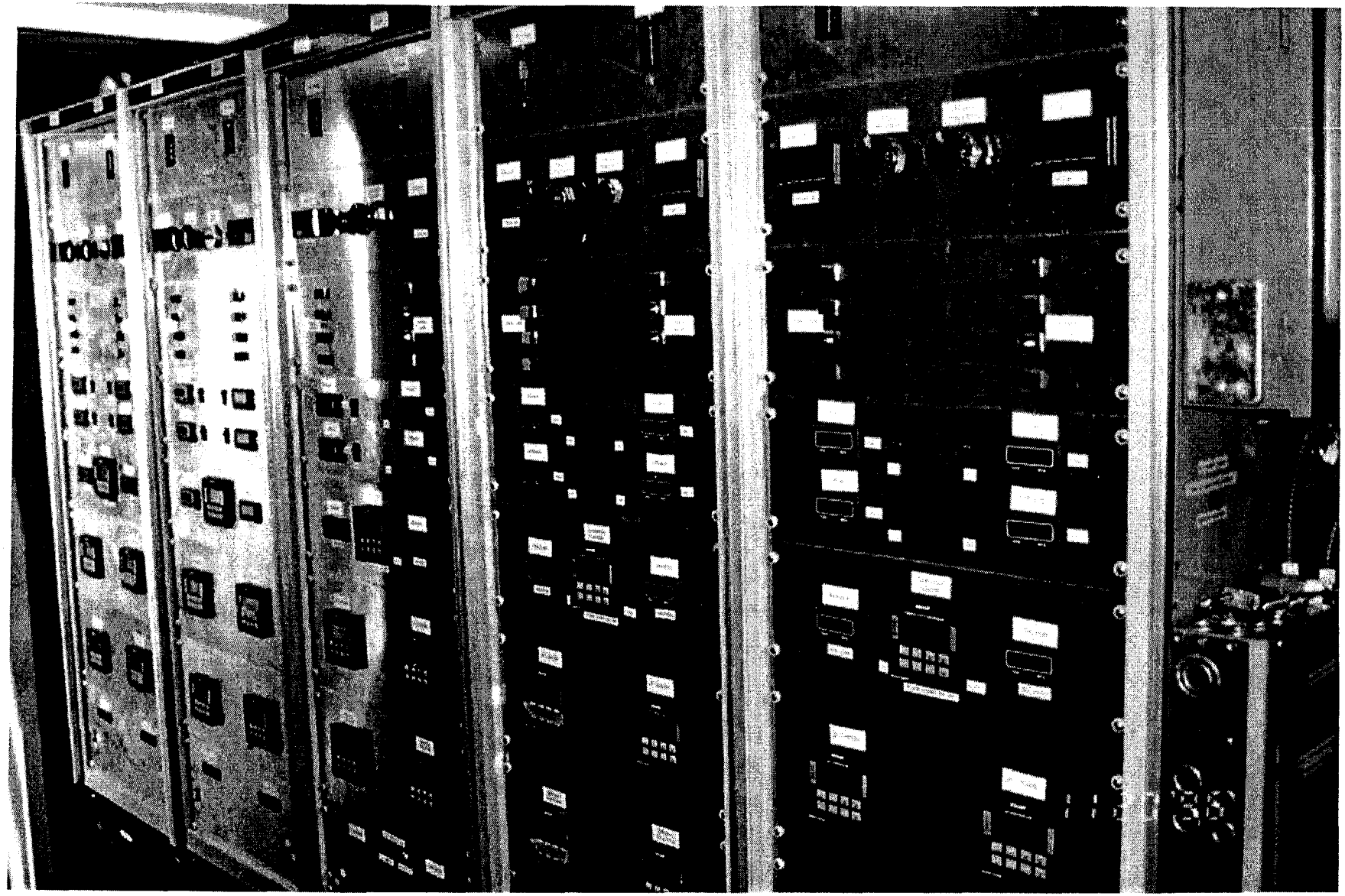

Photograph 2. EK Control Panels Housed in the Control Trailer.

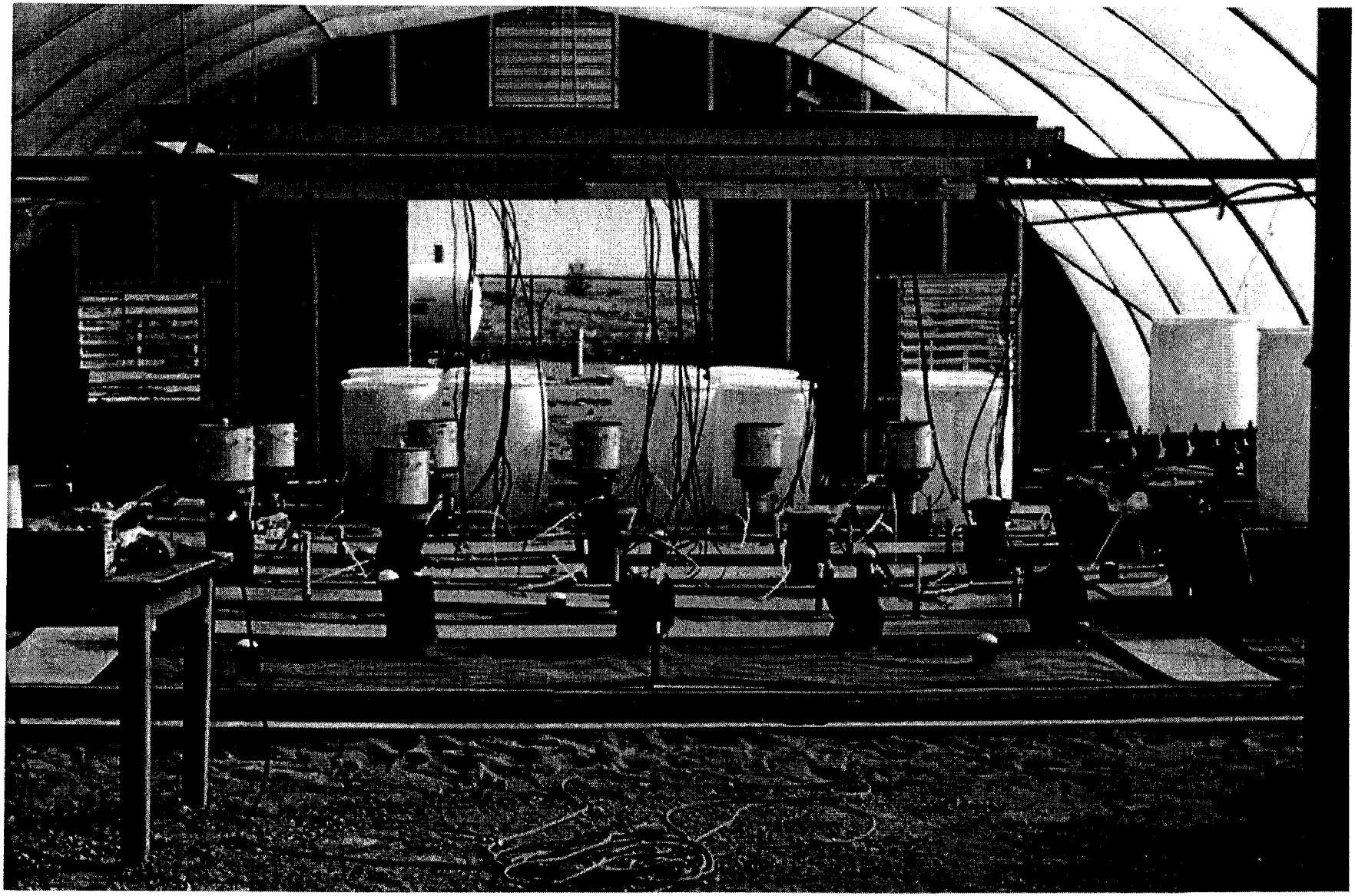

Photograph 3. Interior of the Greenhouse with Some Equipment Installed.

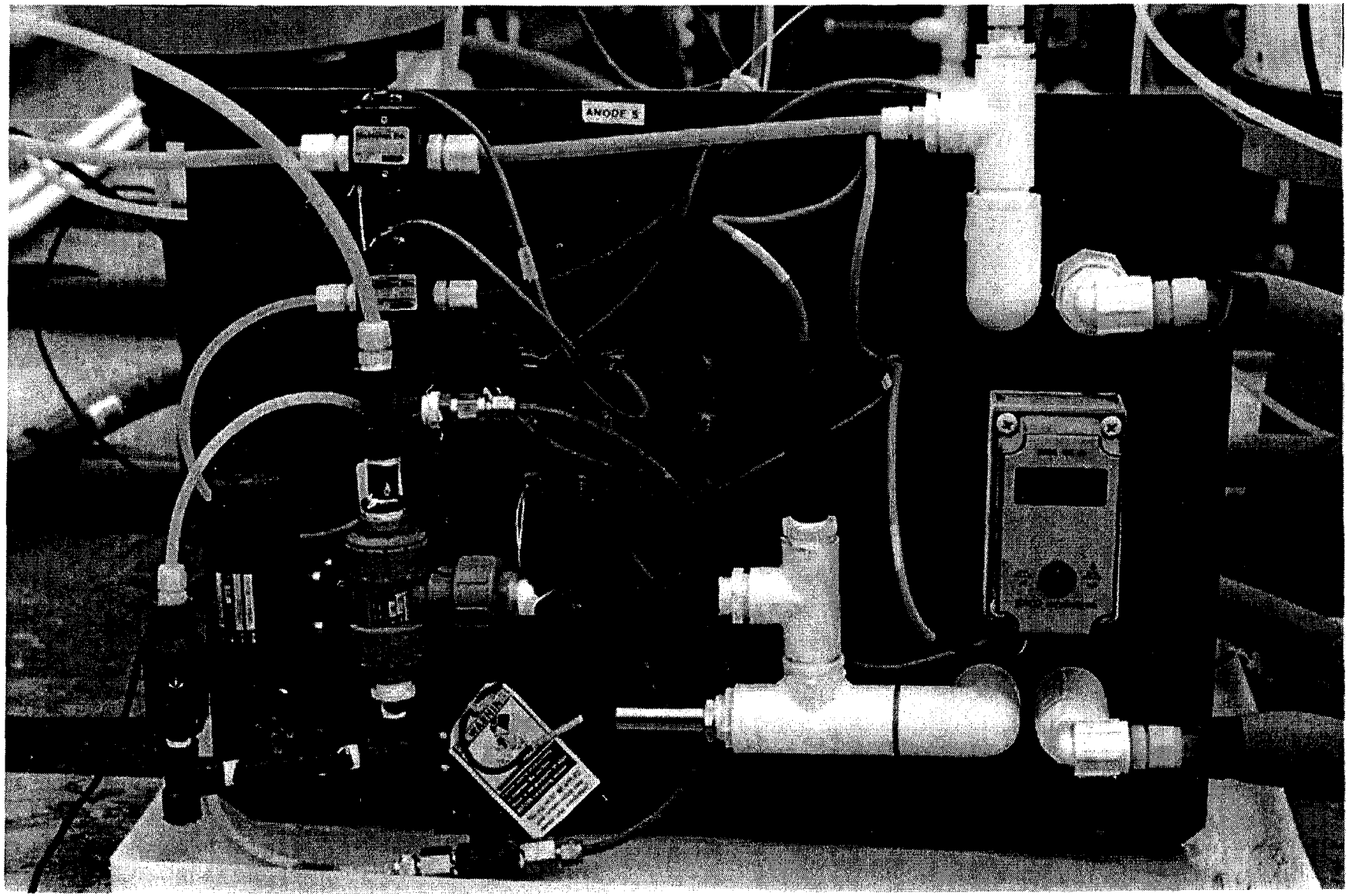

Photograph 4. Recycle Board for Anode 5.

DISTRIBUTION:

1 Kim Abott
U.S. Department of Energy
Oakland Operations Office
Room 700 N
1301 Clay Street
Oakland, CA 94612-5208

1 Robert E. Adams
Deputy Program Manager
Hazardous Waste Remediation Program
Technology Programs
P. O. Box 2003, MS-7606
Oak Ridge, TN 37381-7606

1 Shin Ahu
Tetra Tech EM Inc.
200 E. Randolph Drive, Suite 4700
Chicago, IL 60601

1 Cheryl Allen
Tech Reps, Inc.
5000 Marble N.E.
Albuquerque, NM 87110

1 Ammi Amarnath
Manager, Process Industries
Customer Systems Division
Electrical Power Research Institute
P. O. Box 10412
Palo Alto, CA 94303

1 Tikisa M. Anderson
Lockheed Missiles & Space Co.
B/157 o/81-40
1111 Lockheed Way
Sunnyvale, CA 94086

1 Robert Andrews, Ph.D.
National Research Council
National Academy of Science
Board of Radioactive Waste
Management
2001 Wisconsin Ave., N.W.
Washington, DC 20007

1 Dr. John A. Apps
Senior Research Scientist
Lawrence Berkeley National Laboratory
Building 50 E
1 Cyclotron Road
Berkeley, CA 94720

1 Cynthia Ardito
Duke Engineering & Services
1650 University Blvd., NE, Suite 300
Albuquerque, NM 87102

1 Richard Baker
U.S. Department of Energy
Chicago Operations Office
9800 South Cass Ave.
Argonne, IL 60439

1 Creighton Barry
MSE Technology Applications, Inc.
P.O. Box 4078
Butte, MT 59702

1 Paul Beam
U.S. Department of Energy
EM-40
Cloverleaf Building
19901 Germantown Rd.
Germantown, MD 20874-1290

1 Bob Bedick
U.S. Department of Energy
Federal Energy Technology Center
3610 Collins Ferry Rd.
Morgantown, WV 26507-0880

1 Kay Birdsell
Los Alamos National Laboratory
EES-5, MS F665
Los Alamos, NM 87545

1 Michael D. Brewster
Energy Systems Division
Argonne National Laboratory
9700 South Cass Avenue
Argonne, IL 60439

1 Mark Bricka
U.S. Army Corps of Engineers
Waterways Experimental Station
3909 Hall Ferry Road
Vicksberg, MS 39180

1 Dr. Philip H. Brodsky
Director, Corporate Research and
Environmental Technology
Monsanto
800 N. Lindbergh Boulevard
St. Louis, MO 63167

1 Dr. Mark F. Buehler
Senior Research Engineer
Batelle Pacific Northwest Laboratories
P. O. Box 999
MSIN P8-38
Richland, WA 99352

1 Dr. Charles H. Byers
Section Head, Energy Research
Oak Ridge National Laboratory
P. O. Box 2008
Oak Ridge, TN 37831-6268

1 Kirk Cantrell
Pacific Northwest National Laboratories
MS K6-81
P.O. Box 999
Richland, WA 99352

1 Skip Chamberlain
U.S. Department of Energy
EM-53
Cloverleaf Building
9901 Germantown Rd.
Germantown, MD 20874-1290

1 Elisabeth Reber-Cox
U.S. Department of Energy
Oakland Operations Office
Room 700 N
1301 Clay Street
Oakland, CA 94612-5208

1 David Daniel
University of Texas at Austin
Dept. of Civil Engineering
Cockrell Hall
Room 9.102
Austin, TX 78712

1 Harsh Dev
IIT Research Institute
10 West 35th Street
Chicago, IL 60616-3799

1 Wayne Downs
Idaho National Engineering &
Environmental Laboratory
P.O. Box 1625
Idaho Falls, ID 83415-2110

1 D. Dresp
Thomas Branigan Library
106 W. Hadley St.
Las Cruces, NM 88003

1 Patricia Duda
Ktech Corp.
901 Pennsylvania, NE
Albuquerque, NM 87110

1 Sandy Dalvit-Dunn
Science & Engineering Assoc., Inc.
3205 Richards Lane
Suite A
Santa Fe, NM 87505

1 Steve Eabry
EPRI Consultant
1786 Oceanaire Avenue
San Luis Obispo, CA 93405

1 Dr. Thomas O. Early
Oak Ridge National Laboratory
P. O. Box 2008
Building 3504, MS-6317
Oak Ridge, TN 37831

1 Gillian Eaton
U.S. Department of Energy
Rocky Flats
Tech Site, Bldg. T124A
P.O. Box 928
Golden, CO 80402-0928

1 Dr. Ahmen Elseewi
Southern California Edison
2244 Walnut Grove Avenue
Rosemead, CA 91770

1 Dave Emilia
MSE Technology Applications, Inc.
P.O. Box 4078
Butte, MT 59702

1 Bruce Erdal
Los Alamos National Laboratory
EM-TD, MS J591
Los Alamos, NM 87545

1 J. Espinosa
NM Environment Department
1190 St. Francis Drive
Santa Fe, NM 87503-0968

1 Dr. Robert J. Gale
Department of Chemistry
Louisiana State University
Baton Rouge, LA 70803

1 Thomas Gaughan
Westinghouse Savannah River Company
Savannah River Technology Center
Environmental Sciences Section
P.O. Box 616 / 730-2B
Aiken, SC 29802

1 Phillip Gauglitz
Pacific Northwest National Laboratories
Battelle Blvd.
P.O. Box 999
Richland, WA 99352

1 George A. Gehring
Executive Vice President
Corrpro Companies, Inc.
610 Brandywine Parkway
West Chester, PA 19380

1 John Geiger
U.S. Department of Energy
Savannah River Operations Office
P.O. Box A
Aiken, SC 29802

1 Dr. Donald H. Gray
Professor, Department of Civil
and Environmental Engineering
University of Michigan
Ann Arbor, MI 48104

1 Dennis Green
U.S. Department of Energy
Idaho Operations Office
850 Energy Drive
Idaho Falls, ID 83401-1563

1 Marvin Gross
U.S. Department of Energy
Fernald Field Office
P.O. Box 538704
Cincinnati, OH 45253-8704

1 Ralph Gruebel
AGRA Earth & Environmental, Inc.
4700 Lincoln Rd., N.E.
Albuquerque, NM 87109

1 Andrea Hart
MSE Technology Applications, Inc.
P.O. Box 4078
Butte, MT 59702

1 John Heiser
Brookhaven National Laboratory
Bldg. 830
34 North Railroad Ave.
Upton, NY 11973

1 Dr. Jonathan G. Herrmann
Deputy Director
Rick Reduction Engineering Laboratory
U.S. Environmental Protection Agency
M.S. 497
Cincinnati, OH 45268

1 Thomas Hicks
U.S. Department of Energy
Savannah River Operations Office
Bldg. 703-46A
P.O. Box A
Aiken, SC 29802

1 Dr. Donald G. Hill
Senior Associate
Weiss Associates
5500 Shellmount
Emeryville, CA 94608

1 Dr. Sa V. Ho
Science Fellow, Remediation
Technologies
Environmental Sciences Center
Monsanto Company (U4E)
800 North Lindbergh Boulevard
St. Louis, MO 63167

1 Dr. Dalibor Hodko
Research Scientist
Lynntech, Inc.
7610 Eastmark Drive
College Station, TX 77840

1 Gary Huffman
U.S. Department of Energy
Rocky Flats Office
Highway 93rd & Cactus St.
Golden, CO 80402

1 Tim Jarosch
Westinghouse Savannah River Company
Bldg. 773-42A
Road SR-1
Aiken, SC 29808

1 Robert D. Jeffress
Industrial Program Manager
Electrical Power Research Institute
P. O. Box 10412
Palo Alto, CA 94303

1 Sharon Johnson
U.S. Department of Energy
Savannah River Operations Office
703 A, Rm. B202
Aiken, SC 29802

1 Dr. Fritz R. Kalhammer
Vice President
Office of Exploratory & Applied
Research
Electric Power Research Institute
P. O. Box 10412
Palo Alto, CA 94303

1 Cindy Kendrick
Oak Ridge National Laboratory
P.O. Box 2001, EW-923
Oak Ridge, TN 37831

1 Dr. John Kerr
EO Systems
3445 Greer Road
Palo Alto, CA 94303

1 Kevin Kostelnick
Idaho National Engineering &
Environmental Laboratory
Lockheed Martin Idaho Technologies
P.O. Box 1625
Idaho Falls, ID 83415-3710

1 Dr. S. Y. Lee
Oak Ridge National Laboratory
P. O. Box 2008
Building 1505, MS-6038
Oak Ridge, TN 37831

1 Jeff Lenhert
U.S. Department of Energy
Albuquerque Operations Office
P.O. Box 5400
Albuquerque, NM 87185

1 Julianne Levings
U.S. Department of Energy
Albuquerque Operations Office
P.O. Box 5400
Albuquerque, NM 87185

1 Brent Lewis
Bureau of Land Management
Denver Service Center
Bldg. 50
Denver, CO 80225-0047

1 Steven Limback
Los Alamos National Laboratory
ESA-EPE, MS J576
Los Alamos, NM 87545

1 Henry L. Lomasney
President
ISOTRON Corporation
13152 Chef Menteur Highway
New Orleans, LA 70129

1 Brian Looney
Westinghouse Savannah River Company
Bldg. 773-42A
Road SR-1
Aiken, SC 29808

1 Bill Lowry
Science & Engineering Assoc., Inc.
3205 Richards Lane
Suite A
Santa Fe, NM 87505

20 Earl Mattson
Sat-Unsat, Inc.
12004 Del Rey, NE
Albuquerque, NM 87122

1 Gerry B. Maybach
Project Manager
Waste Water Management Program
Environmental Division, HSTC
Electric Power Research Institute
P. O. Box 242
Barker, NY 14012

1 Doug Maynor
U.S. Department of Energy
Ohio Operations Office
P.O. Box 3020
Miamisburg, OH 45343-3020

1 Scott McMullin
U.S. Department of Energy
Savannah River Operations Office
Bldg. 703-46A
P.O. Box A
Aiken, SC 29802

1 Dr. James K. Mitchell
Cahill Professor Emeritus
Department of Civil Engineering
University of California, Berkeley
Berkeley, CA 94720

1 Johnny Moore
U.S. Department of Energy
Oak Ridge Operations Office
EW-923
P.O. Box 2001
Oak Ridge, TN 37831-8620

1 Chuck Morgan
U.S. Department of Energy
Nevada Operations Office
2753 S. Highland Rd.
Las Vegas, NV 89109

1 Dr. Ishwar Murarka
Manager, Business Development
Land Waste & Water Environmental Div
Electric Power Research Institute
P.O. Box 10412
Palo Alto, CA 94303

1 New Mexico Junior College
Pannell Library
Lovington Highway
Hobbs, NM 88240

1 New Mexico State Library
325 Don Gaspar
Santa Fe, NM 87503

1 New Mexico Tech
Martin Speere Memorial Library
Campus Street
Socorro, NM 87810

1 Stephanie Odell
Bureau of Land Management
Farmington District Office
1235 LaPlata Highway
Farmington, NM 87401

1 Dennis Olona
U.S. Department of Energy
Albuquerque Operations Office
P.O. Box 5400
Albuquerque, NM 87185

1 Arturo Palomares
U.S. Environmental Protection Agency
Region 8
999 18th Street
Suite 500
Denver, CO 80202

1 Dr. Sibel Pamukcu
Associate Professor
Civil Engineering Department
Lehigh University
Fritz Engineering Laboratory
13 East Packard Avenue
Bethlehem, PA 18015

1 Randy Parker
Office of Research & Development
U.S. Environmental Protection Agency
26 W. Martin Luther King Drive
Cincinnati, OH 45268

1 Charles G. Patterson
Department of Geological Science
University of Colorado
Boulder, CO 80309-0250

1 Jim Paulson
U.S. Department of Energy
9800 S. Cass Avenue
Argonne, IL 60439

1 Dr. Robert W. Peters
Energy Systems Division
Argonne National Laboratory
9700 South Cass Avenue
Argonne, IL 60439

1 Dale Pflug
U.S. Department of Energy
Chicago Operations Office
EAD/900
9800 South Cass Ave.
Argonne, IL 60439-4832

1 Elizabeth Phillips
U.S. Department of Energy
Oak Ridge Operations Office
P.O. Box 2001
Oak Ridge, TN 37830

1 Dr. Ronald J. Phillips
Assistant Professor, Department of
Chemical Engineering and Material
Science
University of California, Davis
Davis, CA 95616

1 Dr. Gautam Pillay
Advanced Technologies Group
Batelle Pacific Northwest Laboratory
P7-41, P. O. Box 999
Richland, WA 99352

1 Dr. Ronald F. Probstein
Professor, Department of Mechanical Engineering
Massachusetts Institute of Technology
Cambridge, MA 02138

1 Dr. Brian Reed
Assistant Professor
Department of Civil and Environmental Engineering
West Virginia University
P. O. Box 6101
Morgantown, WV 26506-6101

1 Eric Rogoff
MDM/Lamb, Inc.
6121 Indian School Rd., N.E.
Suite 105
Albuquerque, NM 87110

1 Nina Rosenberg
Los Alamos National Laboratory
EES-DO, MS D446
Los Alamos, NM 87545

1 Dr. Donald D. Runnells
Shepherd-Miller, Inc.
1600 Specht Point Drive
Fort Collins, CO 80525

1 Shannon Saget
U.S. Department of Energy
Richland Operations Office
P.O. Box 550, K8-50
Richland, WA 99352

1 Dr. Donald E. Sanning
Senior Environmental Scientist
Office of Research and Development
U.S. Environmental Protection Agency
Risk Reduction Engineering Laboratory
26 W. Martin Luther King Drive
Cincinnati, OH 45268

1 George Schneider
U.S. Department of Energy
Idaho Operations Office
785 DOE Place
Idaho Falls, ID 83402

1 Dr. Dale S. Schultz
DuPont Company
Glasgow Site
Building 300, P. O. Box 6101
Newark, DE 19714

1 Dr. Daniel T. Schwartz
Assistant Professor
Department of Chemical Engineering
University of Washington
Mail Stop BF-10
Seattle, WA 98195

1 Dr. Steven Schwartzkopf
Research & Development Division
Lockheed Missiles & Space Company
3251 Hanover Street
Org. 93-50, Building 204
Palo Alto, CA 94304-1191

1 Michael Serrato
Westinghouse Savannah River Company
Savannah River Technology Center
Environmental Sciences Section
P.O. Box 616 / 773-42A
Aiken, SC 29802

1 Ahmet Seur
Westinghouse Savannah River Company
Savannah River Technology Center
Environmental Sciences Section
P.O. Box 616 / 730-2B
Aiken, SC 29802

1 Joe Shinn
Lawrence Livermore National Laboratory
MS L453
P.O. Box 808
Livermore, CA 94551-9900

1 Mel Shupe
U.S. Department of Energy
Federal Energy Technology Center
Industrial Park
P.O. Box 3462
Butte, MT 59702

1 Dr. Donald C. Slack
Professor & Head
Department of Agricultural and
Biosystems Engineering
The University of Arizona
Tucson, AZ 85721

1 Steve Slate
Pacific Northwest National Laboratories
Battelle Blvd.
P.O. Box 999
Richland, WA 99352

1 Dr. Stuart Smedley
SRI International
333 Ravenswood Avenue
Menlo Park, CA 94025

1 Gug Sresty
IIT Research Institute
10 West 35th Street
Chicago, IL 60616-3799

1 Larry Stebbins
FERMCO
MS: 81-2
P.O. Box 538704
Cincinnati, OH 45235

1 Helen Stolz
U.S. Department of Energy
Nevada
P.O. Box 98518
Las Vegas, NV 89193-8518

1 John Stormont
University of New Mexico
Dept. of Civil Engineering
Albuquerque, NM 87131-1351

1 Jim Studer
Intera, Inc.
1650 University Blvd. N.E.
Albuquerque, NM 87102

1 Rick E. Swatzell
Martin Marietta Energy Systems
P.O. Box 2003
Oak Ridge, TN 37831-7606

1 Tsuneo Tamura
Hazardous Waste Remediation Program
M.S. 7606
Oak Ridge, TN 37831-7606

1 Bruce Thompson
University of New Mexico
Dept. of Civil Engineering
Albuquerque, NM 87131-1351

1 Dr. Roy F. Thornton
Environmental Laboratory
General Electric Corporate Research &
Development
P. O. Box 8
K-1, 4B30
Schenectady, NY 12301-0008

1 Dr. Thanos Trezos, P.E.
Environmental Engineer
Southern California Edison
2244 Walnut Grove Avenue
Room #405
Rosemead, CA 91770

1 University of New Mexico
Zimmerman Library
Government Publications Department
Albuquerque, NM 87131

1 Maria Vargas
U.S. Department of Energy
Richland Operations Office
P.O. Box 550
Richland, WA 99352

1 Jef Walker
U.S. Department of Energy
EM-53
Cloverleaf Bldg.
19901 Germantown Rd.
Germantown, MD 20874-1290

1 Rod Warner
U.S. Department of Energy
Ohio Operations Office
P.O. Box 538705
Cincinnati, OH 45030

1 Phillip Washer
U.S. Department of Energy
Savannah River Operations Office
Bldg. 773-A
P.O. Box 616
Aiken, SC 29803

1 Bill Wilborn
U.S. Department of Energy
Nevada Operations Office
2753 S Highland Rd.
Las Vegas, NV 89109

1 Earl Whitney
Los Alamos National Laboratory
EES-5, MS F665
Los Alamos, NM 87545

1 Dr. Fritz G. Will
Research Professor, Chemical Eng.
University of Utah
EPRI Visiting Scientist
Electric Power Research Institute
P. O. Box 10412
Palo Alto, CA 94303

1 Thomas Williams
U.S. Department of Energy
Idaho Operations Office
MS1219
785 DOE Pl.
Idaho Falls, ID 83402

1 Dr. J. Kenneth Wittle
Electro-Petroleum, Inc.
996 Old Eagle School Road
Suite 1116
Wayne, PA 19087

1 James Wright
U.S. Department of Energy
Savannah River Operations Office
Bldg. 703-46A
P.O. Box A
Aiken, SC 29803

1 Paul Zielinski
U.S. Department of Energy
EM-443
Cloverleaf Bldg.
19901 Germantown Rd.
Germantown, MD 20874-1290

1 Pete Zionkowski
Westinghouse Savannah River Company
Savannah River Technology Center
Environmental Sciences Section
P.O. Box 616 / 730-2B
Aiken, SC 29802

Internal

1 MS 0710 Richard Lynch, 6100
1 MS 0719 George Allen, 6131
1 MS 0719 Thomas Burford, 6131
1 MS 0719 Matthew Hankins, 6131
20 MS 0719 Eric Lindgren, 6131
1 MS 0719 James Phelan, 6131
1 MS 0724 Joan Woodard, 6000
1 MS 0750 Patrick Brady, 6118
1 MS 0750 Henry Westrich, 6118
1 MS 0876 Rekha Rao, 9111
1 MS 1044 Darlene Moore, 7511
1 MS 1147 Warren Cox, 6132
1 MS 1147 Fran Nimick, 6133
1 MS 1148 Richard Fate, 6134
1 MS 1335 Margaret S.Y. Chu, 6801

Unclassified *Unlimited Release* Documents

1 MS 9018 Central Technical Files, 8940-2
5 MS 0899 Technical Library, 4916
2 MS 0619 Review & Approval Desk, 12690
For DOE/OSTI